CHARACTERIZATION OF PLUS FRACTIONS FOR LOW GAS-OIL RATIO BLACK OIL SAMPLES IN TURKEY

A THESIS SUBMITTED TO
THE GRADUATE SCHOOL OF NATURAL AND APPLIED SCIENCES
OF
MIDDLE EAST TECHNICAL UNIVERSITY

BY

ARTUĞ TÜRKMENOĞLU

IN PARTIAL FULLFILMENT OF THE REQUIREMENTS
FOR
THE DEGREE OF MASTER OF SCIENCE
IN
PETROLEUM AND NATURAL GAS ENGINEERING

FEBRUARY 2016

Approval of the thesis:

CHARACTERIZATION OF PLUS FRACTIONS FOR LOW GAS-OIL RATIO BLACK OIL SAMPLES IN TURKEY

submitted by **ARTUĞ TÜRKMENOĞLU** in partial fulfillment of the requirements for the degree of **Master in Science in Petroleum and Natural Gas Engineering, Middle East Technical University** by,

Prof. Dr. Gülbin DURAL ÜNVER
Director, Graduate School of Natural and Applied Sciences

Prof. Dr. Serhat AKIN
Head of Department, Petroleum and Natural Gas Engineering

Assist. Prof. Dr. Çağlar SINAYUÇ
Supervisor, Petroleum and Natural Gas Engineering, METU

Examining Committee Members:

Prof. Dr. Mahmut PARLAKTUNA
Petroleum and Natural Gas Engineering Dept., METU

Assist. Prof. Dr. Çağlar SINAYUÇ
Petroleum and Natural Gas Engineering Dept., METU

Prof. Dr. Serhat AKIN
Petroleum and Natural Gas Engineering Dept., METU

Assist. Prof. Dr. İsmail DURGUT
Petroleum and Natural Gas Engineering Dept., METU

Assist. Prof. Dr. Emre ARTUN
Petroleum and Natural Gas Engineering Dept., METU-NCC

Date: February 8th, 2016

I hereby declare that all information in this document has been obtained and presented in accordance with academic rules and ethical conduct. I also declare that, as required by these rules and conduct, I have fully cited and referenced all material and results that are not original to this work.

Name, Last name :

Signature :

ABSTRACT

CHARACTERIZATION OF PLUS FRACTIONS FOR LOW GAS-OIL RATIO BLACK OIL SAMPLES IN TURKEY

Türkmenoğlu, Artuğ
M.S., Department of Petroleum and Natural Gas Engineering
Supervisor: Assist. Prof. Dr. Çağlar Sınayuç

February 2016, 120 Pages

Pressure - Volume - Temperature (PVT) analyses simulate the reservoir fluid behavior while flowing from the reservoir to the surface under varying pressure, volume and temperature conditions. There are several PVT simulators that perform PVT calculations. Accurate characterization of a fluid is very important for further studies and reservoir simulations in all reservoir engineering aspects. Because there are a few equations of state and many types of reservoir and reservoir fluids, experimental data does not perfectly match with the PVT simulation results. Low API black oils include heavy hydrocarbons. Therefore, regression and characterization of plus fractions are needed in order to get better results from the PVT simulators. PVT data is usually used for field development program, reserve calculations, and EOR/IOR implementations such as gas flooding.

In this study, PVT experiments, which are Constant Composition Experiment, 0 - Flash Experiment, Gas and Oil Compositional Analysis and Viscosity Measurement at reservoir temperature, are conducted on low GOR (20.7 scf/STB

< GOR < 62.3 scf/STB) black oil samples. Reservoir fluid samples are obtained from different fields in Turkey. After laboratory experiments, in order to compare the experimental data, PVT simulation studies are performed. During simulation study, with respect to EOS models (SRK and PR with Peneloux Correction), bubble points, oil densities and oil viscosities are used as regression data. Heavier hydrocarbons are lumped together as C7+, C10+ and C20+, which is called as pseudoization process. Effects of critical properties and degree of pseudoization of plus fractions are investigated. Also, correlations to predict critical properties are used. The predictive ability of EOS models after tuning is analysed also by comparing simulational and experimental oil formation volume factors at bubble point pressure. The reason of selecting these parameters is that those are not used as inputs into compositional simulator for regression.

PR - Pen EoS is more successful in density predictions than SRK - Pen EoS. Also, pseudoization is highly effective on density predictions. However, for heavy hydrocarbons, small degree of pseudoization gives acceptable results. Viscosity predictions are not effected by both EoS models and pseudoization but, they depend on viscosity correction factors of CSP model. Good agreements with experimental data suggest that PVT simulators can be used as a good alternative, especially when there is no possibility to conduct the experiments.

Key Words: Pressure - Volume - Temperature (PVT) Analysis, PVT Simulation, Equation of State

ÖZ

TÜRKİYE'DEKİ DÜŞÜK GAZ-PETROL ORANINA SAHİP PETROL ÖRNEKLERİNDE ARTI UÇLARIN KARAKTERİZAYONU

Türkmenoğlu, Artuğ

Yüksek Lisans : Petrol ve Doğal Gaz Mühendisliği Bölümü

Tez Yöneticisi : Yrd. Doç. Dr. Çağlar Sınayuç

Şubat 2016, 120 Sayfa

Basınç-Hacim-Sıcaklık (PVT) analizi, rezervuar akışkanının rezervuardan yüzeye gelene kadarki akışını değişken basınç, sıcaklık ve hacim koşullarında simüle etmektedir. PVT hesaplamalarını gerçekleştiren pek çok PVT simülatörü bulunmaktadır. Bir akışkanın doğru karakterizasyonu, ileri çalışmalar ve tüm rezervuar mühendisliği simülasyonları için çok önemlidir. Pek az hal denklemi ve çok fazla karakteristikte rezervuar ve rezervuar sıvısı olduğundan dolayı, deney verisi, PVT simülasyon sonuçlarıyla mükemmel bir şekilde eşleşmemektedir. Bundan dolayı, regresyon ve ağır uçların karakterizasyonu gerekmektedir. PVT verisi, genellikle saha geliştirme programları, rezerv hesaplamaları ve gaz öteleme gibi EOR/IOR uygulamaları için kullanılmaktadır.

Bu çalışmada, düşük gaz-petrol (20.7 scf/STB < GOR < 62.3 scf/STB) oranına sahip petrol örnekleri üzerinde, Sabit Bileşim Testi, 0 - Flash Testi, Gaz ve Petrolün Kompozisyon Analizleri ve rezervuar sıcaklığında Viskozite ölçümleri gibi PVT laboratuvar deneyleri yapılmıştır. Rezervuar petrolü örnekleri, Türkiye'deki farklı sahalardan alınmıştır. Laboratuvar deneylerinden sonra, deney sonuçlarıyla kıyaslayabilmek amacıyla, PVT simülasyon çalışmaları yapılmaktadır. Bu kısımda, EOS modellerine (Peneloux düzeltmeli SRK ve PR) göre; kabarcık basınçları, petrol yoğunluk ve viskoziteleri regresyon verisi olarak kullanılmıştır. Daha ağır hidrokarbonlar C7+, C10+ ve C20+ olacak şekilde gruplanmış olup, bu sadeleştirme aşaması olarak adlandırılmaktadır. Artı uçların kritik özellikleri ve sadeleştirilme derecesinin etkileri araştırılmıştır. Ayrıca, kritik özellikleri tahmin edecek korelasyonlar kullanılmıştır. EOS modellerinin ayarlamadan sonra tahmin kapasitesi, simülasyon ve deney sonucu elde edilen kabarcık basıncındaki petrol formasyon hacim katsayılarını kıyaslayarak analiz edilmiştir. Bu verilerin seçilmesinin sebebi, simülatörde regresyon amacıyla girdi olarak kullanılmamış olmamalarıdır.

PR - Pen hal denklemi yoğunluk tahminlerinde SRK - Pen hal denklemine göre daha iyi sonuçlar vermiştir. Ayrıca, sadeleştirme yoğunluk tahminlerinde oldukça yüksek derecede etkilidir. Ancak, ağır hidrokarbonlar için, daha az derecede sadeleştirme de etkili olabilmektedir. Viskozite tahminleri hem hal denklemlerinden hem de sadeleştirmeden etkilenmemektedir ama CSP modelinin viskozite düzeltme faktörlerine bağlıdırlar. Deney verisiyle iyi eşleşme, özellikle deneyi yapma olanağı bulunmadığı zamanlarda, PVT simülatörlerinin iyi bir alternatif olarak kullanılabileceğini göstermektedir.

Anahtar Sözcükler: Basınç - Hacim - Sıcaklık (PVT) Analizi, PVT Simülasyonu, Hal Denklemi

ACKNOWLEDGEMENTS

I would like to express my gratitude to Assist. Prof. Dr. Çağlar SINAYUÇ for his patience and guidance, to Mr. Uğur KARABAKAL and Mr. Hüseyin ÇALIŞGAN for their flexibility through the completion of this study and their guidance.

I would like to thank to Turkish Petroleum Research Centre for their allowance of using company data and their flexibility.

I would like to give my thanks to PVT analysis technician, Mr. R. İbrahim ŞAHİN for his excellent care during the experimental part of this study.

TABLE OF CONTENTS

ABSTRACT .... **v**
ÖZ .... **vii**
ACKNOWLEDGEMENTS .... **ix**
TABLE OF CONTENTS .... **x**
LIST OF TABLES .... **xiii**
LIST OF FIGURES .... **xvi**
NOMENCLATURE .... **xx**

CHAPTERS

1. INTRODUCTION **1**
2. LITERATURE REVIEW **5**
    2.1.CLASSIFICATION OF HYDROCARBON RESERVOIR 5
        2.1.1. Dry Gas 6
        2.1.2. Wet Gas 7
        2.1.3. Retrograde Gas 8
        2.1.4. Volatile Oil 9
        2.1.5. Black Oil 10
    2.2.EQUATION OF STATE 11
        2.2.1. Soave - Redlich - Kwong (SRK) EoS 11
        2.2.2. Peng - Robinson (PR) EoS 13
    2.3.MODIFICATIONS TO EQUATIONS OF STATE 14
    2.4.LUMPING PROCEDURE 15
    2.5.CORRELATIONS OF CRITICAL PROPERTIES 15
        2.5.1. Edmister (1958) Correlation 16
        2.5.2. Sancet (2007) Correlation 16
        2.5.3. Pedersen (1992) Correlation 16
        2.5.4. Riazi - Daubert (1987) Correlation 17

2.5.5. Katz and Firoozabadi (1978) Correlation 18

2.6.VISCOSITY MODELS 18

2.6.1. Corresponding States (CSP) Theory 18

2.6.2. Lohrenz - Bray - Clark (LBC) Viscosity Model 19

2.6.3. Comparison of CSP and LBC Viscosity Models 19

2.7. PVT EXPERIMENTS 20

2.7.1. Fluid Sampling 20

2.7.1.1. Bottom Hole Sampling 21

2.7.1.2. Surface Sampling 21

2.7.1.3. Wireline Sampling 22

2.7.2. Constant Composition Expansion (CCE) Experiment 22

2.7.3. 0-Flash Experiment 23

2.7.4. Differential Liberation (DL) Experiment 24

2.7.5. Constant Volume Depletion (CVD) Experiment 25

2.7.6. Multi-Stage Separator Experiment 27

2.7.7. Viscosity Experiment 28

2.7.8. Compositional Analysis 28

3. STATEMENT OF THE PROBLEM 31

4. METHODOLOGY 33

4.1.EXPERIMENTAL PROCEDURE 33

4.2.PVT SIMULATION STUDY 34

5. RESULTS AND DISCUSSIONS 37

5.1.INTRODUCTION 37

5.2.LABORATORY STUDIES 37

5.2.1. Well B60 Sample 37

5.2.2. Well DS1 Sample 41

5.2.3. Well E2 Sample 44

5.2.4. Well BSS1 Sample 47

5.3.SIMULATION STUDIES 53

5.3.1. Well B60 Sample 54

5.3.2. Well DS1 Sample 67

5.3.3. Well E2 Sample 80
5.3.4. Well BSS1 Sample.. 92
6. CONCLUSIONS 105
7. RECOMMENDATIONS... 107

REFERENCES 109

APPENDICES

APPENDIX A - INSTRUMENTS OF THE PVT TEST SYSTEM 115
APPENDIX B - SAMPLE CHROMATOGRAM.. 119

LIST OF TABLES

TABLES

5.1 CCE Results for Well B60 Sample 38
5.2 Flash Experiment Results for Well B60 Sample 39
5.3 Viscosity Experiment Result for Well B60 Sample 39
5.4 Gas and Oil Compositions for B60 Well Sample 40
5.5 CCE Results for Well DS1 Sample 41
5.6 Flash Experiment Results for Well DS1 Sample 42
5.7 Viscosity Experiment Result for Well DS1 Sample 42
5.8 Gas and Oil Compositions for DS1 Well Sample 43
5.9 CCE Results for Well E2 Sample 44
5.10 Flash Experiment Results for Well E2 Sample 45
5.11 Viscosity Experiment Result for Well E2 Sample 45
5.12 Gas and Oil Compositions for Well E2 Sample 46
5.13 CCE Results for Well BSS1 Sample 47
5.14 Flash Experiment Results for Well BSS1 Sample 48
5.15 Viscosity Experiment Result for Well BSS1 Sample 48
5.16 Gas and Oil Compositions for Well BSS1 Sample 49
5.17 Lumped Reservoir Fluid Compositions for Well B60 Sample 54
5.18 Parameters of Plus Fractions for Well B60 Sample 55
5.19 Parameters of Plus Fractions After MW Adjustment for Well B60 Sample 55
5.20 B_{ob} Comparison for Well B60 Sample (SRK - Pen EoS) 59
5.21 B_{ob} Comparison for Well B60 Sample (PR - Pen EoS) 59
5.22 Correlation – Calculated Critical Properties of Plus Fraction for Well B60 Sample 60

5.23 B_{ob} Comparison for Well B60 Sample (SRK-Pen EoS with S and E values) 64
5.24 B_{ob} Comparison for Well B60 Sample (PR-Pen EoS with S and E values) 65
5.25 CSP Viscosity Coefficient for Well B60 Sample (SRK-Pen EoS) 65
5.26 CSP Viscosity Coefficient for Well B60 Sample (PR-Pen EoS) 66
5.27 Lumped Reservoir Fluid Compositions for Well DS1 Sample 68
5.28 Parameters of Plus Fractions for Well DS1 Sample 68
5.29 Parameters of Plus Fractions After MW Adjustment for Well DS1 Sample 69
5.30 B_{ob} Comparison for Well DS1 Sample (SRK-Pen EoS) 72
5.31 B_{ob} Comparison for Well DS1 Sample (PR-Pen EoS) 73
5.32 Correlation – Calculated Critical Properties of Plus Fraction for Well DS1 Sample 73
5.33 B_{ob} Comparison for Well DS1 Sample (SRK-Pen EoS with S and E values) 77
5.34 B_{ob} Comparison for Well DS1 Sample (PR-Pen EoS with S and E values) 77
5.35 CSP Viscosity Coefficient for Well DS1 Sample (SRK-Pen EoS) 78
5.36 CSP Viscosity Coefficient for Well DS1 Sample (PR-Pen EoS) 78
5.37 Lumped Reservoir Fluid Compositions for Well E2 Sample 80
5.38 Parameters of Plus Fractions for Well E2 Sample 81
5.39 Parameters of Plus Fractions After MW Adjustment for Well E2 Sample 81
5.40 B_{ob} Comparison for Well E2 Sample (SRK - Pen EoS) 84
5.41 B_{ob} Comparison for Well E2 Sample (PR - Pen EoS) 85
5.42 Correlation – Calculated Critical Properties of Plus Fraction for Well E2 Sample 85
5.43 B_{ob} Comparison for Well E2 Sample (SRK-Pen EoS with S and E values) 89

5.44 B_{ob} Comparison for Well E2 Sample
(PR-Pen EoS with S and E values) 89
5.45 CSP Viscosity Coefficient for Well E2 Sample (SRK - Pen EoS) 90
5.46 CSP Viscosity Coefficient for Well E2 Sample (PR - Pen EoS) 90
5.47 Lumped Reservoir Fluid Compositions for Well BSS1 Sample 92
5.48 Parameters of Plus Fractions for Well BSS1 Sample 93
5.49 Parameters of Plus Fractions After MW Adjustment
for Well BSS1 Sample 93
5.50 B_{ob} Comparison for Well BSS1 Sample (SRK - Pen EoS) 96
5.51 B_{ob} Comparison for Well BSS1 Sample (PR - Pen EoS) 97
5.52 Correlation – Calculated Critical Properties of Plus Fraction for
Well BSS1 Sample 97
5.53 B_{ob} Comparison for Well BSS1 Sample
(SRK - Pen EoS with S and E values) 100
5.54 B_{ob} Comparison for Well BSS1 Sample
(PR - Pen EoS with S and E values) 101
5.55 CSP Viscosity Coefficient for Well BSS1 Sample (SRK - Pen EoS) 101
5.56 CSP Viscosity Coefficient for Well BSS1 Sample (PR - Pen EoS) 102
A.1. Technical Specifications of Fluid-Eval Standard®
(VINCI Technologies, 2012, p.6) 115
A.2 Technical Specifications of EV1000®
(VINCI Technologies, 2012, p.23) 116
A.3 Technical Specifications of Automated Gasometer®
(VINCI Technologies, 2012, p.14) 116

LIST OF FIGURES

FIGURES

2.1 Phase diagram of a typical dry gas with line of isothermal reduction of reservoir temperature, 12, and surface conditions (McCain, 1990) 6

2.2 Phase diagram of a typical wet gas with line of isothermal reduction of reservoir temperature, 12, and surface conditions (McCain, 1990) 7

2.3 Phase diagram of a typical retrograde gas with line of isothermal reduction of reservoir temperature, 123, and surface conditions (McCain, 1990) 8

2.4 Phase diagram of a typical volatile oil with line of isothermal reduction of reservoir temperature, 123, and surface conditions (McCain, 1990) 9

2.5 Phase diagram of typical black oil with line of isothermal reduction of reservoir temperature, 123, and surface conditions (McCain, 1990) 10

2.6 Schematic of a CCE Experiment for oil 23

2.7 Schematic of a 0-Flash Experiment for oil 24

2.8 Schematic of a DL Experiment for oil... 25

2.9 Schematic of a CVD Experiment for gas 26

2.10 Schematic of a Multi-Stage Separator Experiment for oil 27

2.11 Schematic of a Gas Chromatograph 29

5.1 Pressure - Density Relationship for All Wells... 50

5.2 Pressure - Viscosity Relationship for All Wells... 51

5.3 Gas Components for All Wells.. 51

5.4 Oil Components for All Wells... 52

5.5 Radar Graph of Oil Components for All Wells.. 53

5.6 Pressure – Density Relationship for Well B60 Sample (C7+ Adjustment)... 56

5.7 Pressure – Density Relationship for Well B60 Sample (C10+ Adjustment). 56

5.8 Pressure – Density Relationship for Well B60 Sample (C20+ Adjustment). 57

5.9 SRK-Pen EoS Predictions of GOR and P_b for Well B60 Sample 58

5.10 PR-Pen EoS Predictions of GOR and P_b for Well B60 Sample 59
5.11 Pressure – Density Relationship for Well B60 Sample (C7+ Adjustment – Correlated). 61
5.12 Pressure – Density Relationship for Well B60 Sample (C10+ Adjustment – Correlated) 62
5.13 Pressure – Density Relationship for Well B60 Sample (C20+ Adjustment – Correlated) 62
5.14 SRK - Pen EoS Predictions of GOR and P_b for Well B60 Sample (with S and E Values) 63
5.15 PR - Pen EoS Predictions of GOR and P_b for Well B60 Sample (with S and E Values) 64
5.16 Pressure and Viscosity Relationship for Well B60 Sample (SRK-PEN EoS).. 66
5.17 Pressure and Viscosity Relationship for Well B60 Sample (PR-PEN EoS).. 67
5.18 Pressure – Density Relationship for Well DS1 Sample (C7+ Adjustment)... 69
5.19 Pressure – Density Relationship for Well DS1 Sample (C10+ Adjustment). 70
5.20 Pressure – Density Relationship for Well DS1 Sample (C20+ Adjustment). 70
5.21 SRK-Pen EoS Predictions of GOR and P_b for Well DS1 Sample 71
5.22 PR-Pen EoS Predictions of GOR and P_b for Well DS1 Sample 72
5.23 Pressure – Density Relationship for Well DS1 Sample (C7+ Adjustment – Correlated) 74
5.24 Pressure – Density Relationship for Well DS1 Sample (C10+ Adjustment – Correlated) 75
5.25 Pressure – Density Relationship for Well DS1 Sample (C20+ Adjustment – Correlated) 75
5.26 SRK - Pen EoS Predictions of GOR and P_b for Well DS1 Sample (with S and E Values) 76
5.27 PR - Pen EoS Predictions of GOR and P_b for Well DS1 Sample (with S and E Values) 76
5.28 Pressure and Viscosity Relationship for Well DS1 Sample (SRK-PEN EoS).. 79

5.29 Pressure and Viscosity Relationship for Well DS1 Sample (PR-PEN EoS). 79
5.30 Pressure – Density Relationship for Well E2 Sample (C7+ Adjustment)..... 82
5.31 Pressure – Density Relationship for Well E2 Sample (C10+ Adjustment)... 82
5.32 Pressure – Density Relationship for Well E2 Sample (C20+ Adjustment)... 83
5.33 SRK - Pen EoS Predictions of GOR and P_b for Well E2 Sample 83
5.34 PR - Pen EoS Predictions of GOR and P_b for Well E2 Sample 84
5.35 Pressure – Density Relationship for Well E2 Sample (C7+ Adjustment – Correlated) 86
5.36 Pressure – Density Relationship for Well E2 Sample (C10+ Adjustment – Correlated) 87
5.37 Pressure – Density Relationship for Well E2 Sample (C20+ Adjustment – Correlated) 87
5.38 SRK - Pen EoS Predictions of GOR and P_b for Well E2 Sample (with S and E Values)... 88
5.39 PR - Pen EoS Predictions of GOR and P_b for Well E2 Sample (with S and E Values)... 88
5.40 Pressure and Viscosity Relationship for Well E2 Sample (SRK - PEN EoS) 91
5.41 Pressure and Viscosity Relationship for Well E2 Sample (PR - PEN EoS).. 91
5.42 Pressure – Density Relationship for Well BSS1 Sample (C7+ Adjustment) 94
5.43 Pressure – Density Relationship for Well BSS1 Sample (C10+ Adjustment)... 94
5.44 Pressure – Density Relationship for Well BSS1 Sample (C20+ Adjustment)... 95
5.45 SRK - Pen EoS Predictions of GOR and P_b for Well BSS1 Sample............ 95
5.46 PR - Pen EoS Predictions of GOR and P_b for Well BSS1 Sample............... 96
5.47 Pressure – Density Relationship for Well BSS1 Sample (C7+ Adjustment – Correlated) 98
5.48 Pressure – Density Relationship for Well BSS1 Sample (C10+ Adjustment – Correlated) 98

5.49 Pressure – Density Relationship for Well BSS1 Sample (C20+ Adjustment – Correlated) 99

5.50 SRK - Pen EoS Predictions of GOR and P_b for Well E2 Sample (with S and E Values) 99

5.51 PR - Pen EoS Predictions of GOR and P_b for Well E2 Sample (with S and E Values) 100

5.52 Pressure and Viscosity Relationship for Well BSS1 Sample (SRK - PEN EoS).................... 102

5.53 Pressure and Viscosity Relationship for Well BSS1 Sample (PR - PEN EoS) 103

B.1. Liquid Chromatogram Sample for Well B6.................... 120

NOMENCLATURE

Roman Symbols :

a	Constant in SRK and PR Equations of State
b	Constant in SRK and PR Equations of State
c_1,c_2,c_3,c_4	Constants in Eq. 31
d_1,d_2,d_3,d_4	Constants in Eq. 32
e_1,e_2,e_3,e_4	Constants in Eq. 33
API	Liquid Gravity, °API
B	Formation Volume Factor, bbl/STB
C_{pen}	Volume Translation Parameter, m^3/mol
K_{ij}	Binary İnteraction Coefficient between Component i and j
P	Pressure, psig
P_{ci}	Absolute Critical Pressure of Component i
R	Gas Constant
T	Temperature, °F
T_b	Normal Boiling Point Temperature, °F
T_{ci}	Absolute Critical temperature of Component i
V	Volume, cc
V_i	Volume corresponding to i’th step, cc
Z	Compressibility Factor in SRK and PR Equations of State
z_i	Mole Fraction of Component i

Z_{RA}	Rackett’s Compressibility Factor

Greek Symbols :

ω	Acentric Factor, dimensionless
ρ	Density, g/cc
μ	Viscosity, cp
μ^*	Viscosity of a Gas Mixture at low pressure in Eq. 37, cp
α	Constant in SRK and PR Equations of State
ψ	Fugacity
ψ_i	Fugacity corresponding to Component i
θ	Physical Property in Eq. 36
ξ	Viscosity Reducing Parameter in Eq. 38
Ωa, Ωb	Pure Component Parameters in Eq. 3 and 4

Abbreviations :

Adj.	Adjusted
CCE	Constant Composition Expansion
CSP	Corresponding State
CVD	Constant Volume Depletion
DL	Differential Liberation
E	Edmister
EoS	Equation of State
GOR	Gas - Oil Ratio, scf/STB

LBC	Lohrenz - Bray - Clark
MW	Molecular Weight, g/mole
Para.	Parameter
Pen	Peneloux correction
PR	Peng -Robinson
S	Sancet
SRK	Soave - Redlich - Kwong

Subscripts :

b	Bubble point
c	Critical
i	i’th
o	Oil
r	Reduced
sat	Saturation
st	Stock Tank

CHAPTER 1

INTRODUCTION

According to Moses (1986), a good planning is required for the development and production of a reservoir. Also, this planning scheme should be done for data gathering procedure. Not only electric logs and core samples, but also the reservoir fluid samples should be studied. The properties of reservoir fluid must be known in order to make reservoir engineering calculations, such as production optimization and EOR.

Hydrocarbons in reservoirs show a great variety. According to hydrocarbon composition, reservoir and surface conditions, reservoir fluids may be called as black oil, volatile oil, retrograde gas, wet gas or dry gas. Identification of the reservoir fluid is important to determine further strategies.

Equation of state (EoS) models show the relationship of two or more phases. After the equation of state of van der Waals (1873), many authors have studied those equations, such as Soave - Redlich - Kwong (1972), Peng and Robinson (1976), Schmidt and Wenzel (1980), Heyen (1983) etc.

Pedersen et. al. (2015) states that most of the calculations of PVT relationship, performed on hydrocarbon mixtures, are based on cubic equations of states and improvements in computer technology result in performance of many multicomponent phase equilibrium and physical property calculations with an equation of state as a base, at a short time.

Fluid characterization is a requirement for compositional simulators. Critical properties for pure components are known, however critical properties of lumped components, such as C7+, C10+ and C20+ are not directly known. In the literature, there are many correlations that can be used to calculate the critical properties of components, such as Edmister (1958), Pedersen et. al. (1992), Riazi and Daubert (1987), Whitson (1983) etc. Whitson (1984) states that the critical properties of oil fractions are estimated with correlations and these correlations require the information of boiling point and specific gravity.

Aim of this study includes; (1) PVT analysis of black oil samples, (2) investigating PVT properties according to equations of state, pseudoization schemes and critical properties of plus fractions, (3) measuring the reliability of Peng - Robinson and Soave - Redlich - Kwong equations of state with their Peneloux corrections.

For this purpose, four black oil samples taken with bottom hole sampler are used for PVT analysis at reservoir temperature. PVT analysis for each sample consists of Constant Composition Expansion (CCE) experiment, 0-Flash experiment, determination of viscosity - pressure relation under reservoir temperature and compositional analysis of gas and oil samples. Due to low Gas - Oil ratio values (GOR) and bubble point pressures (P_b), differential liberation (DL) experiment is not conducted on samples.

In the next step, the gas and oil compositions, the Gas - Oil ratios (GOR), the density and the viscosity values at the reservoir conditions and the bubble point pressures (P_b) of each sample are used in PVT simulator. Peng - Robinson (PR) and Soave - Redlich - Kwong (SRK) equations of state with Peneloux correction are used to investigate the effect of EoS model. Reservoir composition is lumped in three ways as heptane plus (C7+), decane plus (C10+) and eicosane plus (C20+), to determine the extent of pseudoization effect on density, viscosity, GOR, P_b and oil formation volume factor at P_b (B_{ob}) predictions. Also, the critical properties of plus fractions are obtained in two ways: (1) Sancet and Edmister's correlations and (2) Pedersen's correlations.

At the end, experimental oil formation volume factors at bubble point pressure, (B_{ob}), are compared with simulation results. This value is not used in PVT simulator for regression and by doing so, it is tried to measure the reliability of EoS models.

CHAPTER 2

LITERATURE REVIEW

In this section, the literature about the hydrocarbon reservoir types, equations of state and their modifications and correlations to predict critical properties is given.

2.1. CLASSIFICATION OF HYDROCARBON RESERVOIRS

Hydrocarbon reservoirs consist of many components and each component has a characteristic behavior with respect to pressure and temperature. Therefore, the amount of each component affects the phase behavior of hydrocarbon reservoir. After the determination of phase envelope, definition of initial and final points, or in other terms reservoir and separator/stock tank conditions are used to obtain the phase behavior along the production path.

Reservoir and production engineers should determine the fluid type in the early life of reservoir because, each reservoir fluid types including black oil, volatile oil, retrograde gas, wet and dry gas need different strategies. Initial producing gas/oil ratio, API gravity and color of stock tank liquid give clues about the fluid type however; evaluation should be done by conducting laboratory experiments (McCain, 1990).

2.1.1. Dry Gas

Dry gas is mainly composed of methane and other gases such as carbon dioxide and nitrogen. Along the production path, gas phase is observed; however, water condensation may be seen owing to gas cooling (Danesh, 1998). The phase behavior may be seen in the Figure 2.1. If gas -oil ratio of a system exceeds 100000 scf/STB, it is accepted as dry gas (Ahmed, 1989).

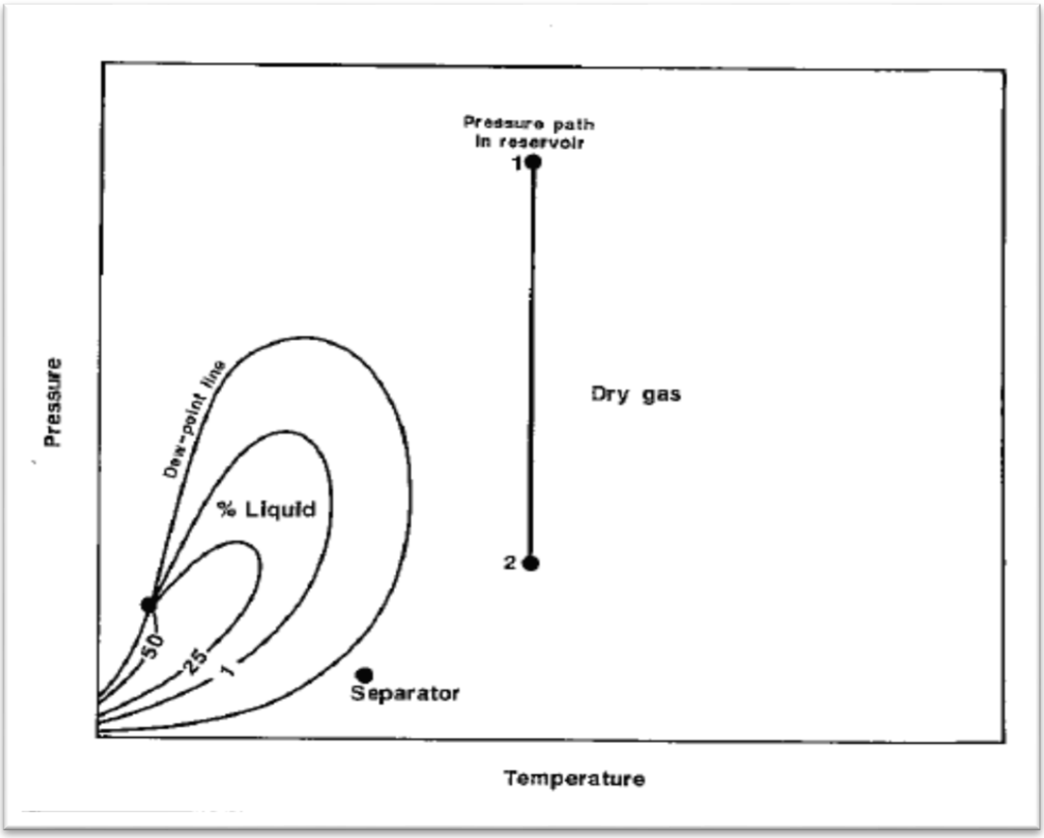

Figure 2.1 Phase diagram of a typical dry gas with line of isothermal reduction of reservoir temperature, 12, and surface conditions (McCain, 1990)

2.1.2. Wet Gas

Phase behavior of this type is located over a temperature range below reservoir temperature. Hence, no liquid drop-out will be observed in the reservoir. Separator conditions within the envelope point out condensation at the surface (Danesh, 1998). Production path and phase behavior of wet gas is, as shown in Figure 2.2.

Gas-oil ratio between 60000 and 100000 scf/STB, API gravity more than 60 °API, colorless liquid in the stock tank and separator conditions in two phase region are characteristics of wet gas (Ahmed, 1989).

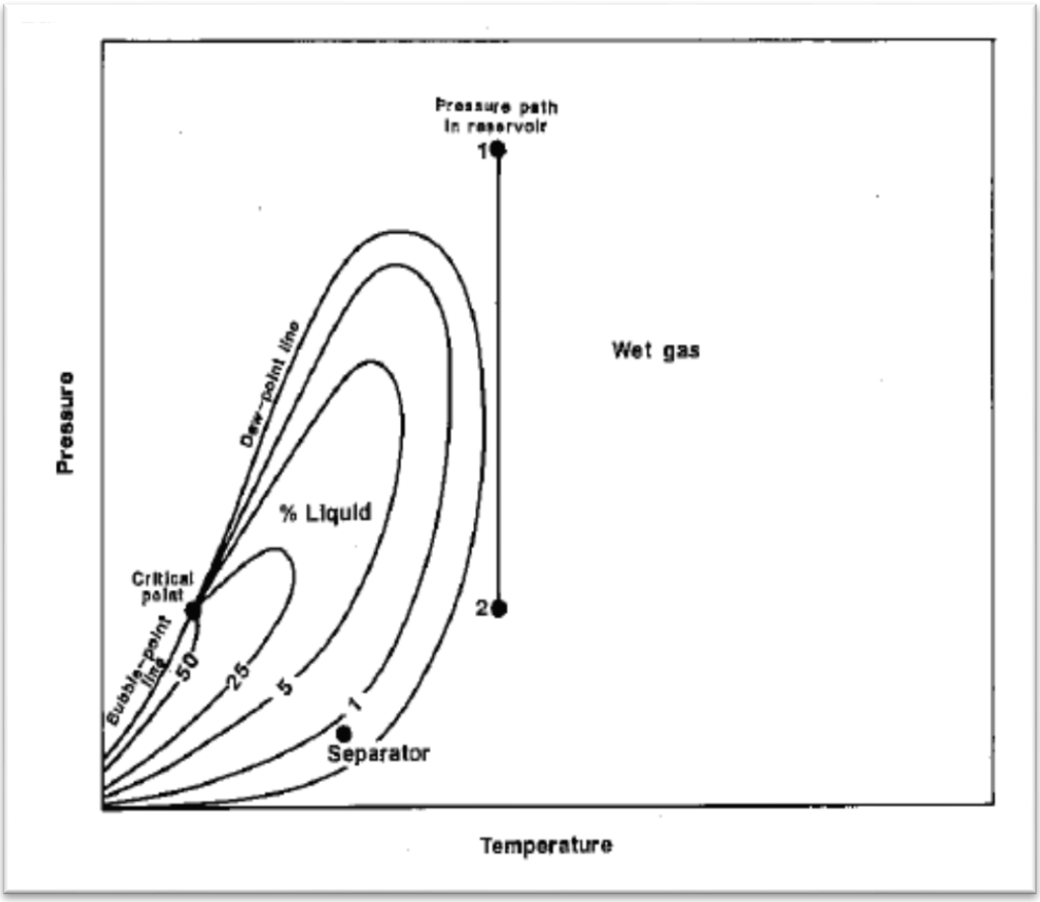

Figure 2.2 Phase diagram of a typical wet gas with line of isothermal reduction of reservoir temperature, 12, and surface conditions (McCain, 1990)

2.1.3. Retrograde Gas

Heavier hydrocarbons increase the width of the envelope of condensate relative to wet gas so, reservoir temperature falls between the critical point and cricondentherm, which is the highest temperature on the envelope. As long as pressure decreases during depletion, retrograde condensation will cause liquid drop out, as shown in Figure 2.3. In addition, because of the decrease in temperature, second condensation of produced gas occurs (Danesh, 1998).

Gas-oil ratio changes between 8000 and 70000 scf/STB and increases during pressure depletion because of liquid drop-out and the loss of heavier components. Stock tank API gravity is more than 50 °API and liquid is usually colorless or slightly colored (Ahmed, 1989).

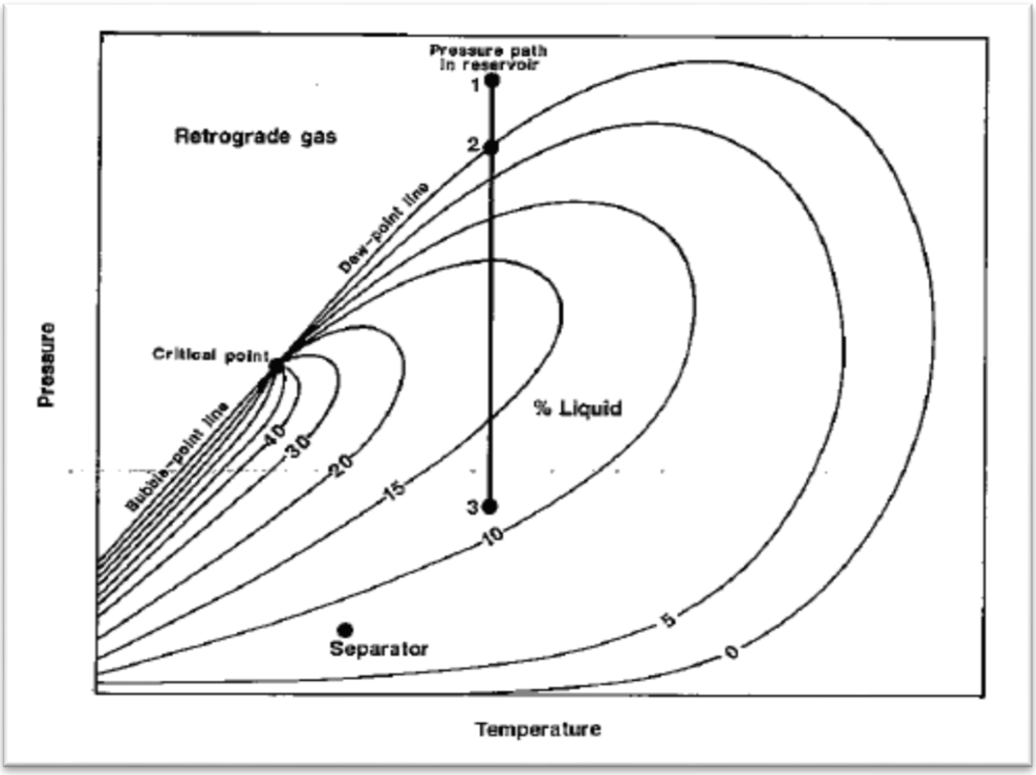

Figure 2.3 Phase diagram of a typical retrograde gas with line of isothermal reduction of reservoir temperature, 123, and surface conditions (McCain, 1990)

2.1.4. Volatile Oil

Volatile oils contain heavier fractions than dry gas, wet gas and gas condensate. Therefore, phase envelope of volatile oil is relatively larger than these cases. As shown in Figure 2.4, close reservoir temperature to critical point and tighter iso-volume lines result in vaporization of significant amounts of oil, when a small decrease in pressure occurs (Danesh, 1998).

Gas-oil ratios vary from 2000 to 3500 scf/STB. Low liquid recovery at the surface and higher stock tank gravities (45 - 55 °API) are observed. Colors of volatile oil change from greenish to orange (Ahmed, 1989).

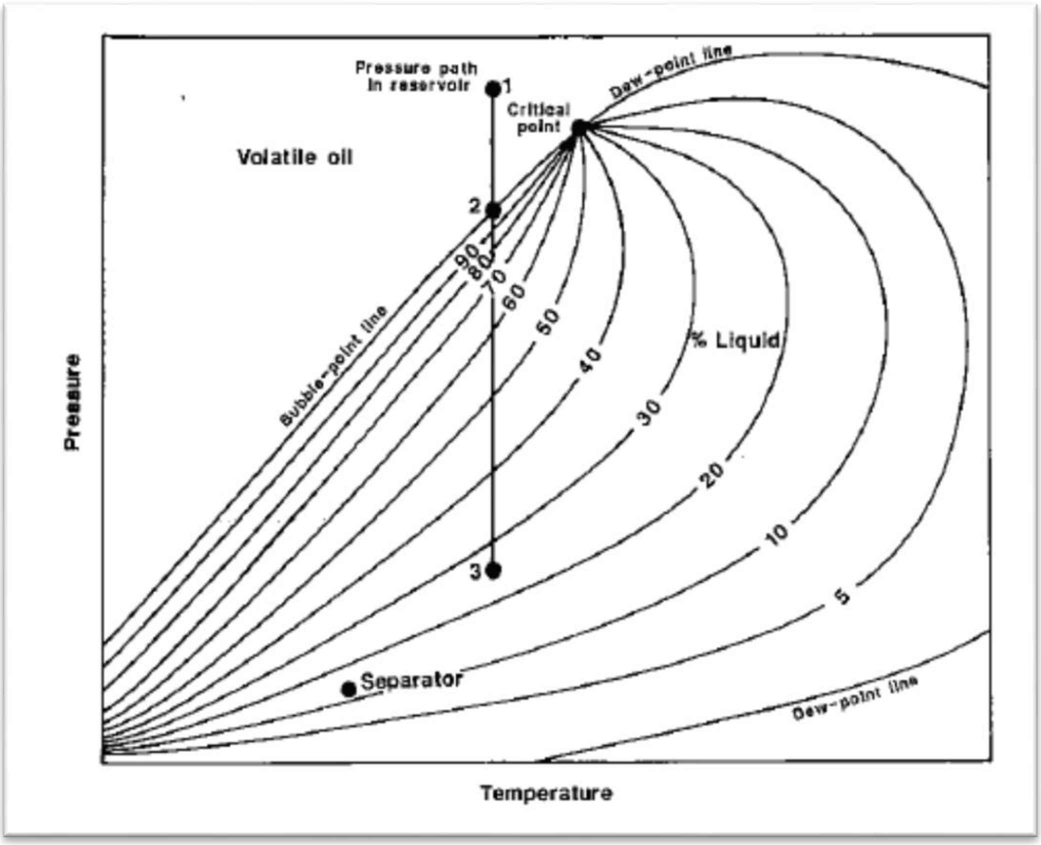

Figure 2.4 Phase diagram of a typical volatile oil with line of isothermal reduction of reservoir temperature, 123, and surface conditions (McCain, 1990)

2.1.5. Black Oil

This type is the most common fluid of oil reservoirs. Abundance of heptane plus fraction, relative to the other types, causes its phase envelope be the largest, with a critical temperature more than reservoir temperature (Danesh, 1998). Phase path during pressure depletion and phase envelope can be seen in Figure 2.5.

Gas-oil ratios between 200 - 700 scf/STB are observed, during production. API gravities may vary from 15 to 40 °API and stock tank black oil has a brown to dark green color (Ahmed, 1989).

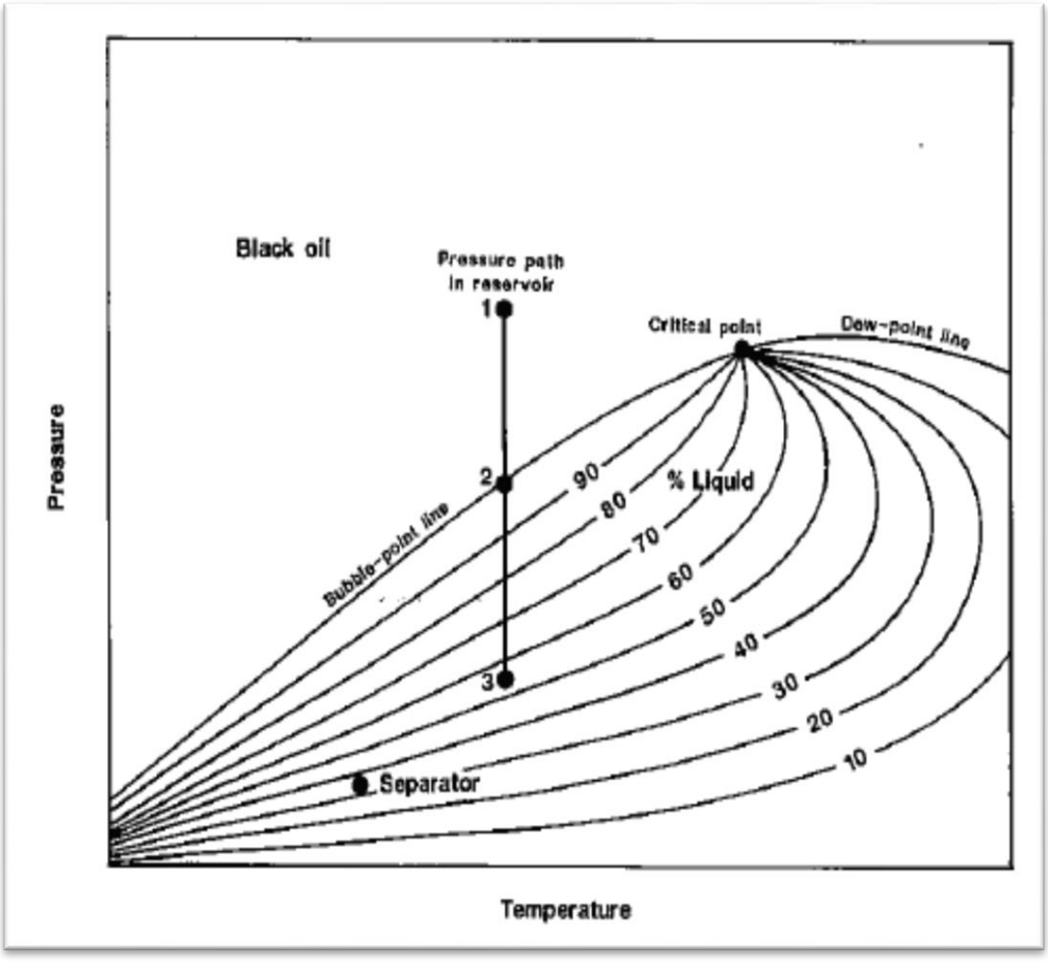

Figure 2.5 Phase diagram of typical black oil with line of isothermal reduction of reservoir temperature, 123, and surface conditions (McCain, 1990)

2.2. EQUATION OF STATE

Equations of State (EoS) models are used to represent thermodynamic and volumetric behavior of fluids. After van der Waals (1873) equation, equations of state attract many authors (Soave, 1972; Peng and Robinson, 1976; Schmidt and Wenzel, 1980; Patel and Teja, 1982; Heyen, 1983). Ahmed (1989) claims that a modification, done in parameter α of the attractive term of Redlich - Kwong EoS by Soave, is the most important point in the development of cubic equations of state.

2.2.1. Soave - Redlich - Kwong (SRK) EoS

The EoS has a form like van der Waals EoS. SRK (Soave, 1972) EoS is given as follows:

$$P = \frac{RT}{(V-b)} - \frac{a\alpha}{[V(V-b)]} \quad (1)$$

where

$$\alpha = [\,1 + m(1 - T_r^{0.5})]^2 \quad (2)$$

$$a = \Omega_a R^2 T_c^2 / P_c \quad (3)$$

$$b = \Omega_b R T_c / P_c \quad (4)$$

The slope, m, is defined in terms of acentric factor, ω, and it is correlated as below:

$$m = 0.480 + 1.574\omega - 0.176\omega^2 \quad (5)$$

The parameters of SRK EoS in Eq. 3 and 4, Ω_a and Ω_b, are 0.42747 and 0.8664, respectively.

SRK EoS in terms of compressibility factor is defined as:

$$Z^3 - Z^2 + (A - B - B^2)Z - AB = 0 \tag{6}$$

where

$$A = a\alpha P/(RT)^2 \tag{7}$$

$$B = bP/RT \tag{8}$$

For the calculation of Vapor - Liquid Equilibrium (VLE) of mixtures, mixing rule, used by Soave, is:

$$(a\alpha)_m = \sum_i \sum_j z_i z_j (a_i a_j)(1 - K_{ij}) \tag{9}$$

$$b_m = \sum_i z_i b_i \tag{10}$$

Where z_i is the mole fraction of phase and K_{ij} values are binary interaction coefficients.

The fugacity coefficient, $\phi_{i,}$ is as in Eq. 11, for a component:

$$\ln(\phi_i) = \frac{b_i(Z-1)}{b_m} - \ln(Z - B) - (\frac{A}{B})(\frac{2\psi_i}{\psi} - \frac{b_i}{b_m})\ln(1 + \frac{B}{Z}) \tag{11}$$

where

$$\psi = \sum_i \sum_j z_i z_j (a_i a_j)(1 - K_{ij}) \tag{12}$$

$$\psi_i = \sum_j z_j (a_i a_j)(1 - K_{ij}) \tag{13}$$

2.2.2. Peng - Robinson (PR) EoS

PR (Peng and Robinson, 1976) equation of state is in the formation of:

$$P = \frac{RT}{V-b} - \frac{a\alpha}{[V(V+b)+b(V+b)]} \tag{14}$$

where

$$a = 0.457235(RT_c)^2/P_c \tag{15}$$
$$b = 0.77796RT_c/P_c \tag{16}$$

The dimensionless factor, α, is calculated in the same way for both SRK EoS and PR EoS. Acentric factor is used to calculate the slope, m for this EoS as shown in Eq. 17:

$$m = 0.37464 + 1.54226\omega - 0.26992\omega^2 \tag{17}$$

Eq. 18 presents the expression of PR EoS in terms of compressibility factor is given by:

$$Z^3 + (B-1)Z^2 + (A - 3B^2 - 2B)Z - (AB - B^2 - B^3) = 0 \tag{18}$$

The fugacity coefficient for a component in mixture, ϕ_i, is defined as in Eq. 19:

$$\ln(\phi_i) = \frac{b_i(Z-1)}{b_m} - \ln(Z-B) - A/(2.82843B)(\frac{2\psi_i}{\psi} - \frac{b_i}{b_m})\ln[\frac{Z+2.414B}{Z-0.414B}] \tag{19}$$

2.3. MODIFICATIONS TO EQUATIONS OF STATE

Peneloux et. al. introduce a new parameter called volume-correction parameter, c_i, into the SRK EoS (Peneloux et. al., 1982). SRK equation with volume correction is given in Eq. 20:

$$P = \frac{RT}{V - b} - \frac{a}{(V+c)(V+b+2c)} \tag{20}$$

with

$$c = \sum_{i=1}^{P} c_i x_i \tag{21}$$

and

$$b = \tilde{b} - c \tag{22}$$

They also, suggest that volume correction parameter, c, is correlated well with Rackett compressibility factor, Z_{RA} (Rackett, 1970) and critical properties. The relationship is given by:

$$c = 0.40768(RT_c/P_c)(0.29441 - Z_{RA} \tag{23}$$

Another different approach is expanding alpha parameter as a power series in acentric factor as shown in Eq. 24 (Twu et. al., 1995):

$$\alpha = \alpha^{(0)} + \omega(\alpha^{(1)} - \alpha^{(0)}) \tag{24}$$

$$\alpha^{(0)} = T_r^{-0.171813} e^{0.125283(1 - T_r^{1.77664})} \tag{25}$$

$$\alpha^{(1)} = T_r^{-0.607352} e^{0.511614(1 - T_r^{2.20517})} \tag{26}$$

They conclude that the extension of an EoS to lower reduced temperatures and heavy hydrocarbons is possible by using this new generalized alpha function.

Lately, with improvement in computer science, genetic algorithms and artificial neural networks gain attraction. Osman et. al. (2001) developed an artificial neural network model by using 803 published data sets from many fields for predicting B_{ob}. Gharbi and Elsharkawy (1999) present a model based on artificial neural network, which is more successful to predict PVT behavior than correlations in use. In the study of Sınayuc and Gumrah (2004), difference minimization between equilibrium ratios, obtained by the evaluation of constant volume depletion experiment and by Peng - Robinson EoS, are used by a Genetic Algorithm for the determination of critical properties of plus fractions.

2.4. LUMPING PROCEDURE

Reservoir fluid contains too many components. Those should be lumped in order to make the calculations in a shorter time. Joergensen and Stenby (1995) studied on the compositions, by aiming to formulate the generalized rules for pseudoization. Their twelve lumping approaches could not perform better than each other. Rastegar and Jessen (2009) proposed a flow based lumping scheme and they concluded that the displacement characteristics and phase behavior are predicted very accurately. In the study of Alavian, Whitson and Martinsen (2014), a pseudoization method was proposed for the description of flow processes such as the depletion and the surface processing.

2.5. CORRELATIONS OF CRITICAL PROPERTIES

Critical properties such as critical temperature, T_c, and pressure, P_c, and acentric factor, ω, are requirements for almost all equations of state. Although these values are known for pure components, critical properties of plus fractions are not known. Correlations to determine the critical properties attract many authors

(Edmister, 1958; Katz and Firoozabadi, 1978; Riazi and Daubert, 1987; Whitson, 1983; Sancet, 2007; Pedersen et. al., 1992).

2.5.1. Edmister (1958) Correlation

Edmister's correlation for acentric factor has a simple form and it is a function of critical pressure and temperature and normal boiling point. Correlation is given in Eq. 27:

$$\omega = \frac{3[\log\left(\frac{P_c}{14.70}\right)]}{7[\frac{T_C}{T_b}-1]} - 1 \qquad (27)$$

2.5.2. Sancet (2007) Correlation

A correlation set to determine critical properties as a function of molecular weight of plus fraction is proposed. Normal boiling point temperature is correlated with critical temperature by using Reid's (Reid, 1987) data set. It is claimed that very good density agreements are achieved with compositional simulators when there are heavy hydrocarbons present in the fluid. The equations are as follows:

$$P_C\,[\text{psia}] = 82.82 + 653\ e^{-0.007427\text{MW}} \qquad (28)$$

$$T_C[R] = -778.5 + 383.5\ln(\text{MW} - 4.075) \qquad (29)$$

$$T_b[R] = 194 + 0.001241\ (T_C[R])^{1.869} \qquad (30)$$

2.5.3. Pedersen et. al. (1992) Correlation

Paraffinic - naphthenic and aromatic (PNA) compounds affect density therefore, density should be included into property correlations. They correlate T_c in K, P_c in atm and ω of a fraction with molecular weight in g/mol and density in g/cm^3 as given below (Pedersen et. al., 1992):

$$T_C = c_1\rho + c_2 \ln MW + c_3 MW + \frac{c_4}{MW}$$

(31)

$$\ln P_c = d_1 + d_2\rho^{d_5} + \frac{d_3}{MW} + \frac{d_4}{MW^2} \quad (32)$$

$$m = e_1 + e_2 MW + e_3\rho + e_4 MW^2 \quad (33)$$

m is a function of acentric factor and correlations of m are given below according to SRK EoS and PR EoS, respectively.

$$m = 0.480 + 1.574\omega - 0.176\omega^2 \quad (34)$$

$$m = 0.37464 + 1.54226\omega - 0.26992\omega^2 \quad (35)$$

2.5.4. Riazi - Daubert (1987) Correlation

According to Riazi and Daubert, critical properties are correlated with molecular weight and specific gravity. They propose the same type equation except coefficients as in Eq. 36:

$$\theta = aMW^b\, SG^c \exp[dMW + eSG + f(MW - SG)] \quad (36)$$

where

θ is physical property,

For T_c, a = 544.4, b = 0.2998, c = 1.055,
d = -0.00013478, e = -0.61641 and f = 0.0,

For P_c, a = 45203, b = -0.8063, c = 1.6015,
d = -0.0018078, e = -0.3084 and f = 0.0 and

For T_b, a = 6.77857, b = 0.401673, c = -1.58262,
d = 0.00377409, e = 2.984036 and f = -0.004252888

2.5.5. Katz and Firoozabadi (1978) Correlation

Normal boiling point temperature range in the study of Bergman et. al. (1975) was extended up to 500 °C with the addition of the data from the studies of Hoffmann et. al. (1953) and Evans and Harris (1956). It is suggested that interaction coefficient of last fraction is correlated with boiling point temperature.

2.6. VISCOSITY MODELS

2.6.1. Corresponding States (CSP) Theory

According to Pedersen et. al. (2015), a property of a component is in a relationship with the same property of a reference material in a corresponding state. The fluids are in corresponding states when any two of variable reduced parameters, reduced temperature, reduced pressure and reduced specific volume, have the same value. Any reduced parameters, which can be calculated from PVT data, will be the same, if fluids behave this law. Phase and temperature change the applicability of the law. Smoothing and correlating experimental data on hydrocarbon and generalized liquid and gas phase correlations are the main usage areas of the corresponding states law (Archer and Wall, 1986).

The expression of corresponding states theory on viscosity is that the same reduced viscosity (η_r) is achieved when two components are at the same reduced temperature (T_r) and pressure (P_r) and if the relation among these parameters are known for a component in the mixture, the viscosity of other components in the mixture at any pressure and temperature can be calculated (Lindeloff et. al. 2004).

2.6.2. Lohrenz - Bray - Clark (LBC) Viscosity Model

Phase viscosities are a fourth degree polynom in terms of reduced density (Lohrenz et. al. 1964).

$$[(\mu - \mu^*)\xi + 10^{-4}]^{1/4} = a_1 + a_2\rho_r + a_3\rho_r^2 + a_4\rho_r^3 + a_5\rho_r^4 \qquad (37)$$

where

a_1 = 0.1023, a_2 = 0.023364, a_3 = 0.058533, a_4 = - 0.040758 and a_5 = 0.0093324
Viscosity reducing parameter, ξ, is given as:

$$\xi = [\sum_{i=1}^{N} z_i T_{ci}]^{1/6} [\sum_{i=1}^{N} z_i MW_i]^{-1/2} [\sum_{i=1}^{N} z_i P_{ci}]^{-2/3} \qquad (38)$$

2.6.3. Comparison of CSP and LBC Viscosity Models

Pedersen et. al. (2015) state that, heavy oils with viscosities more than 10 cP are not suitable for classical Corresponding States Model, however the study of Lindeloff et. al. (2004) about averaging the Corresponding States Model and heavy oil correlation provide an advantage for heavy oils.

According to Yang et. al. (2007), Lohrenz - Bray - Clark viscosity model is widely used in the industry; however the mixture density and the critical volumes of heavy fractions highly effect the LBC correlation. In addition to this, tuning of the critical volumes and coefficients of the correlation to match the experimental data is a necessary and not straight-forward process. Also, it is reported that, LBC model predicts oil viscosity poorly.

2.7. PVT EXPERIMENTS

PVT experiments are conducted to determine the phase and volumetric behavior of reservoir fluids. The experiments start with the sampling of the fluid. Experimental studies consist of Constant Composition Expansion Experiment (CCE), Flash Experiment, Compositional Analysis of gas and oil, Viscosity Experiment, Constant Volume Depletion (CVD) Experiment, Differential Liberation (DL) Experiment and multi-stage Separator Experiment.

2.7.1. Fluid Sampling

Fluid samples are obtained in three ways: (1) Bottom hole sampling, (2) Surface sampling and (3) Wireline sampling. According to Bon et. al. (2006), the reasons of the fluid sampling includes:

- The determination of PVT properties,
- The evaluation of the economic value of the reservoir with respect to the composition of reservoir fluid,
- Having an understanding of the contaminants (sulphur compounds, the corrosiveness etc.) in the reservoir fluid for further plans and
- The determination of fluid flow ability for tubing and well design, and the risk of flow assurance problems.

Lawrence et. al. (2008) state that, no production of water, obtaining the expected GOR, high productivity index that provides steady flow by preventing the heading and staying away from Gas-Oil Contact (GOC) and Oil-Water Contact (OWC) should be considered for sampling.

2.7.1.1. Bottom Hole Sampling

To get a representative fluid sample from the well, it is important to perform well conditioning initially and the well shut-in time should be long enough to have complete build-up. Also, before shut-in period, the well should produce enough until reservoir fluid, which does not contain acid and drilling fluid, is observed. Shut in period is followed by pressure gradient survey to determine gas, oil and water columns and contacts such as Oil - Water Contact (OWC) within the well. Pressure gradient survey shows pressures with respect to depth. From pressure gradients, one can easily determine contacts. Bottom hole sample is taken from the oil column, preferentially deeper sections. Bottom hole sample is transferred into the sample tube in a higher pressure than its expected bubble point pressure (P_b).

2.7.1.2. Surface Sampling

Surface samples are taken from the separator and the wellhead. Bon et. al. (2006) states that, while sampling from the separator, flow should be at constant pressure, temperature and GOR. The pressure, temperature and flow rates should be noted very accurately. Even if the well conditioning and the sampling are very well, incorrect GOR to recombine the gas and the oil will result in unrepresentative reservoir fluid. Well head sampling is usually applied to gases. Van Orsdal (1990) reports that, when sampling the gas, no allowance to cool should be taken into consideration to prevent condensation.

2.7.1.3. Wireline Sampling

Recently, wireline sampling is getting more attraction in the industry. Michaels, Moody and Shwe (1995) state that, Wireline Formation Testers (WFT) makes pressure survey along the well and sample the reservoir fluid according to the pressure. According to Bon et. al. (2006), WFT are used in open hole wells and they insert a probe into the selected section of the formation. The fluid is allowed to flow into the probe. Virgin sample, in terms of any flow and drawdown in the reservoir, is taken. Canas et. al. (2005) recommends some practices to reduce the cleanup time and the contamination. These recommendations are about WFT tool selection, sampling level and flow rate selection as per formation stability, the invasion depth, viscosity ratio, anisotropy in permeability and the distance to the top sealing boundary.

2.7.2. Constant Composition Expansion (CCE) Experiment

Transferring is done under laboratory temperature and high pressure and then, system is heated to T_{res}. The volume expansion with respect to heating is evaluated as Thermal Expansion Factor (TEF). After temperature equilibrium is achieved, pressure is decreased gradually and in each step, the equilibrium is waited to occur. Schematic of the experiment is shown in Figure 2.6.

Bubble point pressure (P_b) may be observed visually and calculated volumetrically from pressure versus volume data. Since the compressibility of liquid phase is much less than gas phase compressibility, volume of the sample increases in higher amounts after bubble point pressure. As a result of the experiment, relative volumes, bubble point pressure, oil compressibility and oil densities are obtained.

Adepoju (2006) states that the isothermal oil compressibility seems constant except for the pressures close to P_b.

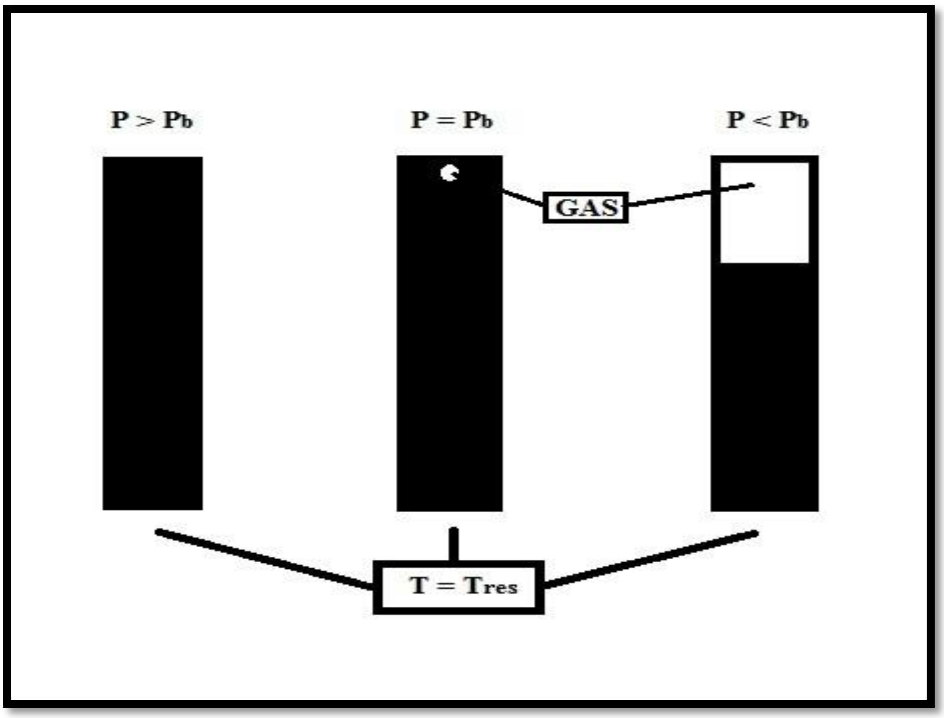

Figure 2.6 Schematic of a CCE Experiment for oil

2.7.3. 0-Flash Experiment

Flashing process in the laboratory is similar to production in the field. PVT cell is set to reservoir temperature and high enough pressure to keep fluid as single phase. Gasometer is connected to the PVT cell with line and the condition of this cell is set to laboratory conditions. A flask is connected to the line to collect oil at atmospheric conditions. Then, the flow from PVT cell to gasometer is allowed. During the flow, pressure of the PVT cell is kept constant by using the piston.

Gas - Oil ratio (GOR) is calculated by dividing the gas volume in the Gasometer to the oil volume in the flask. Produced fluid volume in the PVT cell and collected oil volume in the flask are used to calculate oil formation volume factors (B_o). To calculate B_o at different stages, relative volumes are used. API gravity of oil is also, measured by using collected oil samples.

The experiment is conducted only for one pressure step of the PVT cell and this pressure is defined as system pressure.

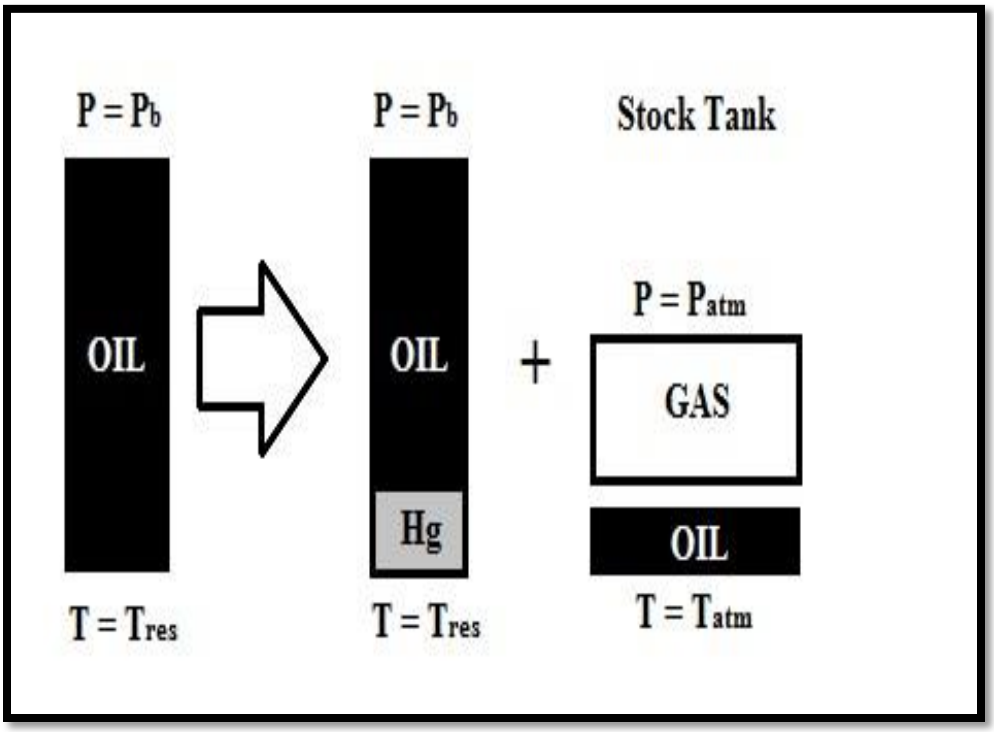

Figure 2.7 Schematic of a 0-Flash Experiment for oil

2.7.4. Differential Liberation (DL) Experiment

Apart from the experiments above, Differential Liberation (DL) Experiment is commonly conducted in the industry for black oil samples. In this experiment, the cell pressure is decreased below the bubble point pressure and as a result, two phases in the system occur. After equilibrium is achieved at constant pressure and temperature, gas is bled out to the separator conditions. Schematic of the experiment is shown in Figure 2.8. Solution GOR, oil and gas FVF, Z factor and specific gravity of gas are achieved for each step.

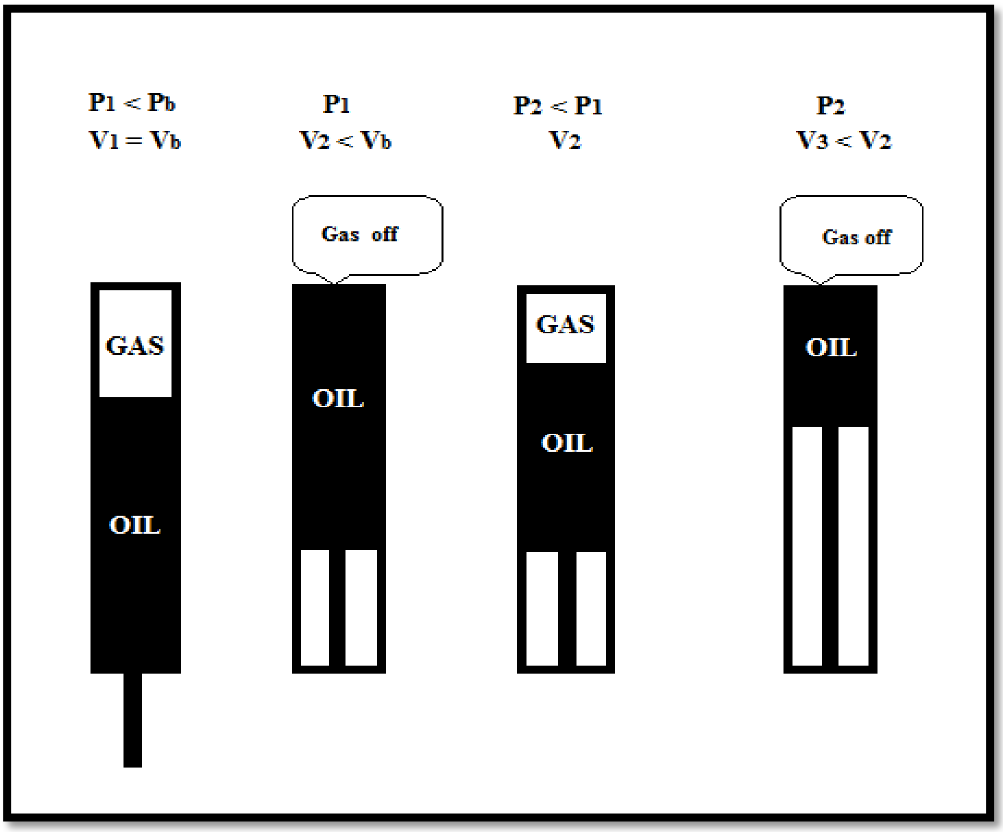

Figure 2.8 Schematic of a DL Experiment for oil

Al-Marhoun (2003) recommends a method for adjusting the DL data to separator conditions. The fluid flow in the reservoir can not be defined as differential liberation or flash liberation process. The method is based on the fact that, the same oil relative density at reservoir conditions should be obtained from the differential liberation and flash liberation experiments.

2.7.5. Constant Volume Depletion (CVD) Experiment

As in CCE experiment, fluid is transferred into the PVT cell. However, a valve on top of the cell should be equipped to remove the gas. The experiment starts at the bubble point pressure. Then, the volume of the sample is increased. The volume of the sample is decreased to the volume at P_b, by removing the gas from the top valve. The volume is increased again and then, depleted to V_b. Schematic of the experiment is presented in Figure 2.9. In each stage, molar composition of the depleted gas, molar amount of gas depleted as a percentage of gas initially in the cell, the liquid volume as a percentage of the volume at P_b and the compressibility factor are determined.

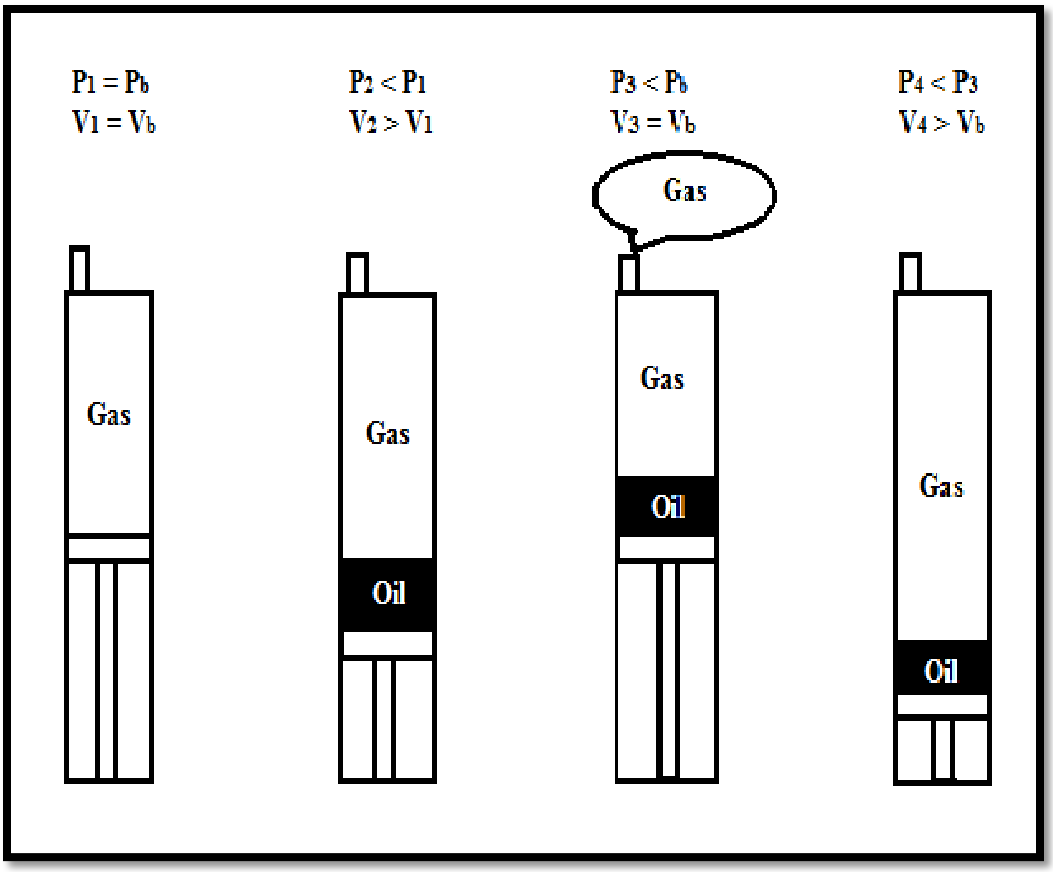

Figure 2.9 Schematic of a CVD Experiment for gas

Imo-Jack and Emelle (2013) present an analytical approach to quality check the CVD material balance and they conclude that, the CVD material balance can be backward or forward. However, widely-used forward material balance is affected from the errors in composition than the backward material balance application.

2.7.6. Multi-Stage Separator Experiment

The aim of the Multi-Stage Separator experiment is to determine the optimum separator conditions. The reservoir fluid is transferred into the PVT cell under reservoir temperature. Then, it is flashed through laboratory multistage separators. The experiment is repeated for different separator conditions in order to determine the optimum conditions. In the last stage, separator oil is flashed to atmospheric conditions. Schematic of the experiment is presented in Figure 2.10.

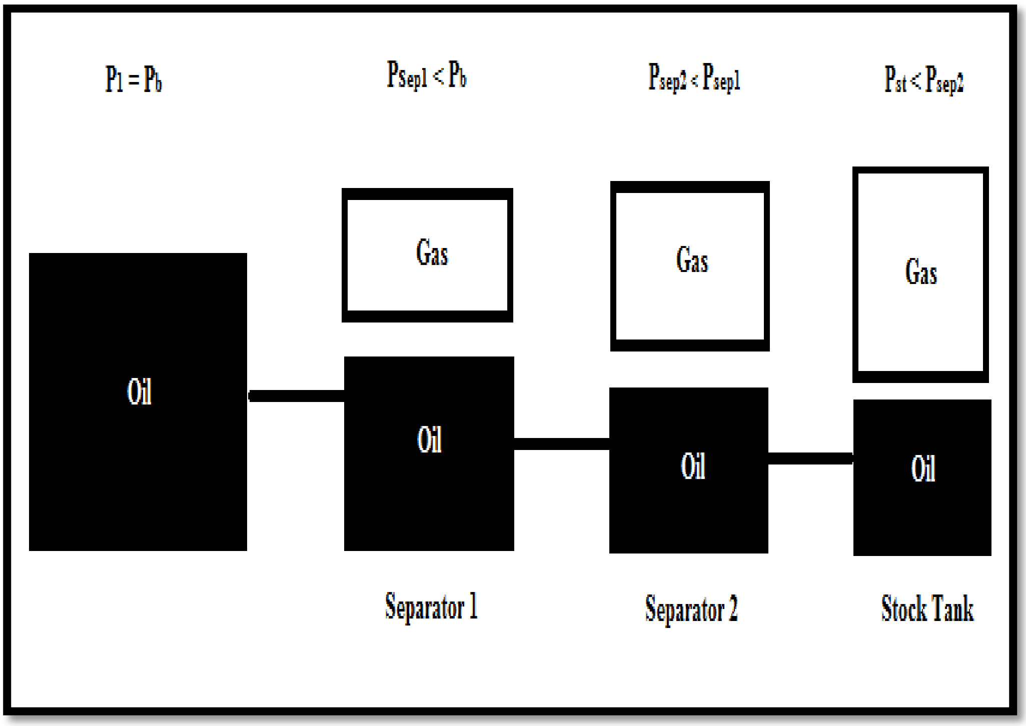

Figure 2.10 Schematic of Multi-Stage Separator Experiment for oil

In the study of Ling et. al. (2013), a method is presented to estimate the optimum separator pressure, using EoS to calculate the liquid and gas compositions in the separator and stock tank conditions. In case where the experiment can not be conducted, the proposed method can be used to determine the optimum pressures. Also, the method can be updated according to changes in the composition of well stream.

2.7.7. Viscosity Experiment

Viscosity of fluid sample is measured at reservoir temperature and different pressure steps starting from above bubble point pressure and oil viscosity is calculated as a function of pressure. Below bubble point pressure, the cell pressure is decreased to measurement point. Then, the solution gas is bled out. After that, cell pressure is increased, in order to achieve single phase fluid. In single phase conditions and at different pressure stages, viscosity is recorded. By extrapolating these viscosities against pressure values, the viscosity at measurement pressure is calculated. This procedure is repeated for every measurement points below bubble point pressure.

In the study of Ashrafi et. al. (2011), the viscosity measurement of Athabasca bitumen is presented. The experiment is conducted with a rotational viscometer up to 300 °C.

2.7.8. Compositional Analysis

For compositional analysis, Gas Chromatograph (GC) is used. A GC, for the separation and analysis of components, usually consists of a capillary column, an oven, a detector, a sample injector, a carrier gas inlet and a vent. Carrier gas (the mobile phase) is usually an inert gas such as helium. The stationary phase is liquid. The gases to be analyzed interact with the stationary phase. Each component reacts within a different time and this time is called as retention time. The retention time is used to analyze the component by Gas Chromatograph. Schematic of a GC is given in Figure 2.11.

Gas chromatographs are widely used in petroleum industry to analyze the oil and gas compositions. In the study of Elias and Gelin (2015), several bitumen extracts of Vaca Muerta Unconventional Shales were analyzed by using different types Gas Chromatographs.

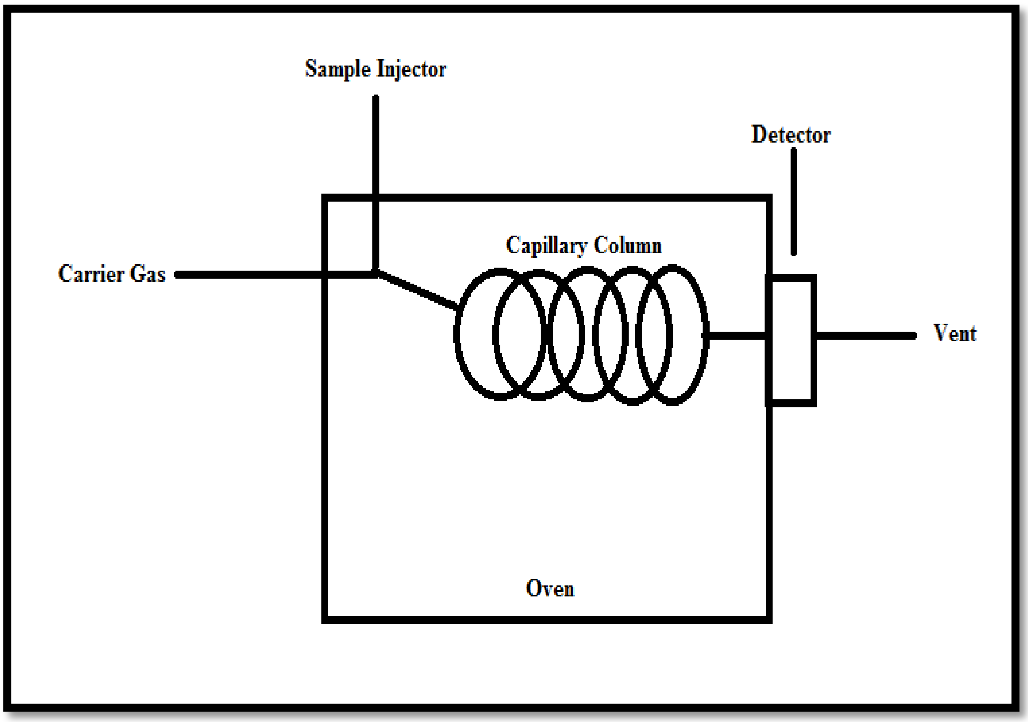

Figure 2.11 Schematic of a Gas Chromatograph

In the paper of Burke et. al. (1991), for the determination of the extended compositional analysis of live oil, a gas chromatographic method is presented. The analysis of the live oil contains the gases such as nitrogen, carbon dioxide, hydrogen sulfide and the hydrocarbons between C1 and C18.

CHAPTER 3

STATEMENT OF THE PROBLEM

Pressure - Volume - Temperature (PVT) properties of oil samples are very important to determine quality and quantity of reservoir. However, due to the abundance of heavy fractions, characterization of black oil samples is difficult to estimate. Most of Turkish oils are classified as black oil, but they have lower Gas - Oil Ratio (GOR) than usual black oils. This situation makes characterization of black oil samples in Turkey harder.

The main objective of this study is therefore to determine a methodology for the characterization of the low GOR black oil samples. In order to achieve this main aim, PVT properties of black oil samples in Turkey are investigated. Different equations of state, pseudoization schemes and correlations to predict the critical properties of plus fractions are used and their effects are investigated. Reliability of equations of states models is measured by comparing experimental and simulational oil formation volume factor values at bubble point pressure.

CHAPTER 4

METHODOLOGY

In this thesis, studies are divided into two groups as experimental and simulational studies.

4.1. EXPERIMENTAL PROCEDURE

PVT experiments start with an appropriate reservoir fluid sampling. For the well conditioning before sampling, wells are shut-in and the fluid level is monitored. Constant or nearly constant level of the fluid is required for the sampling. Bottom hole samples are taken from each of the wells. The depth, at which the sample should be taken, is determined through pressure gradient survey. The sampling depths are chosen within the oil column.

Experimental studies consist of Constant Composition Expansion Experiment (CCE), Flash Experiment, Compositional Analysis of gas and oil and Viscosity Experiment. PVT tests are conducted on original bottom hole sample under reservoir temperature (T_{res}) for each well. Due to low GOR and P_b, Differential Liberation Experiment and multi-stage Separator Experiment could not be conducted. The study consists of 4 black oil samples from Turkey.

During the experiments, Fluid Eval® (Standard Version), Automated Gasometer®, EV 1000® and Hydrocarbon Compositional Analyser® of VINCI Technologies© are used. Technical specifications and other details about the instruments are provided in APPENDIX A.

4.2. PVT SIMULATION STUDY

In the industry, PVT experiments are validated with commercial compositional simulators. Also, the experiments, which are difficult to conduct in laboratory, are calculated by simulators. However, experimental and simulated results are typically different from each other, so regression to experimental data and EOS tuning is highly applied. In this study, Calsep's PVTsim Compositional Simulator is used. Initially, gas and oil compositions are combined according to GOR and oil density.

To investigate the effect of pseudoization, three lumping scenarios are done. In the first scenario, they are recombined and the heavier fractions than C7+ are lumped together. For the second scenario, C10+ components are lumped together and for the last one, C20+ components are lumped as one pseudo component. After that, Christensen's (1999) regression procedure is taken into account:

- To adjust the MW of plus fraction in the range of ± 10%, by making regression to experimental P_b.

- To adjust the volume translation parameter (C_{pen}) of the lumped components in the range of ± 100%, by making regression to experimental density data.

- To adjust two of the critical temperature, the critical pressure and acentric factor of lumped components in the range of ± 20%, by making regression to experimental density data.

Critical properties and acentric factor of plus fraction are directly found from Pedersen et.al.'s correlations, which are the functions of molecular weight of plus fraction and liquid density. For Pedersen et. al.'s correlation, boiling point temperature for plus fraction is calculated from Katz and Firoozabadi’s correlation.

In this study, Soave-Redlich-Kwong (SRK) and Peng-Robinson (PR) Equations of State with their Peneloux corrections are used. Oil viscosity against pressure is another input to the simulator. Corresponding States Method (CSP) is used in our study. In PVTsim, methane is used as reference material for this viscosity model. During the EOS tuning, CSP coefficients are also adjusted in the last step.

Critical properties of plus fractions are determined not only by using Pedersen et. al.’s equations, but also by using Sancet’s correlations for T_c, P_c and T_b and Edmister’s correlation for acentric factor, ω. The reason of using two different sets of correlations is to determine the effect of critical properties of plus fractions. The calculated critical properties are also, used in the simulator and they are regressed in the same amount as stated in Christensen’s procedure above.

In order to measure reliability of compositional simulation, after each simulation, simulated oil formation volume factors at bubble point pressure (B_{ob}) are compared to experimental results. This comparison is done, by using B_{ob} values, because those are not used in the simulation before. The used formula for the comparison is as following:

$$\text{Relative Error (\%)} = \left[\frac{\text{Simulated } B_{ob} - \text{Experimental } B_{ob}}{\text{Experimental } B_{ob}}\right] \text{x}100 \qquad (39)$$

CHAPTER 5

RESULTS AND DISCUSSIONS

5.1. INTRODUCTION

The aim of this study is the characterization of heavy oil plus fractions. In order to reach the aim, laboratory PVT studies are conducted and the results of experiments are used in the simulation studies. The live oil samples, used in this study, are from Well B60, Well DS1, Well E2 and Well BSS1. None of the samples are taken from the same field. In this section, first of all, the results of laboratory studies are given and then simulation results are presented.

5.2. LABORATORY STUDIES

For each well, after sampling from the well, routine PVT analyses are conducted. It should be noted that routine analyses include Constant Composition Experiment (CCE), 0 – Flash Experiment, Compositional Analysis and Viscosity Analysis (See Chapter 2.7 for details of the analyses).

5.2.1. Well B60 Sample

Bottom hole oil sample of Well B60 is taken at 1386 meters depth. Before sampling, for static conditioning, approximately 4 days shut – in period is maintained. Oil column in the static well is determined through pressure gradient survey. Sample is transferred at 3000 psig of pressure, which is assumed to be much higher than the bubble point pressure (P_b). Then, sample is transferred into the PVT cell and the temperature Tres is set to 137 °F. In the following table, Table 5.1, the result of CCE experiment is given. It should be repeated that P_b is determined both visually and volumetrically and it is found as 90.5 psig.

Then, pressure is set back to 3000 psig and gas in the cell is let to dissolve in the oil phase. The next experiment, 0 – Flash experiment (See Chapter 2.7.3) can be thought as simulation of production to the stock tank conditions. Pressure and temperature of gasometer, where the collected gas is deposited, is set to atmospheric conditions at that time. By opening the valve, connected to the cell, slowly, oil and gas dissolved in the oil are produced. Cell pressure is always kept constant during the experiment. Results of the experiment are given in Table 5.2.

Table 5.1 CCE Results for Well B60 Sample

Pressure (psig)	Relative Volume (V_i/V_b)	Oil Compressibility (1/psi) 10^{-6}	Oil Density (g/cc)
3000	0.9797		0.8335
2500	0.9828	6.3530	0.8309
2000	0.9859	6.6559	0.8282
1500	0.9893	6.9642	0.8254
1000	0.9928	7.0138	0.8225
750	0.9946	7.1302	0.8210
500	0.9963	7.3712	0.8196
250	0.9982	7.6013	0.8180
200	0.9986	8.1143	0.8177
150	0.9990	9.3142	0.8173
125	0.9993	13.9674	0.8171
100	0.9997	19.8268	0.8168
90.5	**1.0000**		**0.8166**

Table 5.2 Flash Experiment Results for Well B60 Sample

System Pressure (psig)	3000
System Temperature (°F)	137
Stock Tank Pressure (psi)	13.30
Stock Tank Temperature (°F)	72.3
Stock Tank Oil Gravity (API)	33.7
Stock Tank Gas Gravity	0.83
Gas – Oil Ratio (scf/STB)	22.38
Oil FVF @ P_b (bbl/STB)	1.0527

Next experiment, conducted on the bottom hole sample, is viscosity experiment at reservoir temperature. The result of the experiment is given below.

Table 5.3 Viscosity Experiment Result for Well B60 Sample

Pressure (psig)	Oil Viscosity (cP)
3000	3.762
2500	3.576
2000	3.401
1500	3.235
1000	3.068
500	2.908
250	2.831
150	2.804
100	2.787
90.5	**2.772**
75	2.799
50	2.824
0	2.891

Lastly, compositional analysis of gas, collected in the gasometer after flash experiment, and dead oil are performed using Gas Chromatography. The highest nitrogen mole percentage is seen in the gas composition of this well among all wells. Also, liquid gas chromatogram for Well B60 can be seen in APPENDIX B. Measured gas and oil compositions are presented in Table 5.4.

Table 5.4 Gas and Oil Compositions for B60 Well Sample

Comp.	Gas Mole, % mole	Oil Mole, % mole	Comp.	Gas Mole, % mole	Oil Mole, % mole
N_2	15.33	0.00	C17	0.00	1.70
CO_2	0.26	0.00	C18	0.00	2.62
C1	64.95	0.00	C19	0.00	0.27
C2	7.12	0.18	C20	0.00	0.32
C3	5.84	0.59	C21	0.00	0.88
iC4	0.19	0.42	C22	0.00	0.60
nC4	2.78	1.26	C23	0.00	0.48
iC5	1.51	2.15	C24	0.00	0.38
nC5	1.47	3.22	C25	0.00	0.27
C6	0.10	0.29	C26	0.00	0.31
C7	0.25	14.12	C27	0.00	0.19
C8	0.18	15.21	C28	0.00	0.15
C9	0.00	13.49	C29	0.00	0.21
C10	0.00	11.49	C30	0.00	0.13
C11	0.00	7.94	C31	0.00	0.09
C12	0.00	7.35	C32	0.00	0.07
C13	0.00	4.95	C33	0.00	0.05
C14	0.00	3.74	C34	0.00	0.04
C15	0.00	3.54	C35	0.00	0.03
C16	0.00	1.25	C36	0.00	0.04

5.2.2. Well DS1 Sample

Bottom hole sample for Well DS1 is taken at 1300 meters depth. Shut - in period is approximately 1 day and the pressure at sampling depth is about 1700 psig, which is much higher than the expected bubble point pressure, P_b. After transferring of the sample, PVT tests are conducted under T_{res} = 166 °F. CCE experiment results to determine P_b and single phase oil density, 0 - Flash experiment results to determine Gas – Oil Ratio (GOR) and B_{ob} and pressure - viscosity relationship are given in the following tables, Table 5.5, 5.6 and 5.7, respectively.

Table 5.5 CCE Results for Well DS1 Sample

Pressure (psig)	Relative Volume (V_i/V_b)	Oil Compressibility (1/psi) 10^{-6}	Oil Density (g/cc)
3000	0.9819		0.9082
2500	0.9847	5.7852	0.9056
2000	0.9876	5.9407	0.9029
1500	0.9905	6.1170	0.9002
1000	0.9936	6.3247	0.8974
750	0.9952	6.6676	0.8960
500	0.9969	6.7004	0.8944
250	0.9986	8.5122	0.8930
200	0.9995	10.7173	0.8922
175	0.9998		0.8919
155	**1.0000**		**0.8917**

Table 5.6 Flash Experiment Results for Well DS1 Sample

System Pressure (psig)	3000
System Temperature (°F)	166
Stock Tank Pressure (psi)	13.27
Stock Tank Temperature (°F)	78.8
Stock Tank Oil Gravity (API)	18.9
Stock Tank Gas Gravity	0.70
Gas – Oil Ratio (scf/STB)	20.65
Oil FVF @ P_b (bbl/STB)	1.0570

Table 5.7 Viscosity Experiment Result for Well DS1 Sample

Pressure (psig)	Oil Viscosity (cP)
3000	48.60
2500	46.21
2000	43.45
1500	40.88
1000	38.47
750	37.21
500	36.04
250	34.96
155	**34.48**
0	41.51

The compositions of collected gas and oil samples at the end of 0-Flash test are analyzed and given in Table 5.8. This well differs from the other wells with high mole percentage of methane (>80%) in gas composition and C20+ fractions (>25%) in oil composition.

Table 5.8 Gas and Oil Compositions for DS1 Well Sample

Comp.	Gas Mole, % mole	Oil Mole, % mole	Comp.	Gas Mole, % mole	Oil Mole, % mole
N_2	3.92	0.00	C17	0.00	2.01
CO_2	2.95	0.00	C18	0.00	2.34
C1	81.87	0.00	C19	0.00	0.71
C2	5.38	0.18	C20	0.00	0.88
C3	3.61	0.78	C21	0.00	1.04
iC4	0.67	0.40	C22	0.00	0.85
nC4	1.23	1.65	C23	0.00	0.94
iC5	0.00	1.50	C24	0.00	1.93
nC5	0.00	2.21	C25	0.00	2.84
C6	0.23	5.34	C26	0.00	3.40
C7	0.08	6.06	C27	0.00	4.13
C8	0.04	8.71	C28	0.00	4.12
C9	0.01	6.88	C29	0.00	3.41
C10	0.00	8.63	C30	0.00	3.15
C11	0.00	5.64	C31	0.00	2.71
C12	0.00	4.33	C32	0.00	1.44
C13	0.00	3.03	C33	0.00	0.47
C14	0.00	2.55	C34	0.00	0.14
C15	0.00	3.02	C35	0.00	0.18
C16	0.00	1.96	C36	0.00	0.08

5.2.3. Well E2 Sample

Bottom hole sample was taken from this well at 2000 meters depth. The pressure, measured in this depth, is approximately 2200 psig and before sampling, the well was shut - in approximately 1 day to achieve static conditioning. According to laboratory PVT experiments, it is noted that bubble point pressure, P_b, is 276.5 psig, which is the highest P_b among all samples. CCE, 0 - Flash and viscosity experiment results, conducted in T_{res} = 203 °F, are given in Table 5.9, 5.10 and 5.11, respectively.

Table 5.9 CCE Results for Well E2 Sample

Pressure (psig)	Relative Volume (V_i/V_b)	Oil Compressibility (1/psi) 10^{-6}	Oil Density (g/cc)
3000	0.9772		0.8315
2500	0.9807	7.5488	0.8284
2000	0.9846	7.8713	0.8252
1500	0.9885	8.3051	0.8219
1000	0.9928	8.8223	0.8184
750	0.9951	9.2807	0.8165
500	0.9974	9.6417	0.8146
400	0.9984	10.5627	0.8138
325	0.9993	12.9498	0.8131
300	0.9997	15.3129	0.8127
276.5	**1.0000**		**0.8125**

Table 5.10 Flash Experiment Results for Well E2 Sample

System Pressure (psig)	3000
System Temperature (°F)	203
Stock Tank Pressure (psi)	13.25
Stock Tank Temperature (°F)	76.1
Stock Tank Oil Gravity (API)	28.6
Stock Tank Gas Gravity	0.82
Gas – Oil Ratio (scf/STB)	62.3
Oil FVF @ P_b (bbl/STB)	1.0632

Table 5.11 Viscosity Experiment Result for Well E2 Sample

Pressure (psig)	Oil Viscosity (cP)
3000	1.606
2500	1.520
2000	1.431
1500	1.351
1000	1.264
750	1.213
500	1.171
300	1.137
276.5	**1.132**
0	2.150

Lastly, compositional analyses are done for collected gas and oil samples. These gas and oil samples are obtained from 0 - Flash experiments. Absence of components up to C6 is the most important result in oil composition.

Table 5.12 Gas and Oil Compositions for Well E2 Sample

Comp.	Gas Mole, % mole	Oil Mole, % mole	Comp.	Gas Mole, % mole	Oil Mole, % mole
N_2	3.16	0.00	C17	0.00	1.99
CO_2	4.34	0.00	C18	0.00	2.18
C1	69.65	0.00	C19	0.00	1.11
C2	10.36	0.00	C20	0.00	1.54
C3	7.60	0.00	C21	0.00	2.18
iC4	2.01	0.00	C22	0.00	2.82
nC4	0.88	0.00	C23	0.00	2.82
iC5	0.44	0.00	C24	0.00	2.60
nC5	0.42	0.00	C25	0.00	2.53
C6	1.13	0.11	C26	0.00	2.72
C7	0.01	12.85	C27	0.00	2.88
C8	0.00	5.62	C28	0.00	2.52
C9	0.00	8.74	C29	0.00	2.00
C10	0.00	9.85	C30	0.00	1.99
C11	0.00	7.24	C31	0.00	1.53
C12	0.00	6.20	C32	0.00	1.01
C13	0.00	4.55	C33	0.00	0.42
C14	0.00	3.79	C34	0.00	0.06
C15	0.00	3.10	C35	0.00	0.04
C16	0.00	2.52	C36	0.00	0.03

5.2.4. Well BSS1 Sample

Bottom hole oil sample of this well is taken in 2000 meters depth and the pressure of this depth is 2523 psig. Well was shut - in about 1 day. Reservoir temperature, at which laboratory PVT analysis is conducted, is 234 °F. Below, results of CCE, 0 - Flash and Viscosity experiments are presented in Table 5.13, 5.14 and 5.15, respectively.

Table 5.13 CCE Results for Well BSS1 Sample

Pressure (psig)	Relative Volume (V_i/V_b)	Oil Compressibility (1/psi) 10^{-6}	Oil Density (g/cc)
3000	0.9742		0.8263
2500	0.9779	7.7600	0.8232
2000	0.9818	8.1633	0.8200
1500	0.9859	8.5616	0.8165
1000	0.9903	8.8007	0.8130
750	0.9925	9.1093	0.8112
250	0.9975	15.2237	0.8070
200	0.9983	19.1262	0.8064
180	0.9989	42.1203	0.8060
160	1.0000	51.2671	0.8051
158	**1.0000**		**0.8051**

Oil compressibilities near the bubble point pressure seem higher than the rest but, it is a typical behavior of oil compressibility.

Table 5.14 Flash Experiment Results for Well BSS1 Sample

System Pressure (psig)	3000
System Temperature (°F)	234
Stock Tank Pressure (psi)	13.25
Stock Tank Temperature (°F)	79.3
Stock Tank Oil Gravity (API)	30.5
Stock Tank Gas Gravity	0.84
Gas – Oil Ratio (scf/STB)	36.2
Oil FVF @ P_b (bbl/STB)	1.0937

Table 5.15 Viscosity Experiment Result for Well BSS1 Sample

Pressure (psig)	Oil Viscosity (cP)
3000	1.215
2500	1.145
2000	1.078
1500	1.015
1000	0.953
750	0.924
500	0.895
250	0.867
158	**0.860**
0	1.380

According to CCE result, P_b of this well is very close to P_b of Well DS1. However, pressure - density and pressure - viscosity relationships differ from Well DS1. Also, it should be noted that temperature of reservoir for Well BSS1 is the highest one among all wells. Below, gas and oil compositions of Well BSS1 are given.

Table 5.16 Gas and Oil Compositions for Well BSS1 Sample

Comp.	Gas Mole, % mole	Oil Mole, % mole	Comp.	Gas Mole, % mole	Oil Mole, % mole
N_2	1.99	0.00	C17	0.00	1.38
CO_2	11.29	0.00	C18	0.00	1.59
C1	66.98	0.00	C19	0.00	0.88
C2	9.16	0.16	C20	0.00	1.00
C3	7.02	0.87	C21	0.00	1.08
iC4	1.29	0.43	C22	0.00	1.75
nC4	2.13	2.09	C23	0.00	2.13
iC5	0.00	1.86	C24	0.00	2.05
nC5	0.00	3.11	C25	0.00	2.23
C6	0.02	7.27	C26	0.00	1.97
C7	0.07	7.94	C27	0.00	2.35
C8	0.02	8.32	C28	0.00	2.05
C9	0.00	8.71	C29	0.00	1.75
C10	0.00	8.75	C30	0.00	1.77
C11	0.00	5.98	C31	0.00	1.45
C12	0.00	5.17	C32	0.00	1.12
C13	0.00	3.39	C33	0.00	0.76
C14	0.00	2.99	C34	0.00	0.28
C15	0.00	2.39	C35	0.00	0.05
C16	0.00	2.07	C36	0.00	0.02

Low GOR black oils in Turkey, used in this study, have different density and viscosity values than each other. Although bubble point pressures and GOR of wells are different from each other, maximum bubble point pressure and GOR are 276.5 psig and 62.3 scf/STB, respectively. Density versus pressure relationships and viscosity versus pressure relationships of four wells are given below in Figure 5.1 and 5.2. While Well DS1 and BSS1 have very close bubble point pressures, they do not have close density and viscosity values. Moreover, samples with the lowest (Well B60) and the highest (Well E2) bubble point pressure do not have the lowest and the highest densities and viscosities, respectively. However, for Well B60, BSS1 and E2, density and viscosity values up to 3000 psig are between 0.80 and 0.84 g/cc and 0.8 and 3.8 cp, whereas density and viscosity values of Well DS1 are quite different than the other wells.

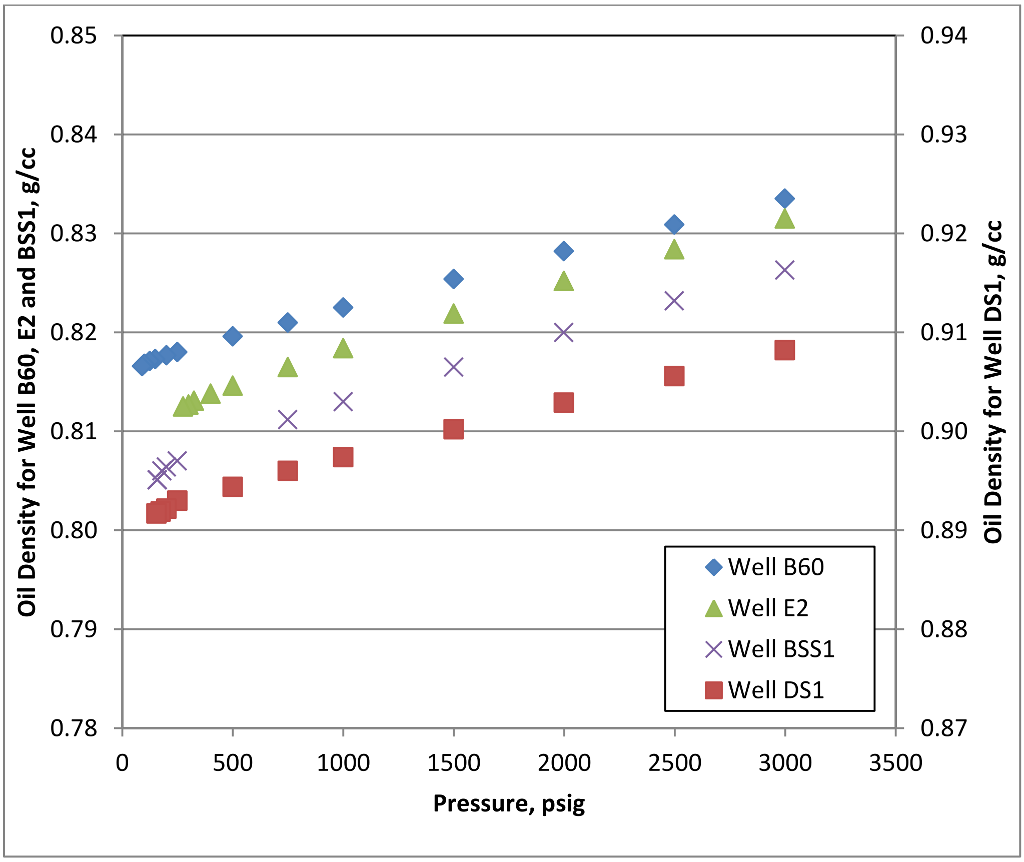

Figure 5.1 Pressure - Density Relationship for All Wells

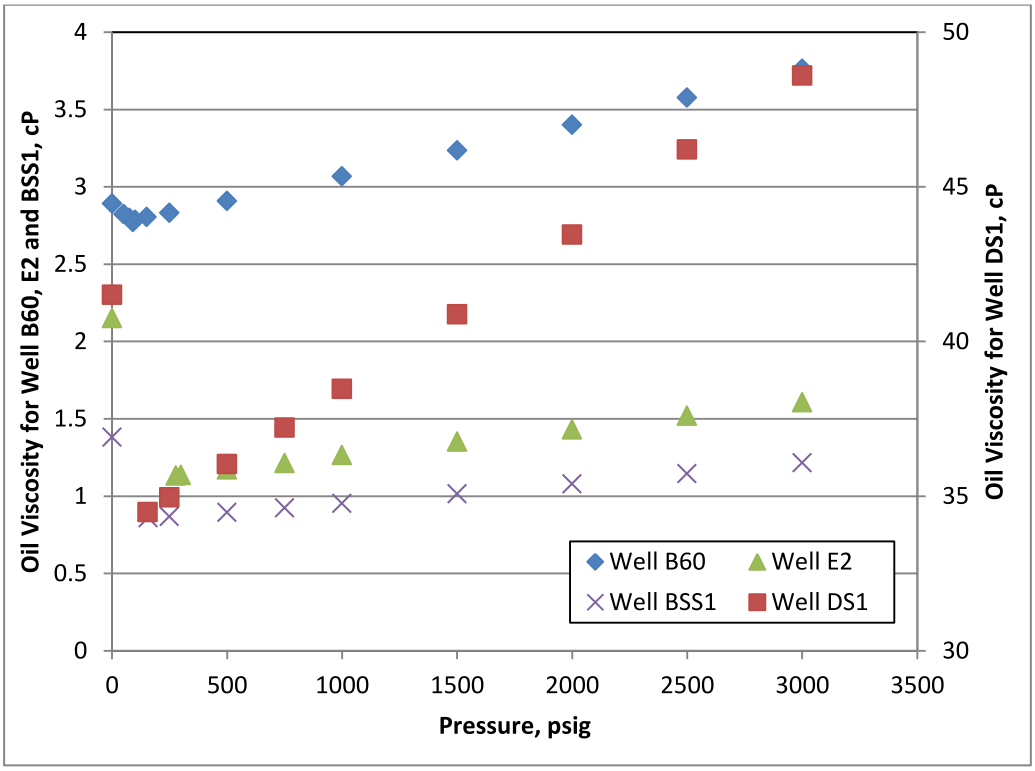

Figure 5.2 Pressure - Viscosity Relationship for All Wells

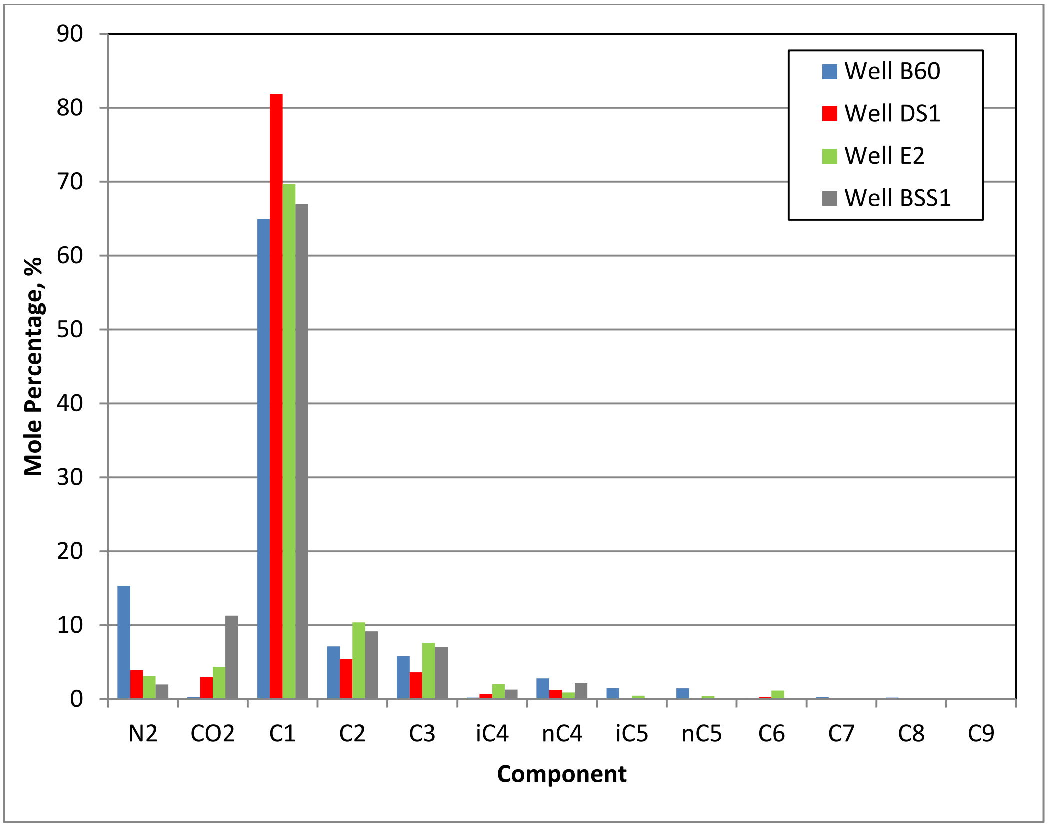

Figure 5.3 Gas Components for All Wells

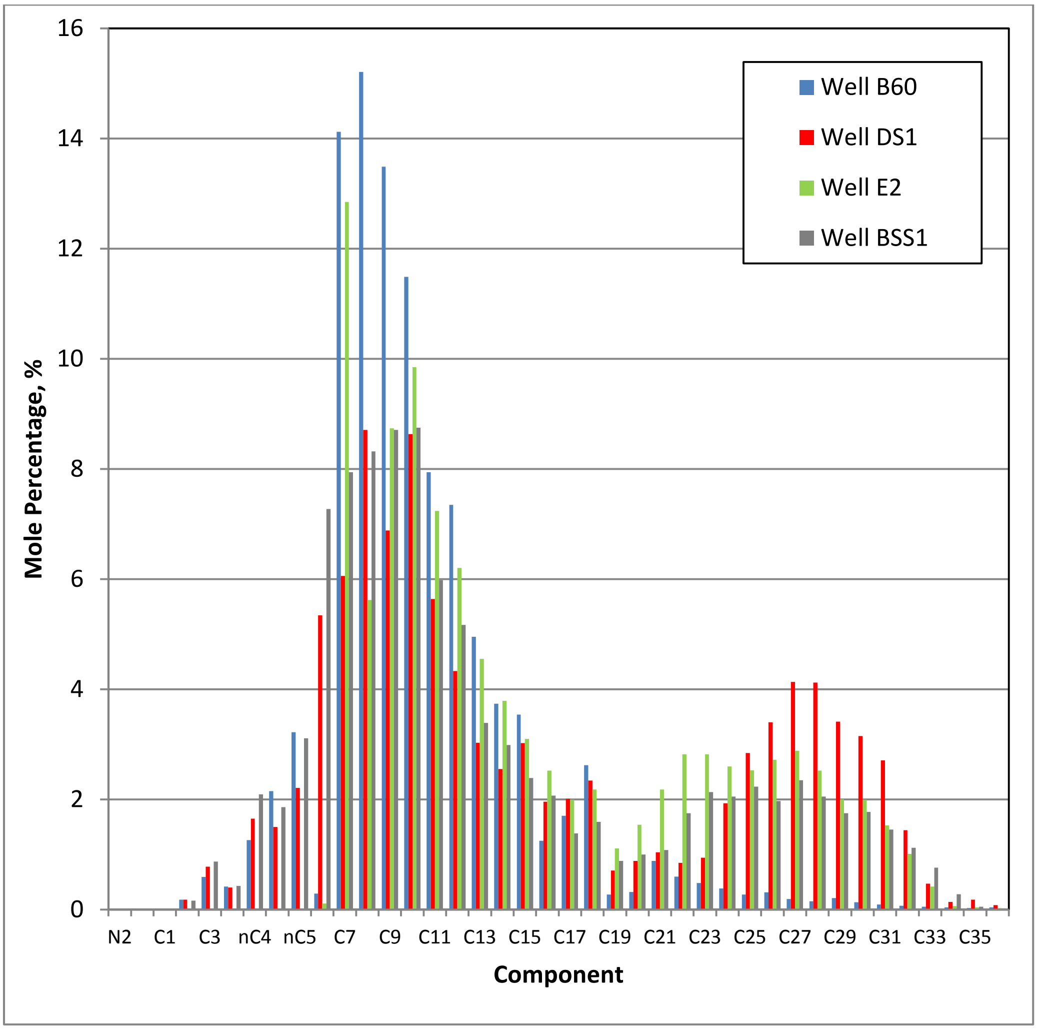

Figure 5.4 Oil Components for All Wells

As shown in Figure 5.3, gas of Well BSS1 contains more CO_2 than the rest of the wells. Also, it is observed that, gas of Well B60 contains the highest mole percentage of N_2 among all wells. In Figure 5.4 and 5.5, components in oil compositions of wells are presented. Oil components of wells become denser between C6 and C12. In addition, relatively high mole percentage of heavy components in oil composition may explain different behavior of Well DS1 in density and viscosity against pressure.

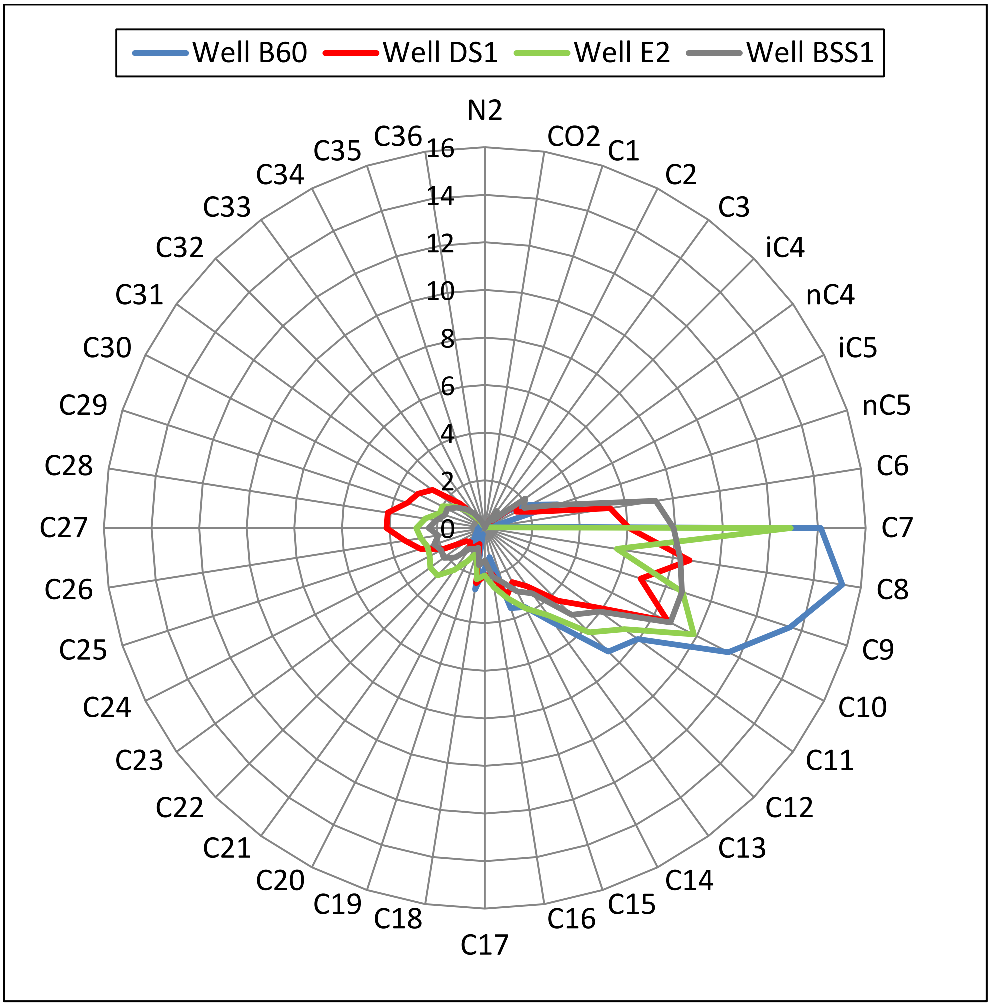

Figure 5.5 Radar Graph of Oil Components for All Wells

5.3. SIMULATION STUDIES

This section contains simulation studies, done on PVT data of bottom hole samples. The aim is to investigate the effect of Equation of State (EoS) Models, critical properties of plus fractions and the pseudoization on phase behavior. PVTsim software is used in this study. Main data required for the study is gas and oil compositions. Pressure vs. oil density relationship from CCE and pressure vs. oil viscosity from viscosity experiments are the other data, which are used in regression. Gas and oil compositions, CCE, 0 - Flash and viscosity results of Well B60, DS1, E2 and BSS1 are used in simulator and they are given in Laboratory Studies section above.

5.3.1. Well B60 Sample

The simulation study for this well starts with entering the oil and gas compositions into the compositional simulator. However, simulation studies are done on reservoir fluid composition instead of gas and oil compositions. In order to do that, these gas and oil compositions are recombined with respect to GOR = 22.38 scf/STB and stock tank oil density, ρ_{liquid} = 0.8555 g/cc, to obtain reservoir fluid composition. The recombined fluid composition is lumped as stated in Methodology Chapter. The reservoir fluid compositions of B60 Well for each scenario are given in Table 5.17. Estimated molecular weight, liquid density and critical properties of plus fractions are given in Table 5.18.

Table 5.17 Lumped Reservoir Fluid Compositions for Well B60 Sample

Comp.	C7+	C10+	C20+	Comp.	C7+	C10+	C20+
N_2	0.369	0.369	0.369	C9		12.788	12.788
CO_2	0.006	0.006	0.006	C10 **(C10+)**		**(46.832)**	10.045
C1	1.563	1.563	1.563	C11			7.890
C2	0.347	0.347	0.347	C12			6.198
C3	0.716	0.716	0.716	C13			4.869
iC4	0.424	0.424	0.424	C14			3.824
nC4	1.296	1.296	1.296	C15			3.004
iC5	2.134	2.134	2.134	C16			2.360
nC5	3.177	3.177	3.177	C17			1.854
C6	0.285	0.285	0.285	C18			1.456
C7 **(C7+)**	**(89.682)**	13.782	13.782	C19			1.144
C8		16.280	16.280	**C20+**			**4.188**

Table 5.18 Parameters of Plus Fractions for Well B60 Sample

Para.	SRK-Pen EoS			PR-Pen EoS		
	C7+	C10+	C20+	C7+	C10+	C20+
MW	148.449	185.788	327.126	148.449	185.788	327.126
ρ_{liquid}	0.8042	0.8324	0.9038	0.8042	0.8324	0.9038
T_c	673.271	743.246	958.584	700.508	781.702	1041.344
P_c	317.67	270.91	211.64	303.07	262.43	198.98
ω	0.6665	0.7526	1.0491	0.5679	0.6680	1.0111
C_{pen}	3.38E-5	4.30E-5	2.28E-5	2.46E-5	2.97E-5	2.33E-5

According to the first stage of Christensen's procedure, molecular weight of plus fractions should be adjusted to predict P_b better. In Table 5.19, adjusted molecular weights, liquid densities and newly-calculated critical properties can be seen.

Table 5.19 Parameters of Plus Fractions After MW Adjustment
for Well B60 Sample

Para.	SRK-Pen EoS			PR-Pen EoS		
	C7+	C10+	C20+	C7+	C10+	C20+
MW	133.605	167.210	294.417	154.402	204.369	359.854
ρ_{liquid}	0.8042	0.8324	0.9038	0.8042	0.8324	0.9038
T_c	636.056	700.643	907.493	725.588	835.637	1111.908
P_c	355.55	299.08	226.03	294.16	246.89	191.00
ω	0.613	0.689	0.977	0.600	0.737	1.066
C_{pen}	2.61E-5	3.35E-5	2.48E-5	2.68E-5	3.18E-5	1.65E-5

In the second stage of Christensen's procedure, the regression to input PVT data is done. Volume translation parameter, C_{pen}, and two of the critical properties (T_c, P_c and ω) are regressed by ± 100% and ± 20%, respectively. Also, viscosity coefficients of corresponding states viscosity model (CSP) are regressed with respect to pressure – viscosity data. Density predictions with respect to different pseudoization schemes are given in Figure 5.6, 5.7 and 5.8.

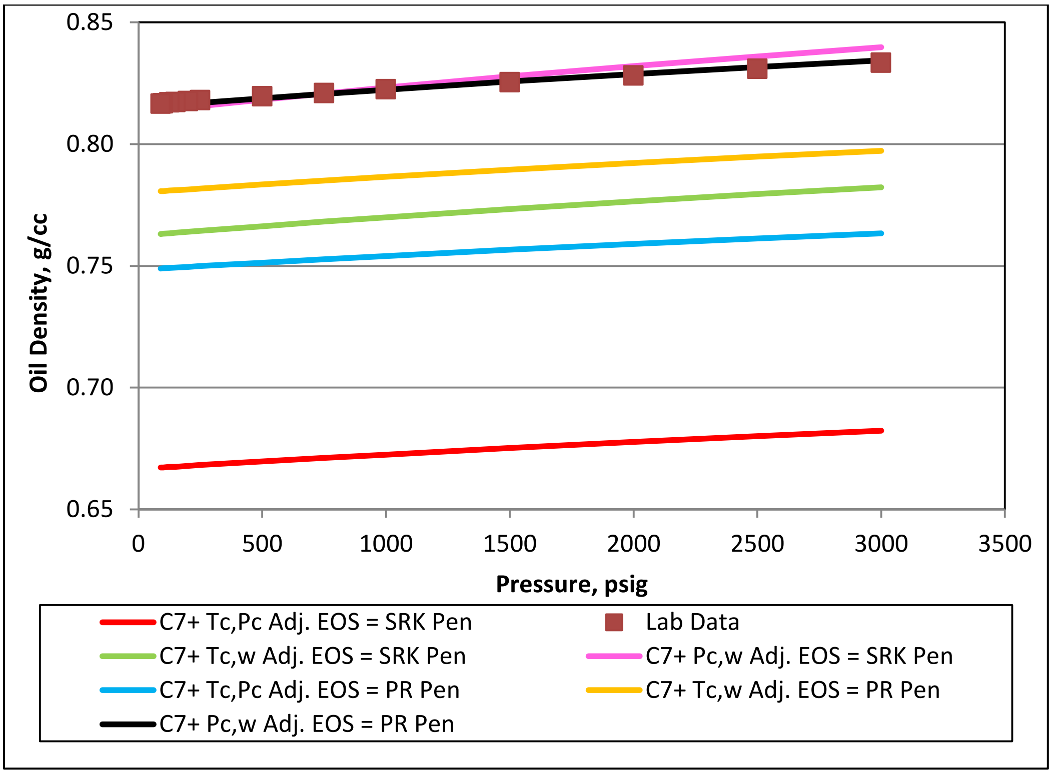

Figure 5.6 Pressure – Density Relationship for Well B60 Sample
(C7+ Adjustment)

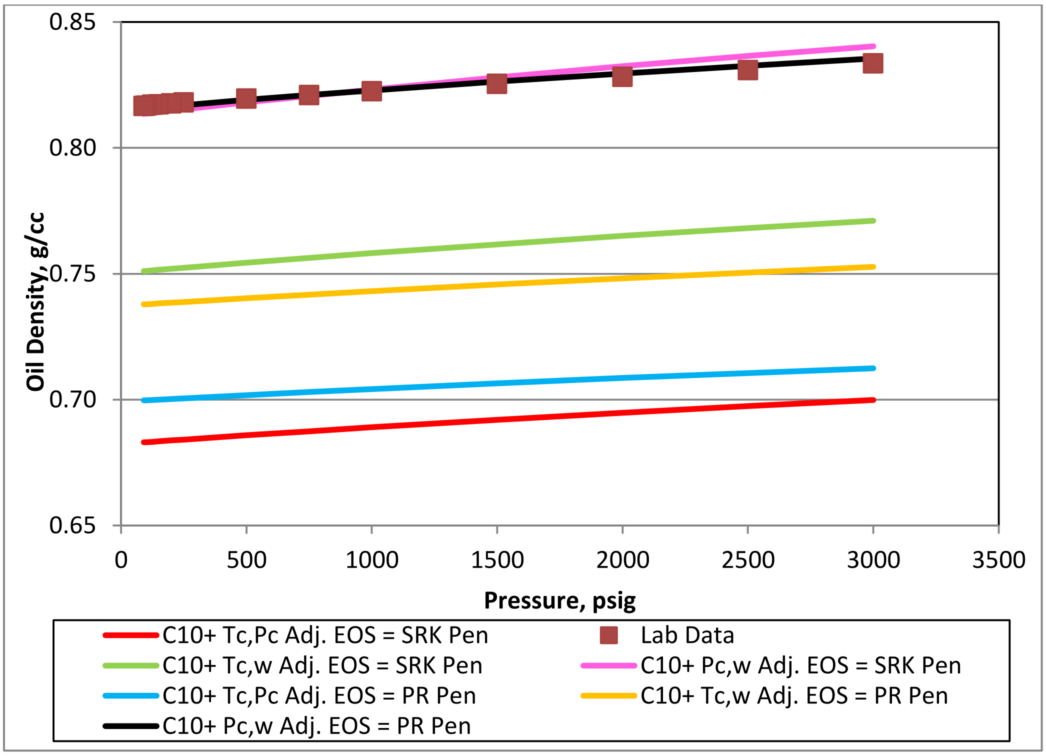

Figure 5.7 Pressure – Density Relationship for Well B60 Sample
(C10+ Adjustment)

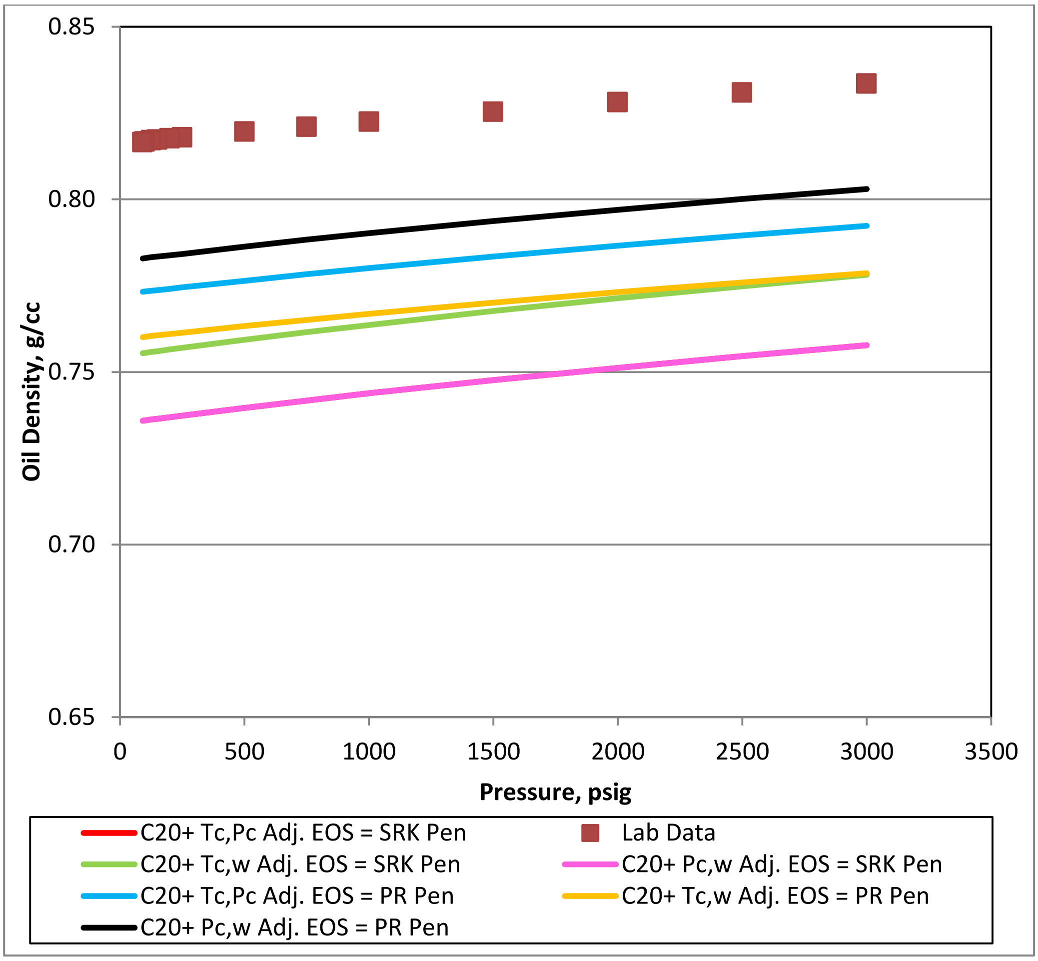

Figure 5.8 Pressure – Density Relationship for Well B60 Sample
(C20+ Adjustment)

From the plots of Pressure – Density curves above, it can be claimed that P_c and ω pair gives the best density predictions. Also, two adjustments, done on C7+ lumped compositions are very close to laboratory results. However, none of the adjustment, done on C20+ lumped compositions, is as close as those. In addition, P_c - ω pair for SRK - Pen EoS predicts density as bad as T_c - P_c pair for SRK - Pen EoS, when C20+ fractions are lumped. Density predictions of two adjustments, done on C10+ lumped compositions, are also very close to experimental data but, the rest of adjustments predicts less than the experimental values.

In this study, predictive ability of EoS models is also studied. Simulation starts with recombination with respect to GOR and then, MW of plus fractions are adjusted to match P_b. At the end of regression, last values of GOR and P_b can be seen in Figure 5.9 for SRK-Pen EoS and in Figure 5.10 for PR-Pen EoS. From Figure 5.9, P_c - ω pairs for all lumping schemes give the closest results. For both EoS models, the minimum difference in GOR prediction is 2.5 scf/STB, which is more than 10% of experimental GOR. Pb predictions vary from 85 to 103 psig, whereas experimental P_b is 90.5 psig.

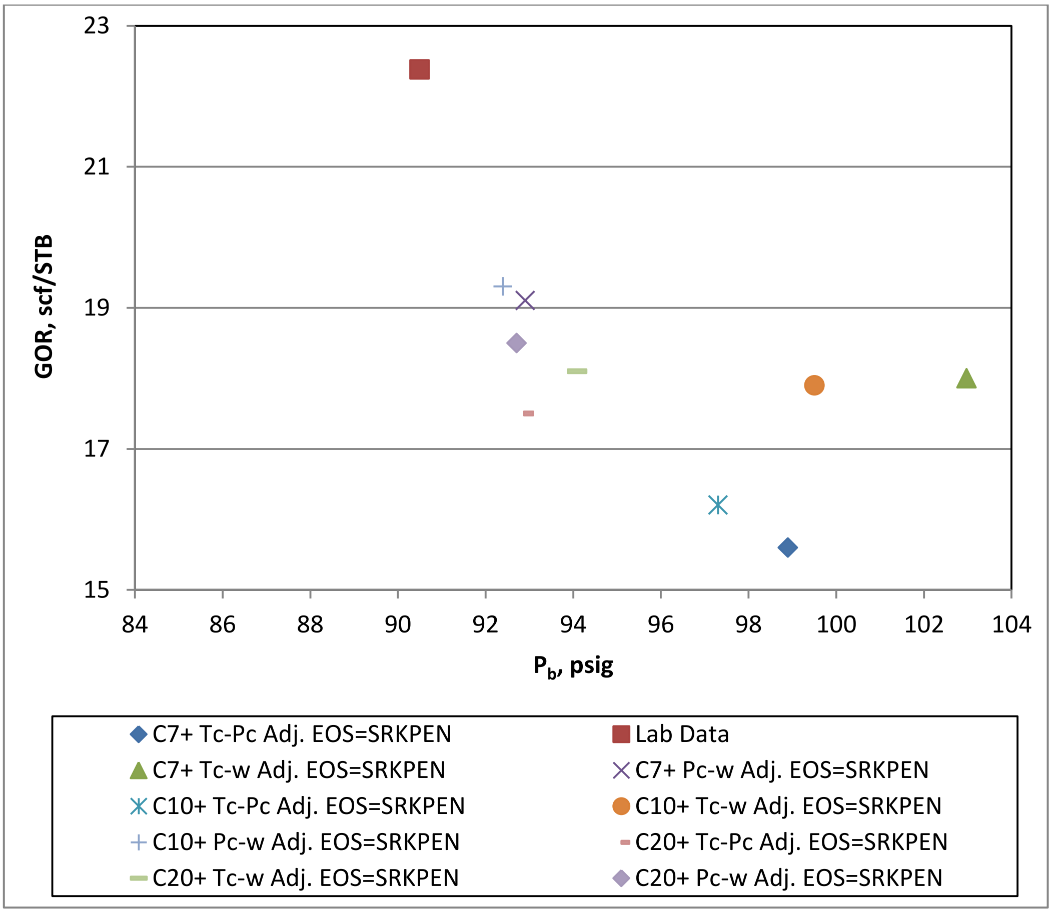

Figure 5.9 SRK-Pen EoS Predictions of GOR and P_b for Well B60 Sample

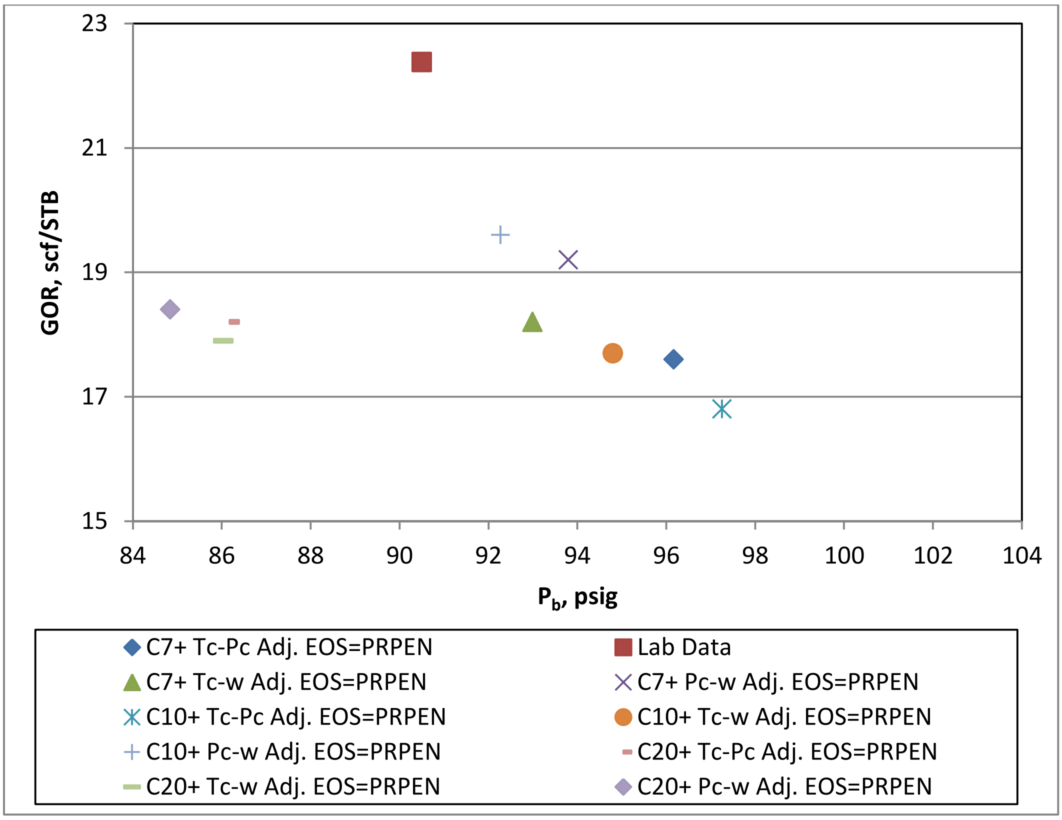

Figure 5.10 PR-Pen EoS Predictions of GOR and P_b for Well B60 Sample

Also, for each scenario, estimated values of B_{ob} are tabulated and compared with the experimental result, B_{ob} = 1.0527 bbl/STB, in Table 5.20 and Table 5.21. SRK-Pen EoS predicts B_{ob} better than PR - Pen EoS. However, all predictions are more than experimental result.

Table 5.20 B_{ob} Comparison for Well B60 Sample (SRK - Pen EoS)

Para.	SRK - Pen EoS								
	C7+			C10+			C20+		
	T_c-P_c	T_c-ω	P_c-ω	T_c-P_c	T_c-ω	P_c-ω	T_c-P_c	T_c-ω	P_c-ω
B_{ob}	1.032	1.035	1.043	1.033	1.036	1.044	1.039	1.040	1.041
Rel. Error, %	1.97	1.68	0.92	1.87	1.59	0.83	1.30	1.21	1.11

Table 5.21 B_{ob} Comparison for Well B60 Sample (PR - Pen EoS)

Para.	PR - Pen EoS								
	C7+			C10+			C20+		
	T_c-P_c	T_c-ω	P_c-ω	T_c-P_c	T_c-ω	P_c-ω	T_c-P_c	T_c-ω	P_c-ω
B_{ob}	1.030	1.031	1.034	1.028	1.030	1.036	1.035	1.035	1.037
Rel. Error, %	2.16	2.06	1.78	2.35	2.16	1.59	1.68	1.68	1.49

In this study, not only Pedersen's correlation but also Sancet and Edmister's (S and E) correlations are used to calculate the critical properties of plus fractions. Sancet's correlations are used to calculate T_c, P_c and T_b as a function of MW and ρ_{liquid} whereas Edmister's correlation is used to calculate ω as a function of Sancet's values. Sancet and Edmister's correlations are used after MW is adjusted by ± 10% to predict P_b. In Table 5.22, correlation – calculated T_c, T_b, P_c and ω values can be seen.

Table 5.22 Correlation – Calculated Critical Properties of Plus Fraction for Well B60 Sample

Para.	SRK-Pen EoS			PR-Pen EoS		
	C7+	C10+	C20+	C7+	C10+	C20+
MW	133.605	167.210	294.417	154.402	204.369	359.854
ρ_{liquid}	0.8042	0.8324	0.9038	0.8042	0.8324	0.9038
T_c	626.810	715.271	936.351	683.914	793.968	1014.298
P_c	310.21	256.74	141.488	275.56	211.25	113.22
ω	0.469	0.567	0.875	0.531	0.664	1.039
T_b	320.602	412.984	671.059	379.519	500.424	771.188

After that, same procedure is repeated for new values of critical properties. Boiling point, T_b, is not regressed, but it is changed because of the fact that Edmister's correlation needs that value to calculate acentric factor, ω. Density versus pressure relationships with respect to new values are given in the following figures, Figure 5.11, 5.12 and 5.13. Density - pressure plots show that adjusted mole percentage is effective on predictive ability. Adjustments on C7+ and C10+ lumped compositions give two close predictions whereas there is no close prediction for C20+ lumped compositions. Also, same adjustment predicts density better when PR - Pen EoS is used.

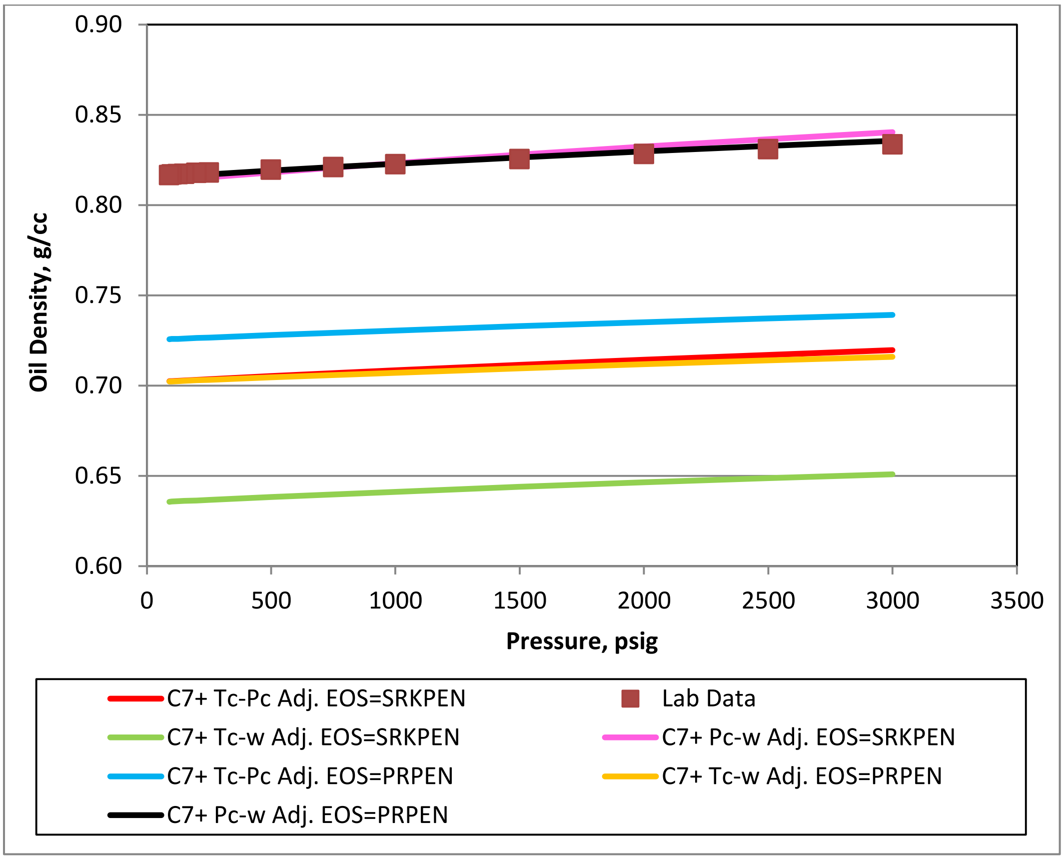

Figure 5.11 Pressure – Density Relationship for Well B60 Sample (C7+ Adjustment – Correlated)

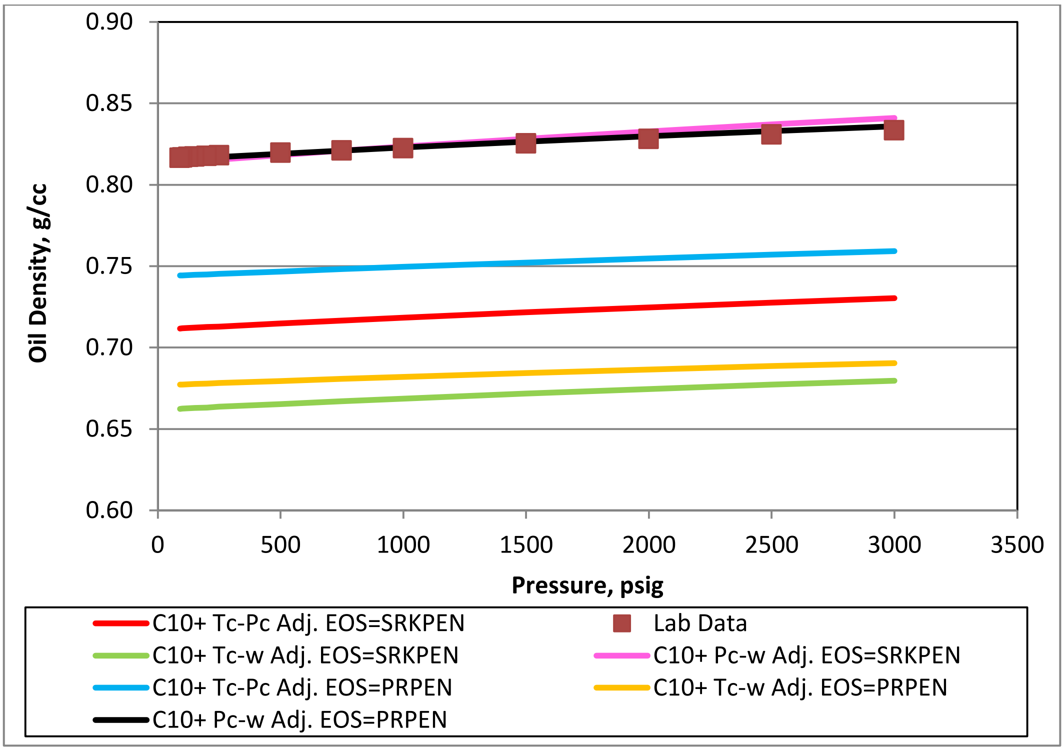

Figure 5.12 Pressure – Density Relationship for Well B60 Sample
(C10+ Adjustment – Correlated)

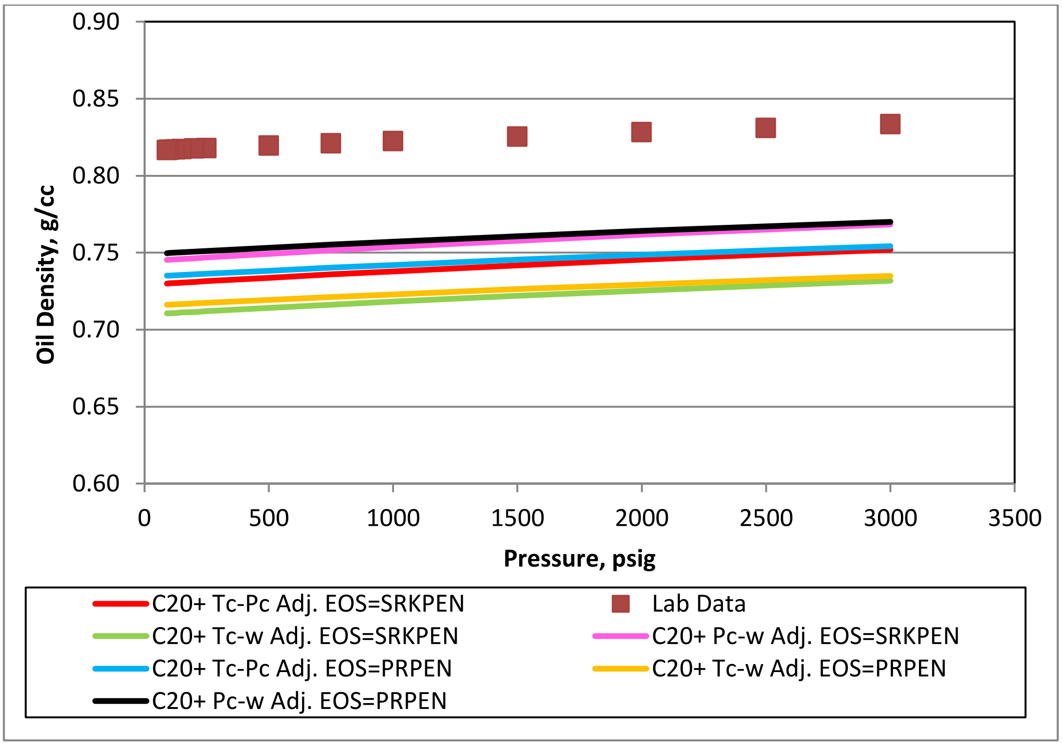

Figure 5.13 Pressure – Density Relationship for Well B60 Sample
(C20+ Adjustment – Correlated)

P_b and GOR values also examined according to EoS models. The points for each scenario are given in Figure 5.14 and Figure 5.15. In Figure 5.14, it can be clearly understood that P_b predictions of SRK-Pen EoS with Sancet and Edmister's values are in good agreement with the experimental value. PR-Pen EoS with Sancet and Edmister's values looks like having a horizontal trend (close GOR values) whereas SRK-PEN EoS with Sancet and Edmister's values has a vertical trend (close P_b values).

In Table 5.23 and 5.24, it can be realized that SRK-Pen EoS with correlation - calculated values predicts B_o better than PR-Pen EoS with correlation - calculated values. Moreover, P_c - ω pair of regression parameters have a better predictive ability than other pairs in all pseudoization schemes.

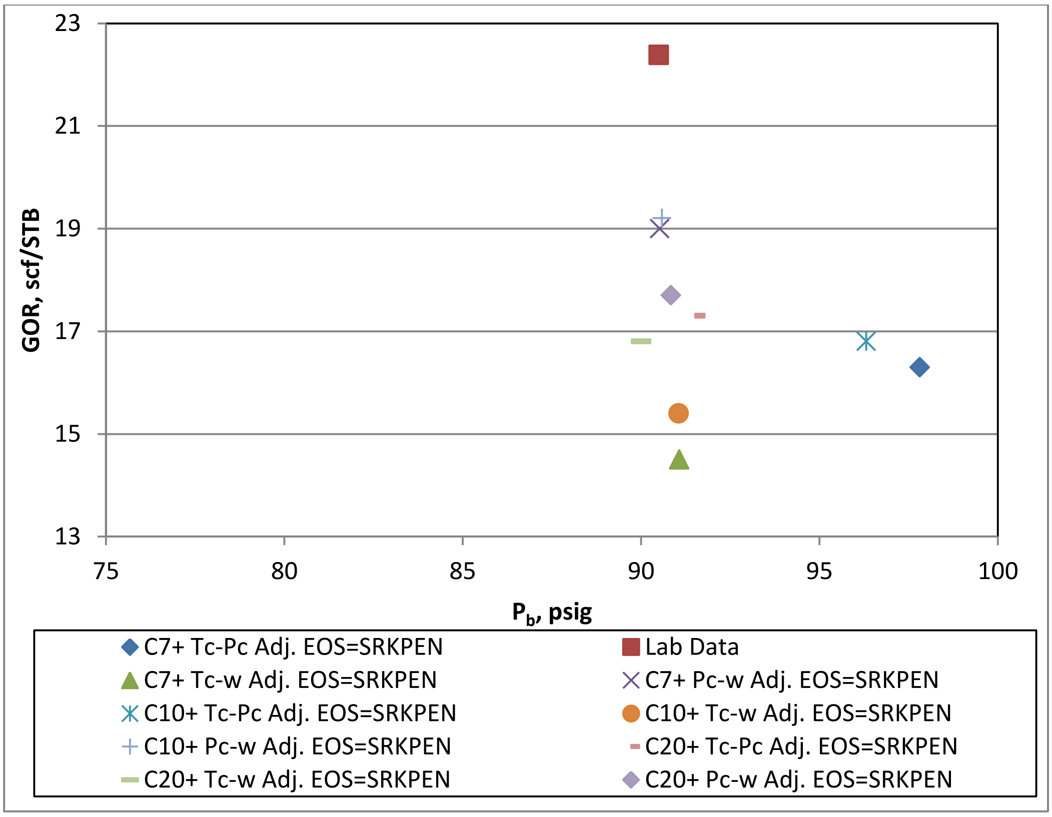

Figure 5.14 SRK - Pen EoS Predictions of GOR and P_b for Well B60 Sample (with S and E Values)

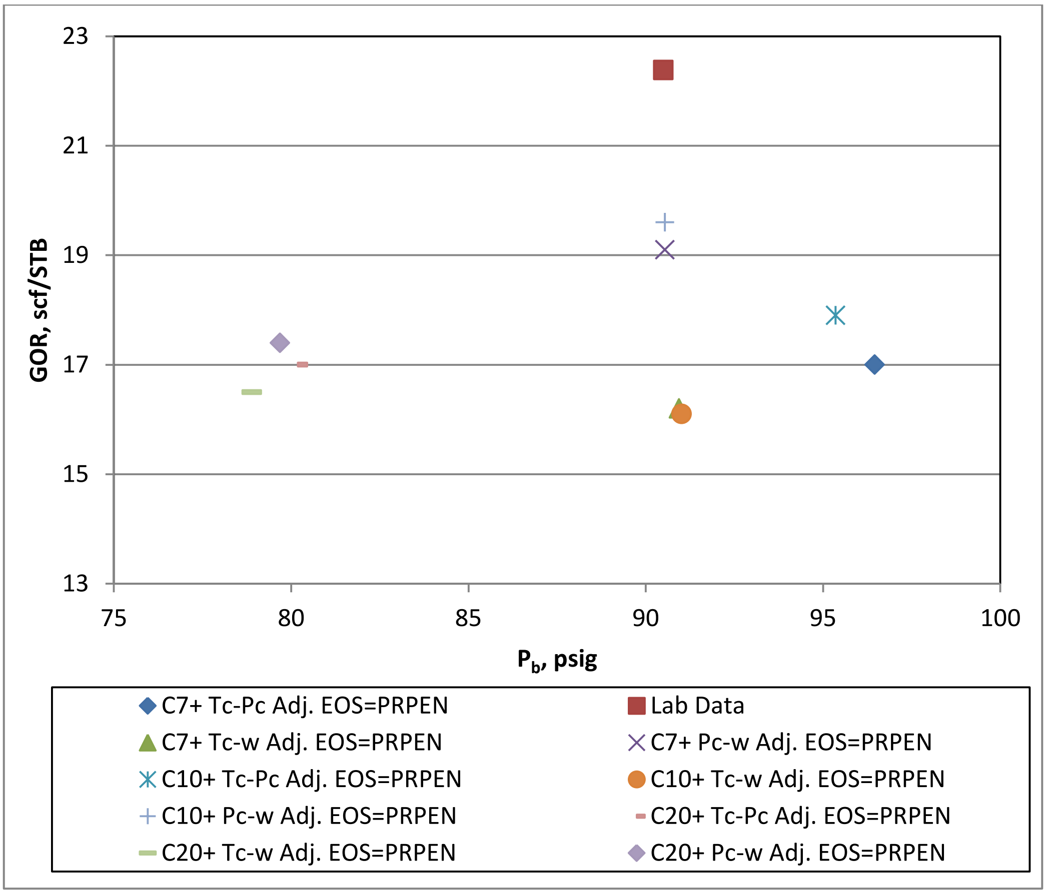

Figure 5.15 PR - Pen EoS Predictions of GOR and P_b for Well B60 Sample (with S and E Values)

Table 5.23 B_{ob} Comparison for Well B60 Sample (SRK-Pen EoS with S and E values)

Para.	SRK-Pen EoS								
	C7+			C10+			C20+		
	T_c-P_c	T_c-ω	P_c-ω	T_c-P_c	T_c-ω	P_c-ω	T_c-P_c	T_c-ω	P_c-ω
B_{ob}	1.033	1.031	1.044	1.035	1.035	1.044	1.039	1.038	1.040
Rel. Error, %	1.87	2.06	0.83	1.68	1.68	0.83	1.30	1.40	1.21

Table 5.24 B_{ob} Comparison for Well B60 Sample
(PR-Pen EoS with S and E values)

Para.	PR-Pen EoS								
	C7+			C10+			C20+		
	T_c-P_c	T_c-ω	P_c-ω	T_c-P_c	T_c-ω	P_c-ω	T_c-P_c	T_c-ω	P_c-ω
B_{ob}	1.028	1.028	1.036	1.030	1.028	1.037	1.036	1.035	1.037
Rel. Error, %	2.35	2.35	1.59	2.16	2.35	1.49	1.59	1.68	1.49

Apart from Pressure versus oil density as an input, pressure versus oil viscosity relationship under reservoir temperature is also introduced to the simulator. CSP coefficients are regressed with respect to this data and given in the following tables, Table 5.25 and Table 5.26. For SRK - Pen EoS, number of non-regressed viscosity correction factor is very high (default = 1.000).

Table 5.25 CSP Viscosity Coefficient for Well B60 Sample (SRK-Pen EoS)

CSP Visc. Corr. Factor	SRK-Pen EoS								
	C7+			C10+			C20+		
	T_c-P_c	T_c-ω	P_c-ω	T_c-P_c	T_c-ω	P_c-ω	T_c-P_c	T_c-ω	P_c-ω
1st	0.986	1.041	1.081	0.930	1.019	1.081	1.080	1.080	1.080
2nd	1.929	1.904	1.998	1.970	2.246	1.998	1.998	1.998	1.998
3rd	0.463	0.502	1.000	0.532	0.543	1.000	1.000	1.000	1.000
4th	0.971	1.093	1.000	1.087	1.127	1.000	1.000	1.000	1.000

Table 5.26 CSP Viscosity Coefficient for Well B60 Sample (PR-Pen EoS)

CSP Visc. Corr. Factor	PR-Pen EoS								
	C7+			C10+			C20+		
	T_c-P_c	T_c-ω	P_c-ω	T_c-P_c	T_c-ω	P_c-ω	T_c-P_c	T_c-ω	P_c-ω
1st	0.952	0.936	1.309	0.810	0.974	1.375	1.407	1.378	1.079
2nd	1.244	1.254	4.946	1.244	1.239	5.817	6.185	5.798	1.998
3rd	0.648	0.654	0.569	0.595	0.624	0.532	0.555	0.646	1.000
4th	1.256	1.283	0.979	1.026	1.126	0.855	1.022	1.379	1.000

Viscosity predictions against pressure under reservoir temperature for each EoS model are given in Figure 5.16 and 5.17. Except some scenarios, most of the regressions give close results with the experimental results. For SRK - Pen EoS, all of P_c - ω regressions can be the worst matches with experimental results.

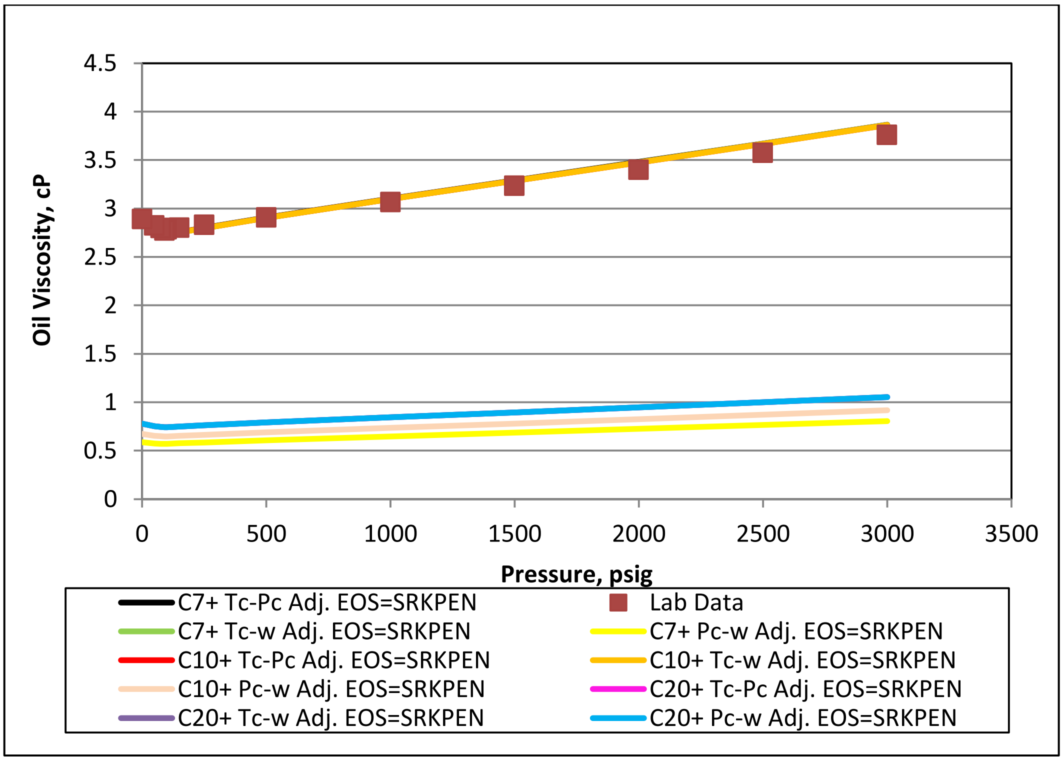

Figure 5.16 Pressure and Viscosity Relationship for Well B60 Sample (SRK-PEN EoS)

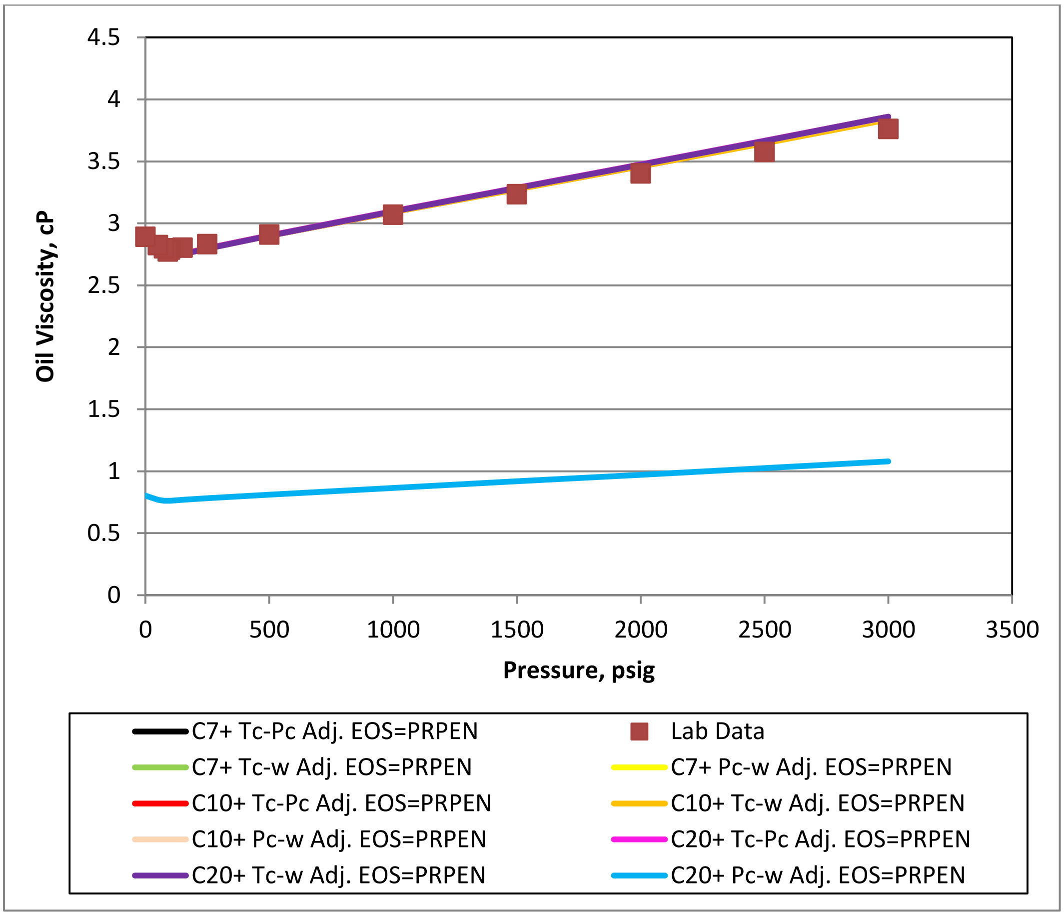

Figure 5.17 Pressure and Viscosity Relationship for Well B60 Sample (PR-PEN EoS)

5.3.2. Well DS1 Sample

Results of laboratory PVT studies are explained in the previous sections for Well DS1. After that, oil and gas compositions, GOR and stock tank oil density, which are obtained from flash experiment, are introduced into the simulator with respect to following scheme. Moreover, in Table 5.28 and 5.29, properties of plus fractions after and before molecular weight adjustment can be seen.

Table 5.27 Lumped Reservoir Fluid Compositions for Well DS1 Sample

Comp.	C7+	C10+	C20+	Comp.	C7+	C10+	C20+
N_2	0.116	0.117	0.116	C9		6.431	6.432
CO_2	0.088	0.088	0.088	C10 **(C10+)**		**(63.989)**	5.845
C1	2.430	2.436	2.430	C11			5.312
C2	0.335	0.335	0.335	C12			4.827
C3	0.867	0.867	0.867	C13			4.387
iC4	0.409	0.409	0.409	C14			3.986
nC4	1.643	1.643	1.643	C15			3.623
iC5	1.461	1.461	1.461	C16			3.292
nC5	2.152	2.152	2.152	C17			2.992
C6	5.207	5.207	5.207	C18			2.719
C7 **(C7+)**	**(85.292)**	7.787	7.788	C19			2.471
C8		7.077	7.077	**C20+**			**24.541**

Table 5.28 Parameters of Plus Fractions for Well DS1 Sample

Para.	SRK-Pen EoS			PR-Pen EoS		
	C7+	C10+	C20+	C7+	C10+	C20+
MW	232.140	273.718	412.848	232.140	273.718	412.848
ρ_{liquid}	0.8552	0.8686	0.9051	0.8552	0.8686	0.9051
T_c	897.666	943.921	1098.557	977.870	1033.996	1227.160
P_c	241.83	218.93	187.46	233.54	214.01	181.10
ω	0.9315	0.9873	1.1679	0.8469	0.9080	1.0936
C_{pen}	5.75E-5	5.47E-5	1.27E-5	4.83E-5	4.39E-5	1.22E-5

Table 5.29 Parameters of Plus Fractions After MW Adjustment for Well DS1 Sample

Para.	SRK-Pen EoS			PR-Pen EoS		
	C7+	C10+	C20+	C7+	C10+	C20+
MW	255.354	301.090	454.133	255.354	301.090	454.133
ρ_{liquid}	0.8552	0.8686	0.9051	0.8552	0.8686	0.9051
T_c	946.841	996.748	1161.556	1042.582	1103.923	1311.744
P_c	255.14	205.60	179.27	221.48	204.200	175.110
ω	0.977	1.032	1.190	0.884	0.940	1.080
C_{pen}	6.24E-5	5.86E-5	5.24E-6	5.11E-5	4.46E-5	4.67E-6

After regression with the density and viscosity data, it is claimed that the regression with more mole percentage gives more successful match in density predictions. Figure 5.19 shows that PR - Pen EoS gives more accurate density predictions than SRK - Pen EoS, when T_c - ω pair is regressed. However, T_c - ω pair gives the least accurate results among all simulations.

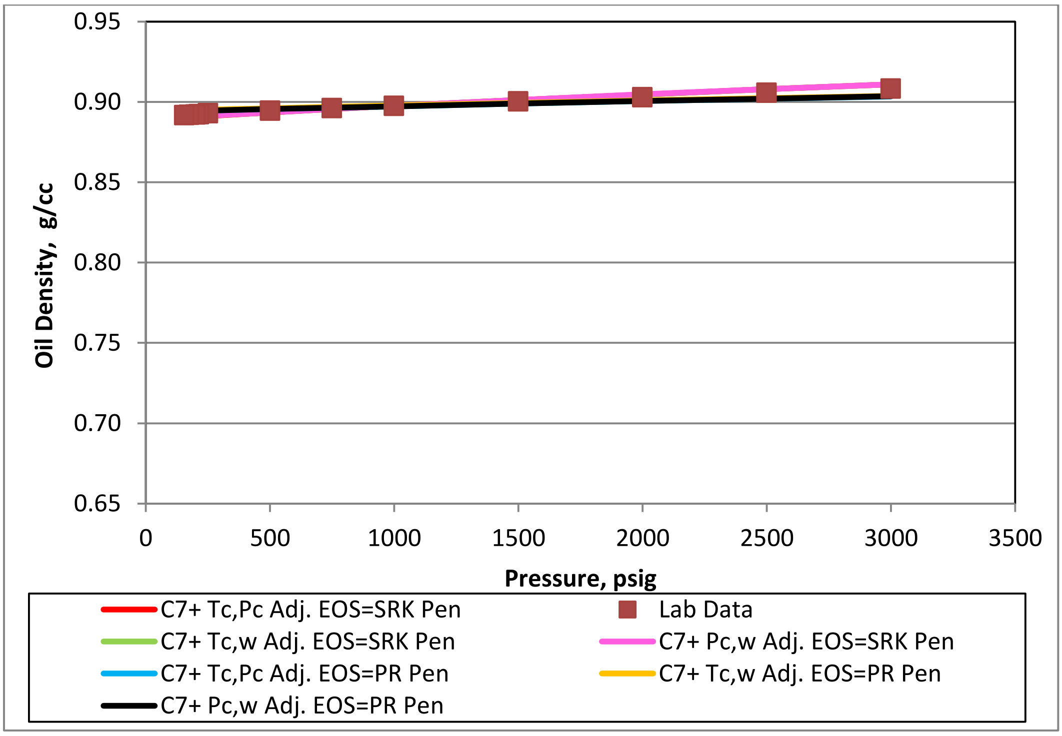

Figure 5.18 Pressure – Density Relationship for Well DS1 Sample (C7+ Adjustment)

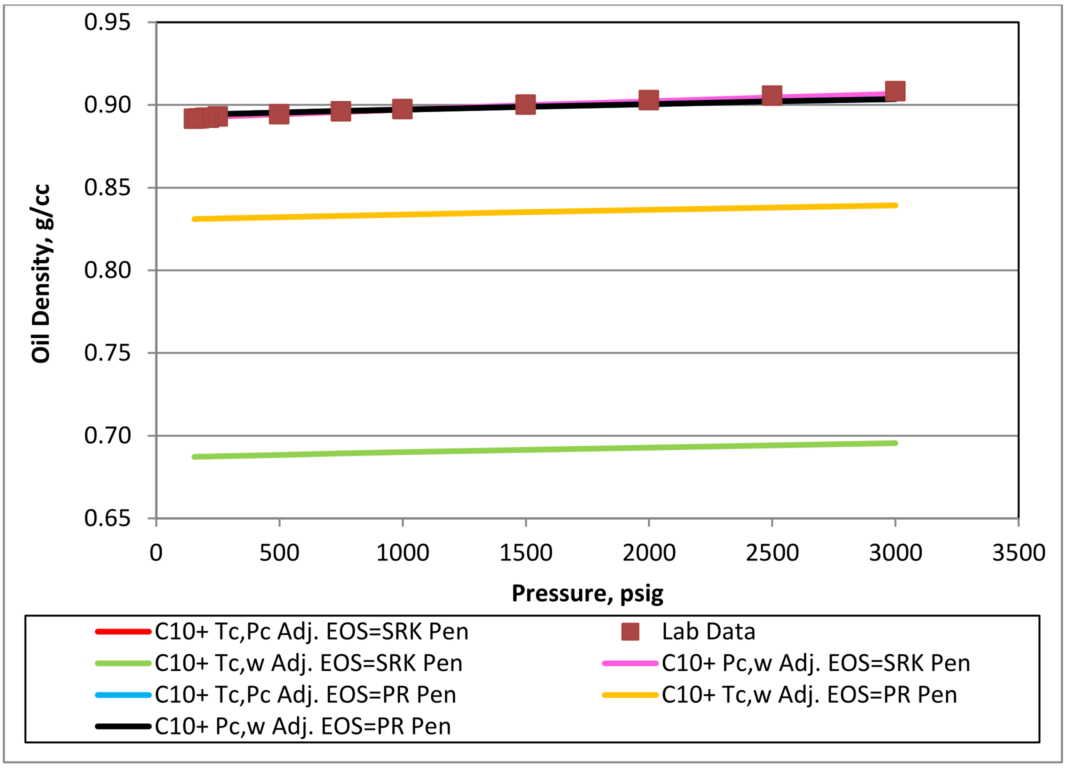

Figure 5.19 Pressure – Density Relationship for Well DS1 Sample
(C10+ Adjustment)

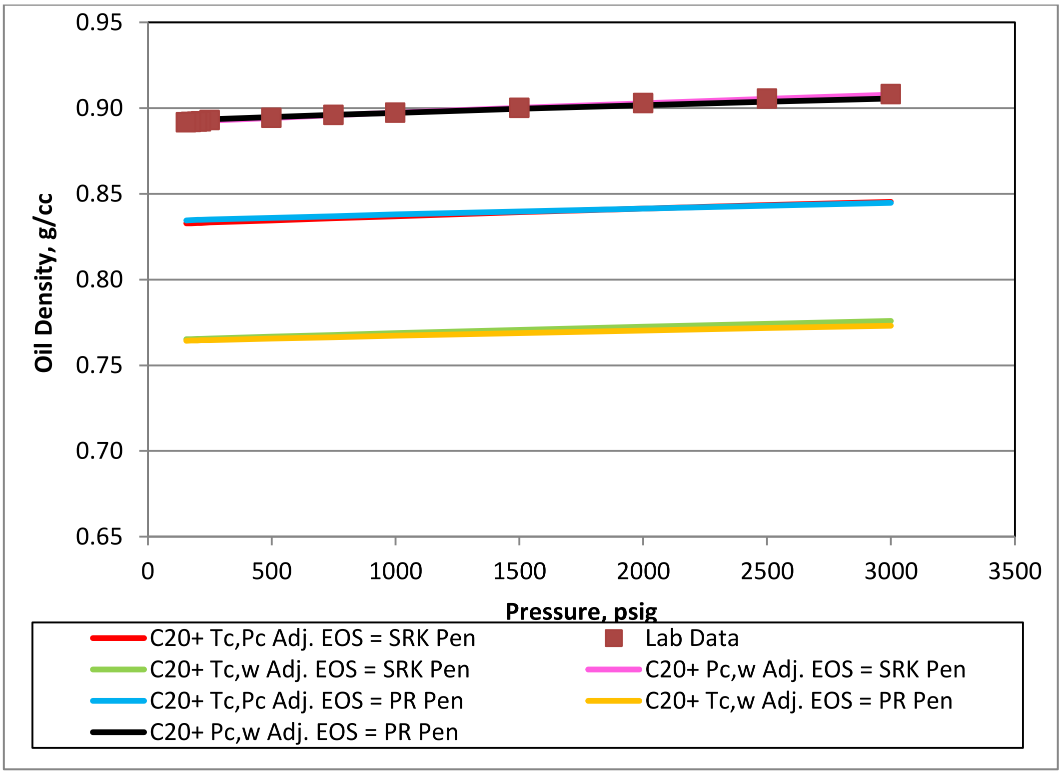

Figure 5.20 Pressure – Density Relationship for Well DS1 Sample
(C20+ Adjustment)

For this well, it is observed in density predictions that, the adjustments on the critical properties of C20+ components result in reasonable density predictions. Abundance of heavy fractions effects the density predictions positively when the adjustments are done on C10+ and C20+.

The P_b vs GOR predictions for EoS models are drawn in the following figures, Figure 5.21 and 5.22. It can be claimed that many of simulations predict GOR values higher than experimental GOR. However, P_b predictions are very close to experimental data, especially for SRK - Pen EoS. For PR-Pen EoS, all C20+ lumped simulations predict P_b worse than other simulations. Pseudoization effect is not seen for both of the equations of state.

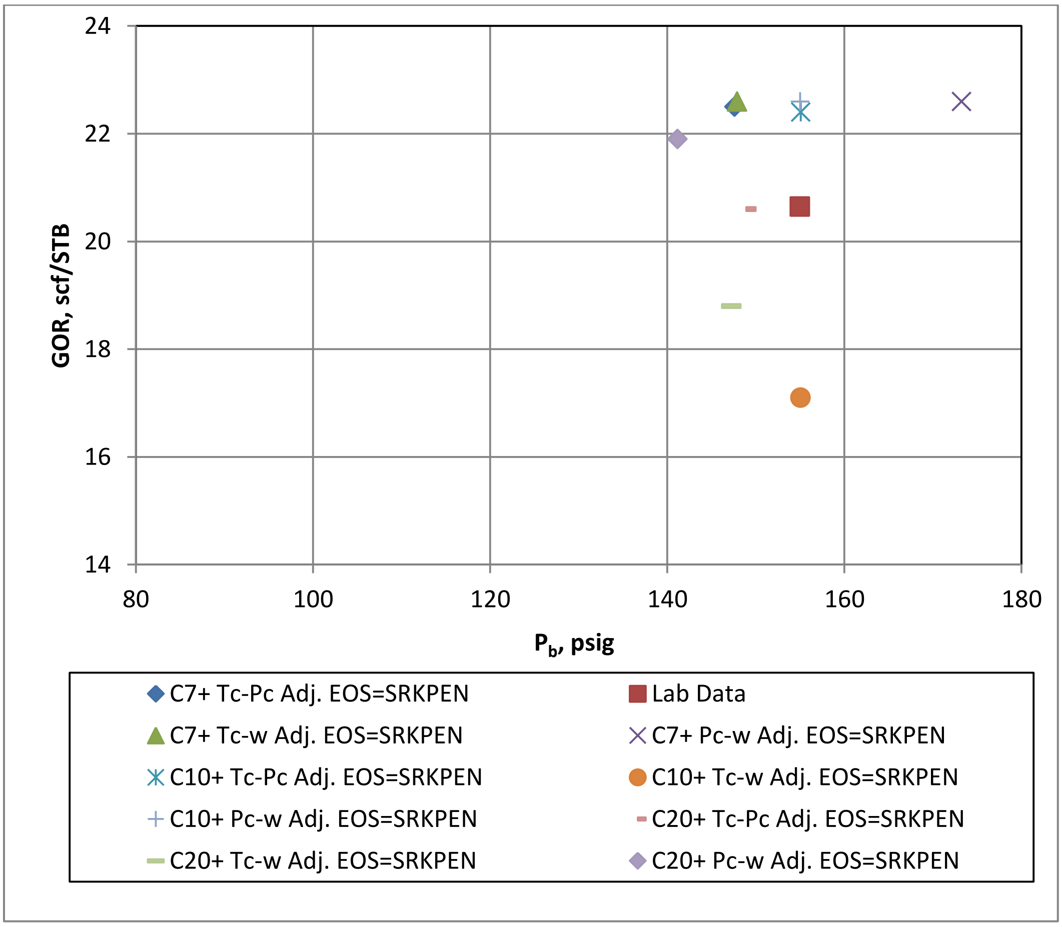

Figure 5.21 SRK-Pen EoS Predictions of GOR and P_b for Well DS1 Sample

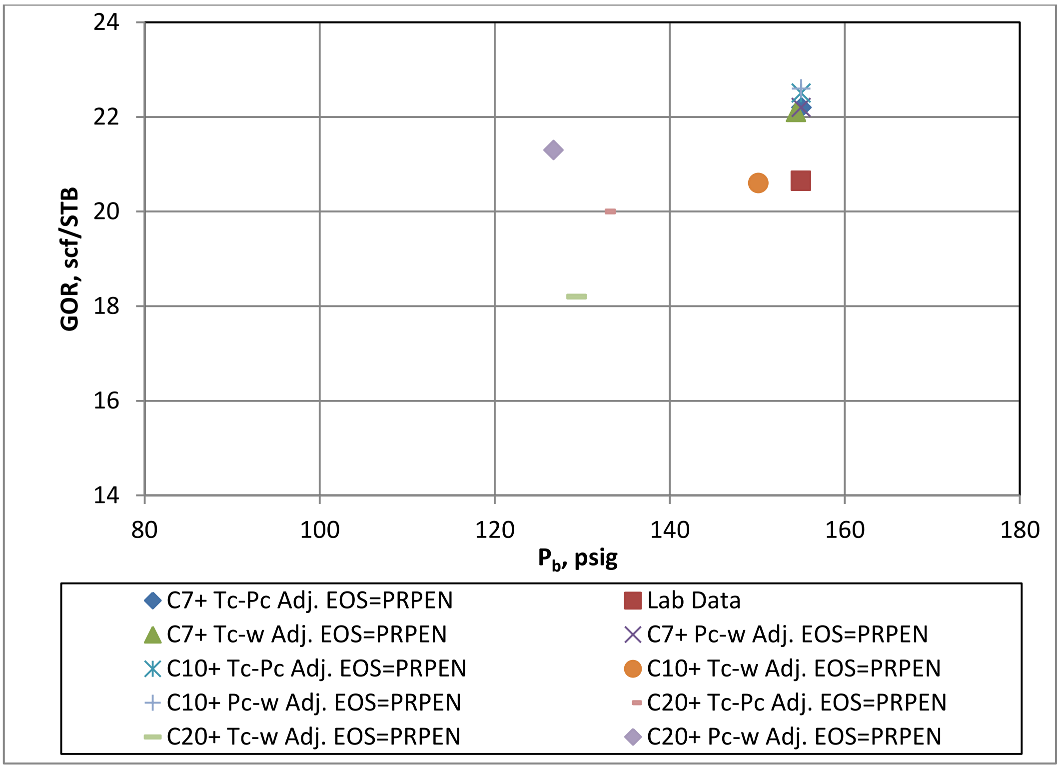

Figure 5.22 PR-Pen EoS Predictions of GOR and P_b for Well DS1 Sample

Comparison of oil FVF at P_b (B_{ob}) between experimental and simulation data is done. According to Table 5.30 and 5.31, SRK-PEN EoS and PR-Pen EoS predict B_{ob} less than the experimental data. Also, predictions of PR-Pen EoS are worse than SRK-Pen EoS.

Table 5.30 B_{ob} Comparison for Well DS1 Sample (SRK-Pen EoS)

Para.	SRK-Pen EoS								
	C7+			C10+			C20+		
	T_c-Pc	T_c-ω	P_c-ω	T_c-P_c	T_c-ω	P_c-ω	T_c-P_c	T_c-ω	P_c-ω
B_{ob}	1.035	1.035	1.035	1.033	1.025	1.034	1.031	1.029	1.036
Rel. Error, %	-2.08	-2.08	-2.08	-2.27	-3.03	-2.18	-2.46	-2.65	-1.99

Table 5.31 B_{ob} Comparison for Well DS1 Sample (PR-Pen EoS)

Para.	PR-Pen EoS								
	C7+			C10+			C20+		
	T_c-Pc	T_c-ω	P_c-ω	T_c-P_c	T_c-ω	P_c-ω	T_c-P_c	T_c-ω	P_c-ω
B_{ob}	1.027	1.027	1.027	1.028	1.026	1.028	1.028	1.026	1.032
Rel. Error, %	-2.84	-2.84	-2.84	-2.74	-2.93	-2.74	-2.74	-2.93	-2.37

As in Well B60, Sancet and Edmister (S and E) Correlations are used to predict T_c, P_c, T_b and ω for this well. Because of the fact that MWs of plus fractions are adjusted by the same amount in the previous stage, values are same for both models. Sancet and Edmister's correlations predict critical properties less than correlations of Pedersen.

Table 5.32 Correlation – Calculated Critical Properties of Plus Fraction for Well DS1 Sample

Para.	SRK-Pen EoS			PR-Pen EoS		
	C7+	C10+	C20+	C7+	C10+	C20+
MW	255.354	301.090	454.133	255.354	301.090	454.133
ρ_{liquid}	0.855	0.869	0.905	0.855	0.869	0.905
T_c	880.937	945.066	1104.446	880.937	945.066	1104.446
P_c	166.129	137.902	90.513	166.129	137.902	90.513
ω	0.785	0.891	1.342	0.785	0.891	1.342
T_b	602.757	682.018	892.862	602.757	682.018	892.862

The pseudoization effect can be easily realized for density predictions with S and E values in following figures. During regression to density data, adjusted mole percentage is highly effective. It is obvious that, using more mole percentage results in more successful density predictions. Also, for this well, Sancet and Edmister correlations seems unsuccessful for P_b and GOR match as can be seen in Figure 5.26 and 5.27.

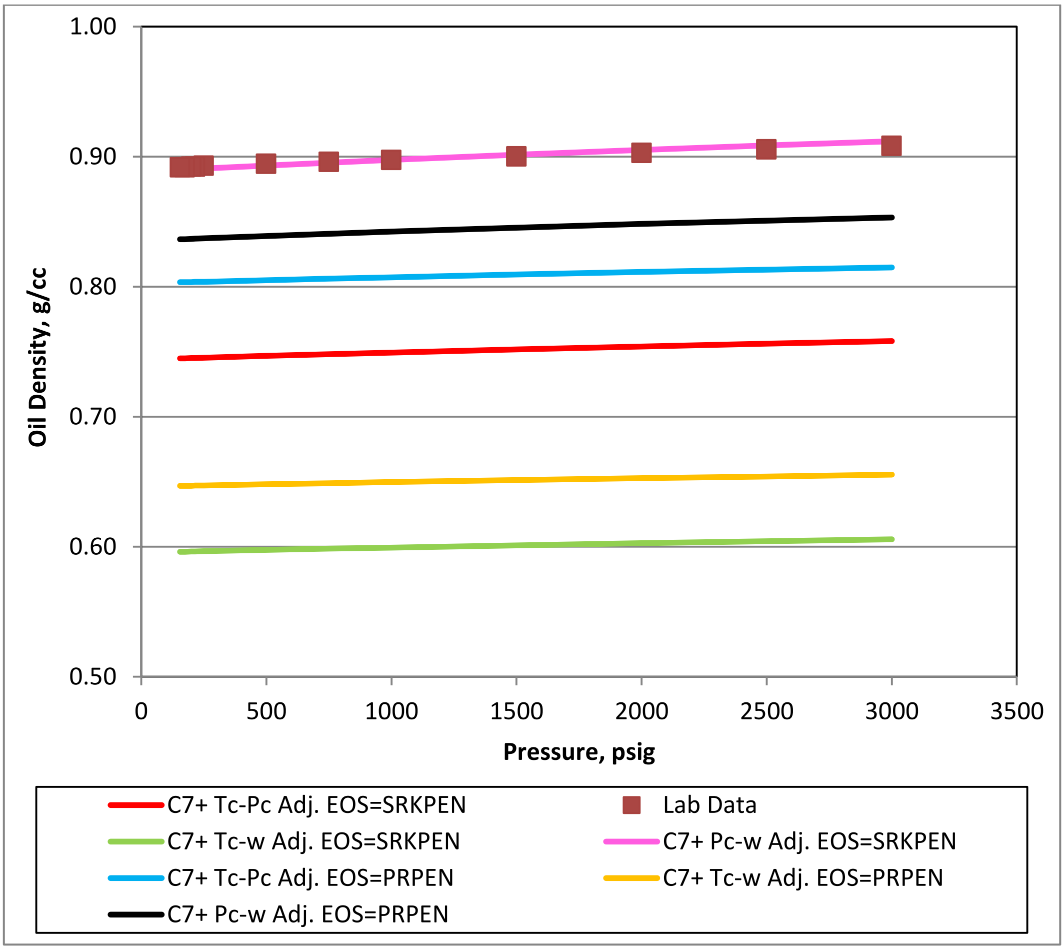

Figure 5.23 Pressure – Density Relationship for Well DS1 Sample
(C7+ Adjustment – Correlated)

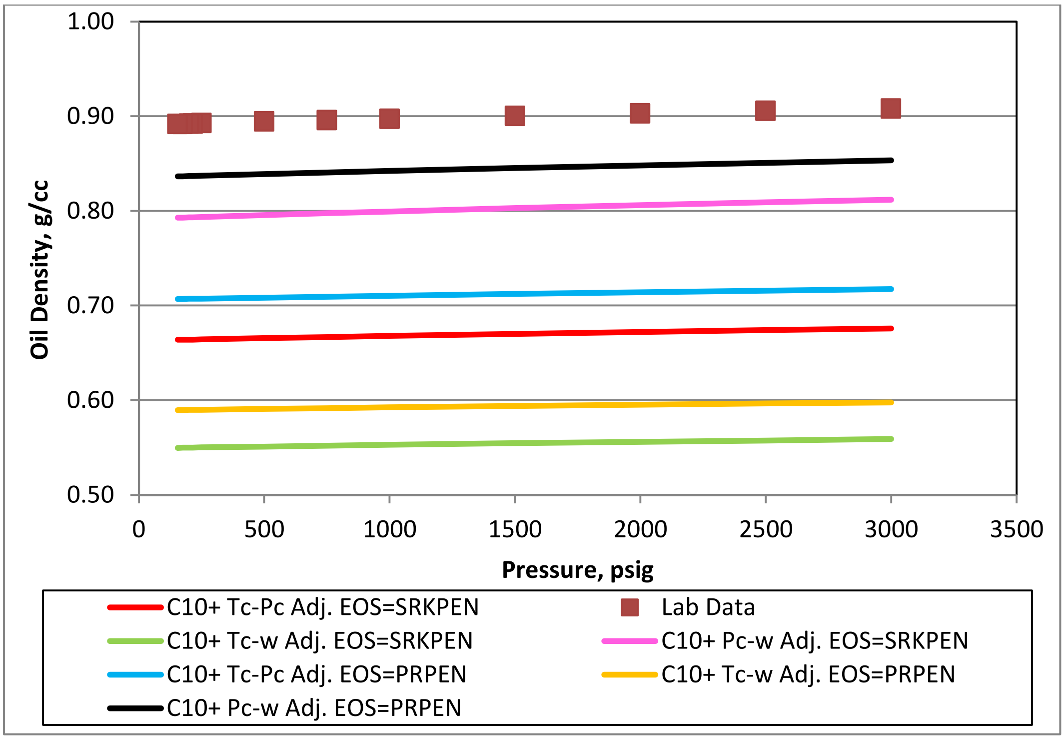

Figure 5.24 Pressure – Density Relationship for Well DS1 Sample
(C10+ Adjustment – Correlated)

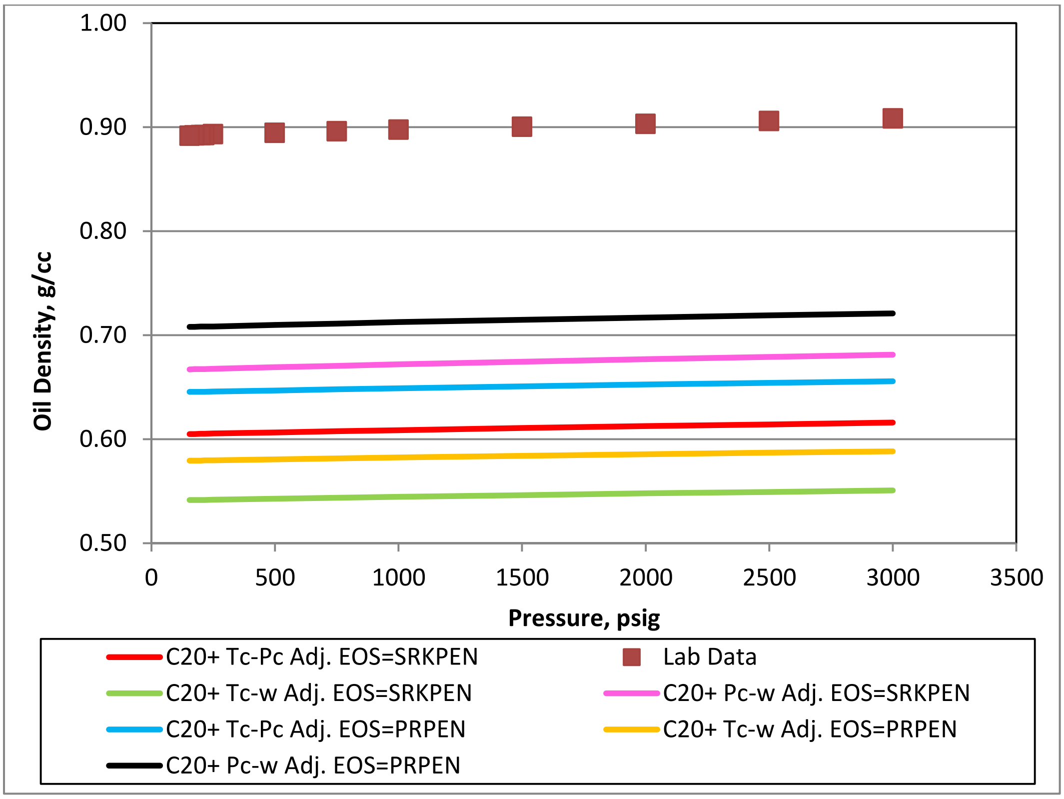

Figure 5.25 Pressure – Density Relationship for Well DS1 Sample
(C20+ Adjustment – Correlated)

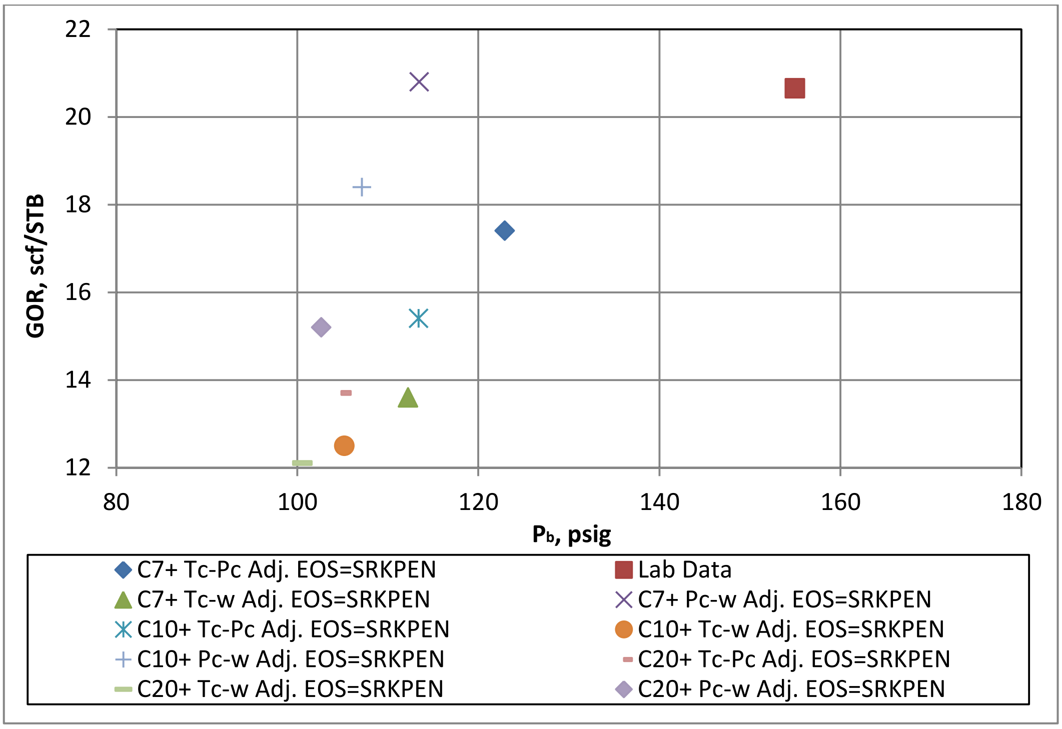

Figure 5.26 SRK - Pen EoS Predictions of GOR and P_b for Well DS1 Sample (with S and E Values)

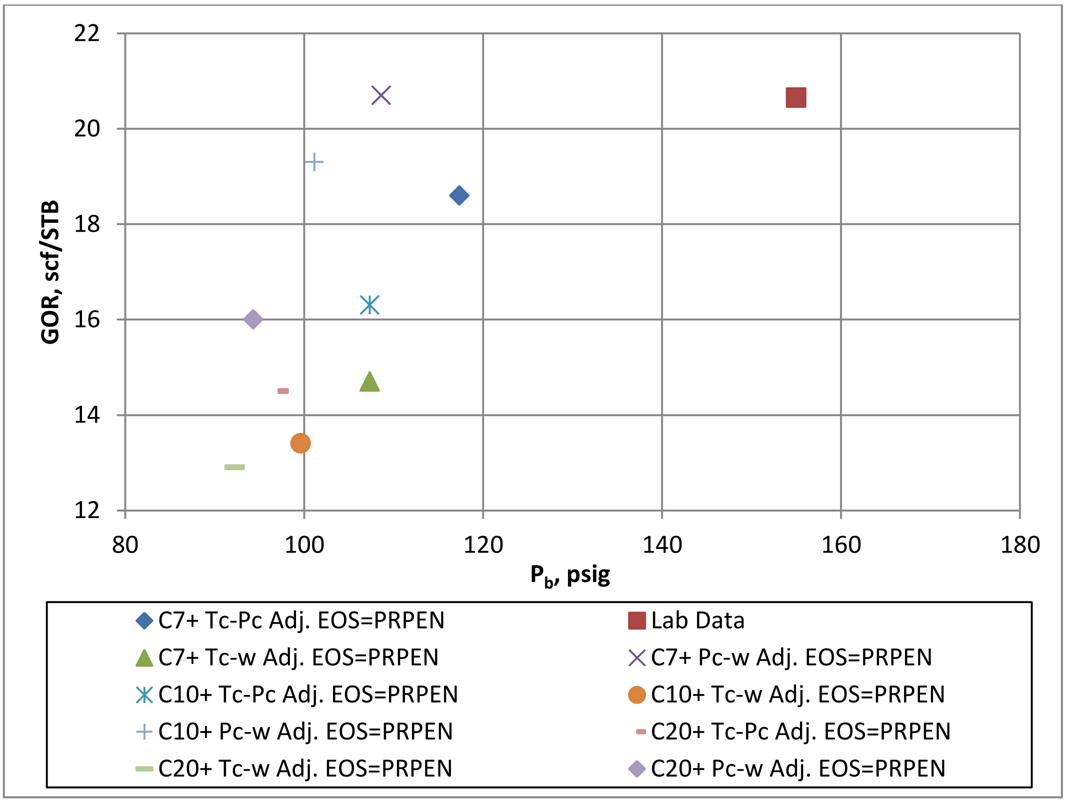

Figure 5.27 PR - Pen EoS Predictions of GOR and P_b for Well DS1 Sample (with S and E Values)

Apart from some exceptions, both models, that use critical properties calculated from Sancet and Edmister's correlations, predict worse than Pedersen's correlations. SRK - Pen EoS seems more successful than PR - Pen EoS, however, all predictions are smaller than the experimental value, B_{ob} = 1.057 bbl/STB.

Table 5.33 B_{ob} Comparison for Well DS1 Sample
(SRK-Pen EoS with S and E values)

Para.	SRK-Pen EoS								
	C7+			C10+			C20+		
	T_c-P_c	T_c-ω	P_c-ω	T_c-P_c	T_c-ω	P_c-ω	T_c-P_c	T_c-ω	P_c-ω
B_{ob}	1.030	1.025	1.041	1.029	1.025	1.038	1.028	1.026	1.033
Rel. Error, %	-2.55	-3.03	-1.51	-2.65	-3.03	-1.80	-2.74	-2.93	-2.27

Table 5.34 B_{ob} Comparison for Well DS1 Sample
(PR-Pen EoS with S and E values)

Para.	PR-Pen EoS								
	C7+			C10+			C20+		
	T_c-Pc	T_c-ω	P_c-ω	T_c-P_c	T_c-ω	P_c-ω	T_c-P_c	T_c-ω	P_c-ω
B_{ob}	1.028	1.024	1.036	1.027	1.024	1.036	1.027	1.026	1.032
Rel. Error, %	-2.74	-3.12	-1.99	-2.84	-3.12	-1.99	-2.84	-2.93	-2.37

In Figure 5.28 and 5.29, viscosity values against pressure under reservoir temperature are presented. Both EoS models predict oil viscosity very well. In Table 5.35 and 5.36, regressed CSP coefficients are given and 3rd viscosity correction coefficients are the most regressed one, for both EoS.

Table 5.35 CSP Viscosity Coefficient for Well DS1 Sample (SRK-Pen EoS)

CSP Visc. Corr. Factor	SRK-Pen EoS								
	C7+			C10+			C20+		
	T_c-P_c	T_c-ω	P_c-ω	T_c-P_c	T_c-ω	P_c-ω	T_c-P_c	T_c-ω	P_c-ω
1st	1.255	1.123	1.205	0.768	1.092	1.433	1.070	0.855	0.396
2nd	1.016	1.036	1.044	0.919	1.066	1.043	1.053	1.052	1.844
3rd	0.468	0.452	0.467	0.498	0.487	0.223	0.297	0.434	0.314
4th	1.020	0.980	1.016	1.112	1.078	0.575	0.730	1.006	0.759

Table 5.36 CSP Viscosity Coefficient for Well DS1 Sample (PR-Pen EoS)

CSP Visc. Corr. Factor	SRK-Pen EoS								
	C7+			C10+			C20+		
	T_c-P_c	T_c-ω	P_c-ω	T_c-P_c	T_c-ω	P_c-ω	T_c-P_c	T_c-ω	P_c-ω
1st	0.994	1.168	0.984	1.085	0.873	0.916	1.091	1.087	0.862
2nd	1.183	0.926	1.053	1.221	0.949	1.013	1.182	1.126	1.319
3rd	0.380	0.446	0.429	0.457	0.354	0.324	0.468	0.468	0.459
4th	0.828	0.966	0.927	1.004	0.794	0.741	1.085	1.085	1.062

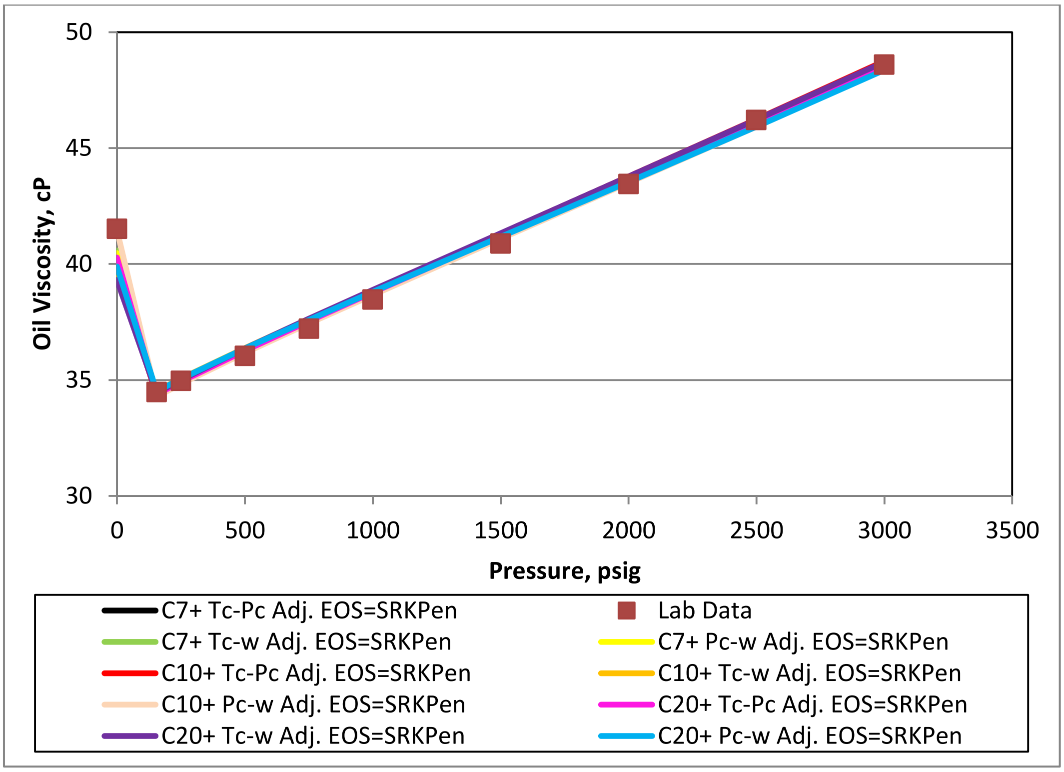

Figure 5.28 Pressure and Viscosity Relationship for Well DS1 Sample (SRK-PEN EoS)

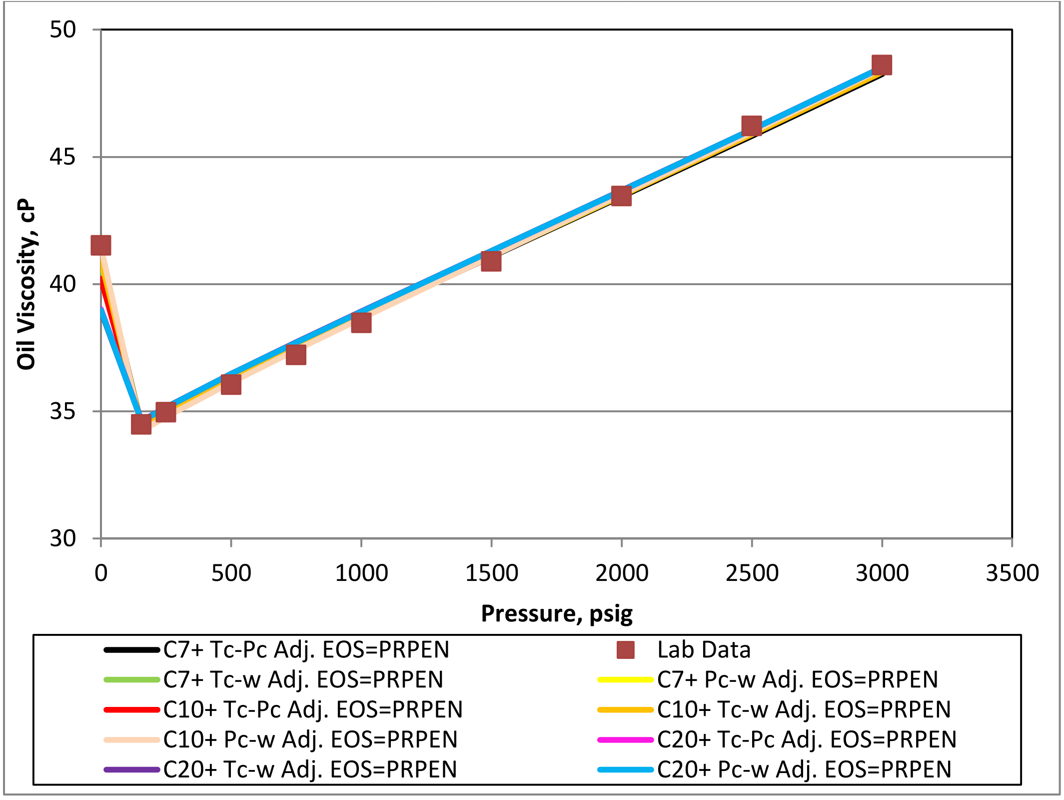

Figure 5.29 Pressure and Viscosity Relationship for Well DS1 Sample (PR-PEN EoS)

5.3.3. Well E2 Sample

In simulation studies of this well, firstly, recombination and lumping procedures take place. Below, in Table 5.37, lumped reservoir fluid compositions, according to three pseudoization schemes, can be seen. Mole fraction of heptane plus components (91%) is the highest among all wells.

Table 5.37 Lumped Reservoir Fluid Compositions for Well E2 Sample

Comp.	C7+	C10+	C20+	Comp.	C7+	C10+	C20+
N_2	0.280	0.280	0.280	C9		7.778	7.778
CO_2	0.385	0.385	0.385	C10 **(C10+)**		**(64.788)**	6.945
C1	6.175	6.175	6.175	C11			6.201
C2	0.918	0.918	0.918	C12			5.536
C3	0.674	0.674	0.674	C13			4.943
iC4	0.178	0.178	0.178	C14			4.413
nC4	0.078	0.078	0.078	C15			3.940
iC5	0.039	0.039	0.039	C16			3.518
nC5	0.037	0.037	0.037	C17			3.141
C6	0.201	0.201	0.201	C18			2.804
C7 **(C7+)**	**(91.035)**	9.757	9.757	C19			2.504
C8		8.712	8.712	**C20+**			**20.843**

Table 5.38 Parameters of Plus Fractions for Well E2 Sample

Para.	SRK-Pen EoS			PR-Pen EoS		
	C7+	C10+	C20+	C7+	C10+	C20+
MW	209.924	251.596	391.691	209.924	251.596	391.691
ρ_{liquid}	0.8440	0.8609	0.9053	0.8440	0.8609	0.9053
T_c	844.065	896.412	1064.665	910.502	973.354	1181.781
P_c	254.64	227.73	192.51	246.07	222.64	184.76
ω	0.8774	0.9420	1.1492	0.7967	0.8690	1.0901
C_{pen}	5.24E-5	5.37E-5	1.55E-5	4.32E-5	4.11E-5	1.54E-5

Table 5.39 Parameters of Plus Fractions After MW Adjustment for Well E2 Sample

Para.	SRK-Pen EoS			PR-Pen EoS		
	C7+	C10+	C20+	C7+	C10+	C20+
MW	188.931	226.437	352.522	188.931	226.437	352.522
ρ_{liquid}	0.844	0.861	0.905	0.844	0.861	0.905
T_c	793.709	842.678	1000.523	844.971	902.941	1096.287
P_c	278.76	246.66	203.77	262.98	236.27	192.830
ω	0.816	0.879	1.097	0.735	0.807	1.056
C_{pen}	4.38E-5	4.71E-5	1.96E-5	3.91E-5	3.88E-5	2.05E-5

According to next stage of Christensen’s procedure, density and viscosity versus pressure are given to simulator. Density against pressure and predicted P_b against predicted GOR are drawn in the following figures for this well. Density versus pressure plots shows that PR - Pen EoS gives more accurate results than SRK - Pen EoS with same pair of critical properties. Adjusted mole percentage is highly effective on accuracy of density predictions. However, it has no effect on bubble point pressure and gas - oil ratio predictions. In Figure 5.33, it is observed that predictions for P_b and GOR form three groups with respect to adjusted critical properties.

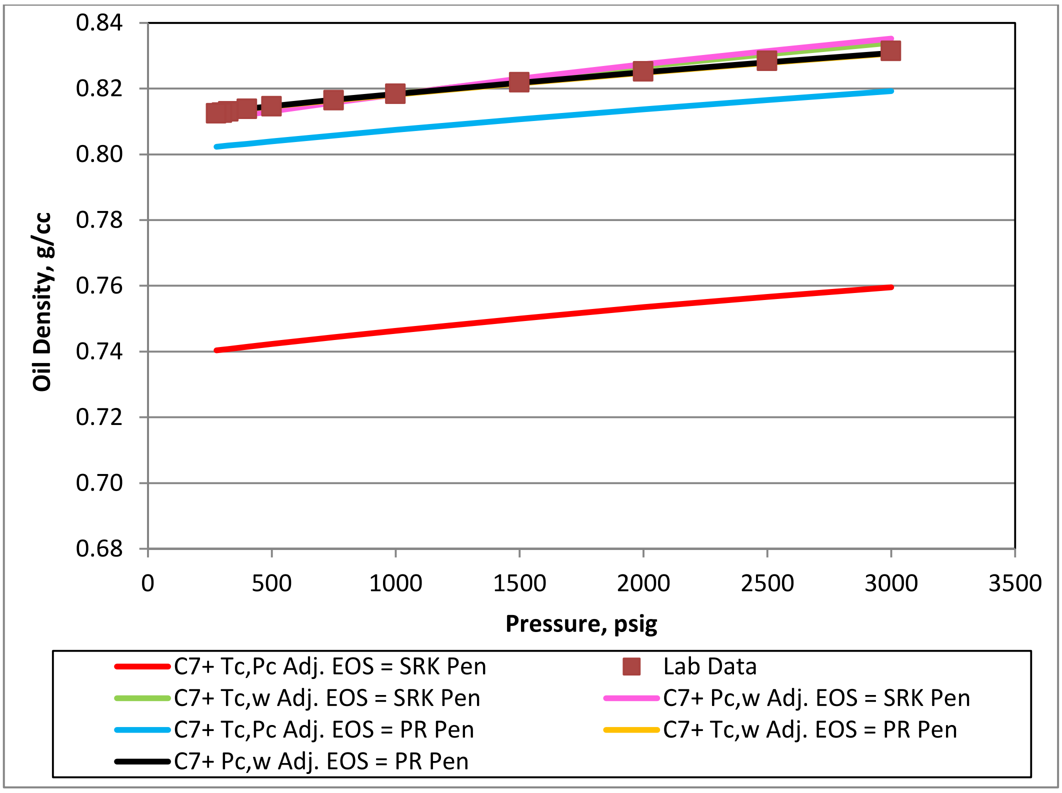

Figure 5.30 Pressure – Density Relationship for Well E2 Sample (C7+ Adjustment)

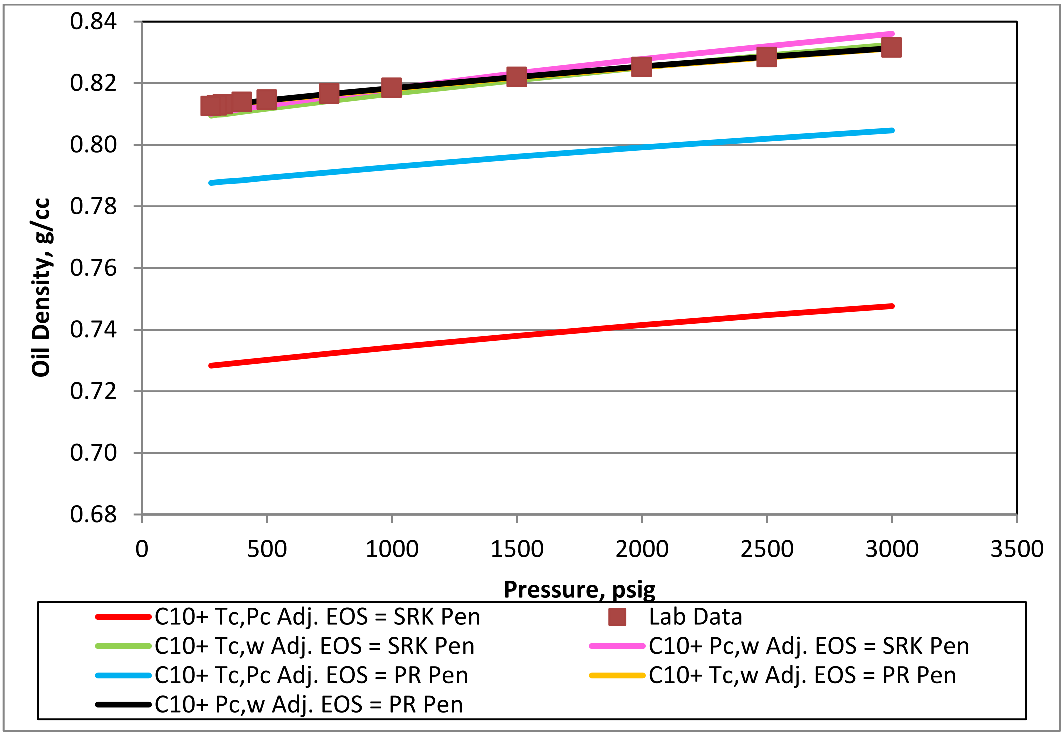

Figure 5.31 Pressure – Density Relationship for Well E2 Sample (C10+ Adjustment)

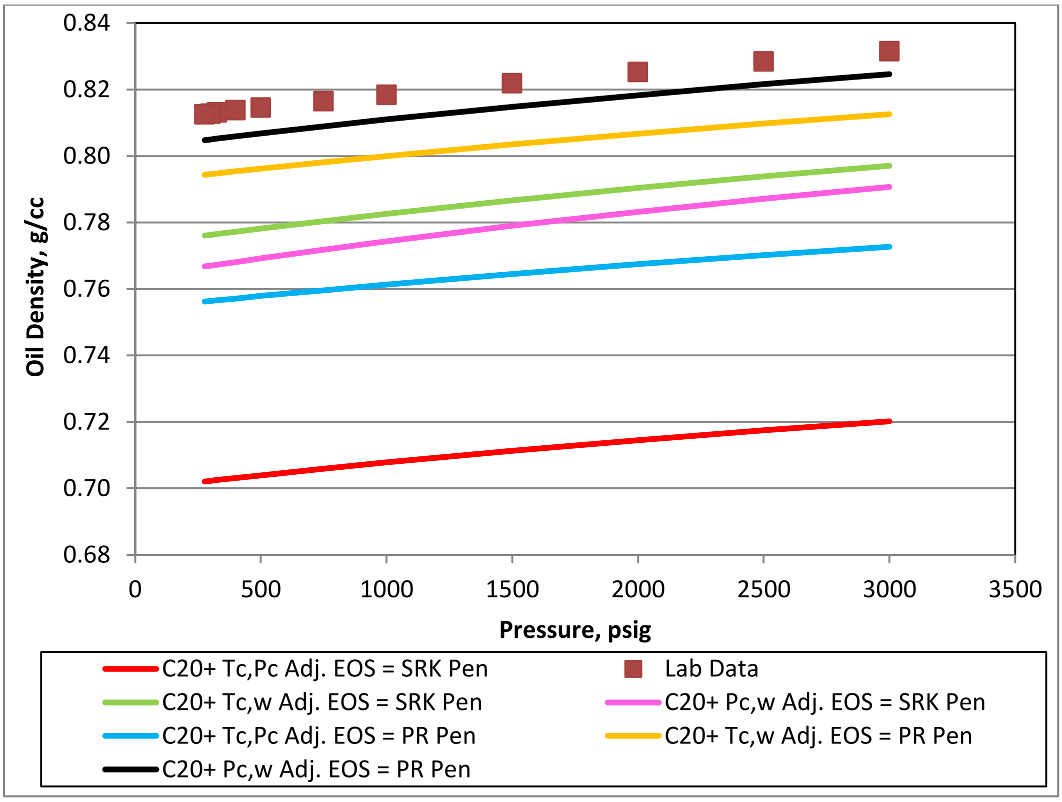

Figure 5.32 Pressure – Density Relationship for Well E2 Sample (C20+ Adjustment)

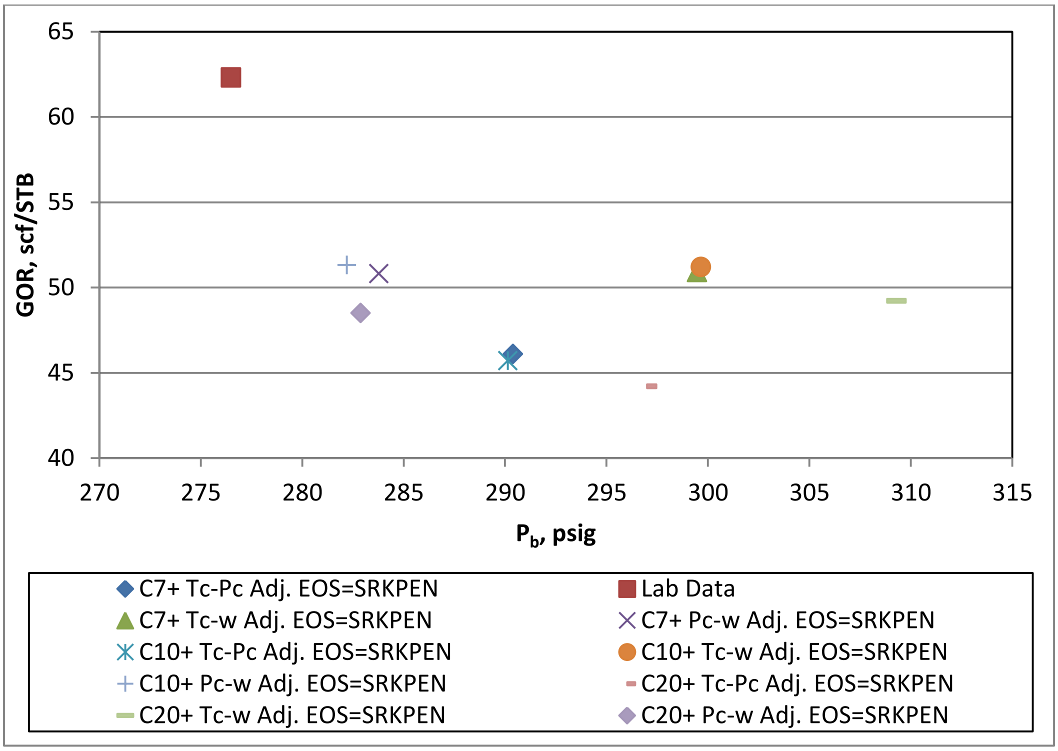

Figure 5.33 SRK - Pen EoS Predictions of GOR and P_b for Well E2 Sample

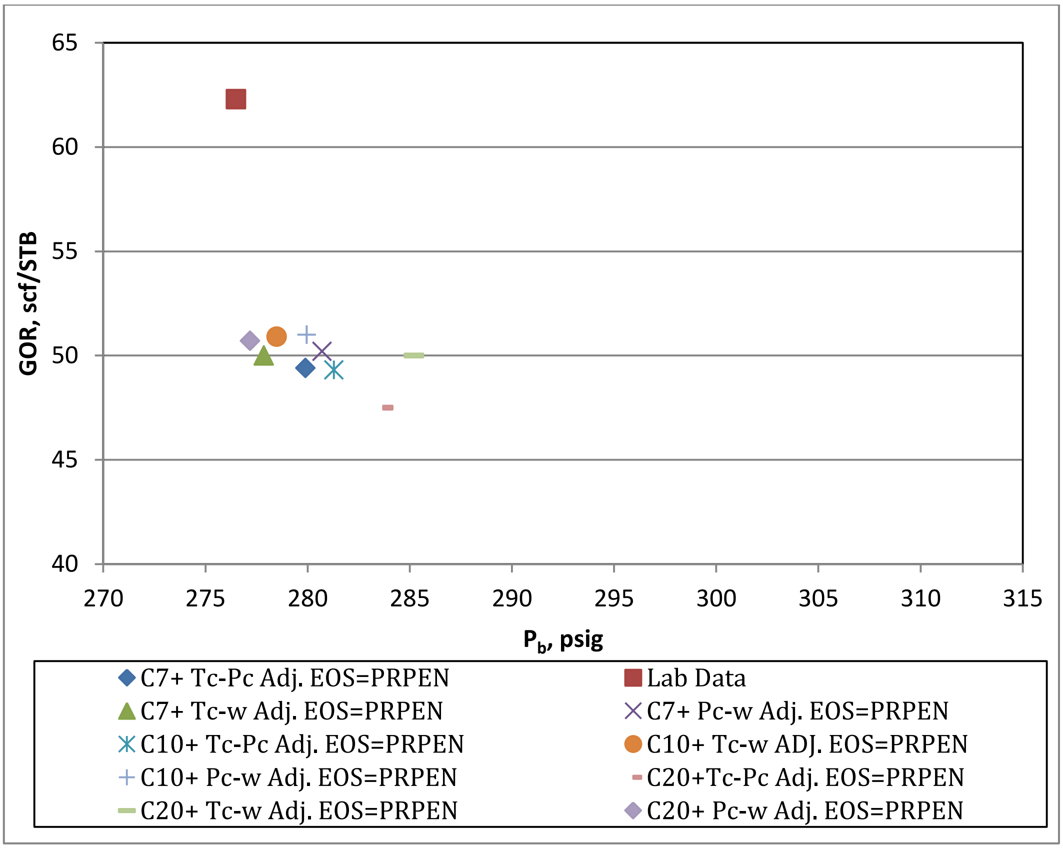

Figure 5.34 PR - Pen EoS Predictions of GOR and P_b for Well E2 Sample

In order to measure predictive ability of EoS models, experimental B_{ob} is compared with the simulation results. Relative errors are very low for both models and pseudoization effect is not observed. The results are tabulated as follows:

Table 5.40 B_{ob} Comparison for Well E2 Sample (SRK - Pen EoS)

Para.	SRK-Pen EoS								
	C7+			C10+			C20+		
	T_c-Pc	T_c-ω	P_c-ω	T_c-P_c	T_c-ω	P_c-ω	T_c-P_c	T_c-ω	P_c-ω
B_{ob}	1.064	1.069	1.073	1.064	1.070	1.075	1.062	1.066	1.072
Rel. Error, %	0.08	0.55	0.92	0.08	0.64	1.11	-0.11	0.26	0.83

Table 5.41 B_{ob} Comparison for Well E2 Sample (PR - Pen EoS)

Para.	PR-Pen EoS								
	C7+			C10+			C20+		
	T_c-Pc	T_c-ω	P_c-ω	T_c-P_c	T_c-ω	P_c-ω	T_c-P_c	T_c-ω	P_c-ω
B_{ob}	1.060	1.061	1.062	1.061	1.063	1.064	1.059	1.062	1.065
Rel. Error, %	-0.30	-0.21	-0.11	-0.21	-0.02	0.08	-0.40	-0.11	0.17

Sancet and Edmister correlations to predict critical properties as a function of MW and ρ_{liquid} of plus fractions are used for Well E2, too. New correlation - calculated critical properties are given in Table 5.42. Since MW of plus fractions are adjusted by the same percentage, final MWs are the same for both models. This results in the same critical values. Again, it is observed that critical values, calculated with Sancet and Edmister's correlation, are less than critical values, calculated with Pedersen's correlations.

Table 5.42 Correlation – Calculated Critical Properties of Plus Fraction for Well E2 Sample

Para.	SRK-Pen EoS			PR-Pen EoS		
	C7+	C10+	C20+	C7+	C10+	C20+
MW	188.931	226.437	352.522	188.931	226.437	352.522
ρ_{liquid}	0.844	0.861	0.905	0.844	0.861	0.905
T_c	763.208	834.052	1006.312	763.208	834.052	1006.312
P_c	228.635	189.610	115.747	228.635	189.610	115.747
ω	0.625	0.717	1.020	0.625	0.717	1.020
T_b	465.661	546.848	760.713	465.661	546.848	760.713

Density - Pressure relationship shows that pseudoization effect is very strong and for the same pairs, modelled with PR - Pen EoS have better density match than the pairs, modelled with SRK - Pen EoS. Also, P_b is predicted between 252 and 284 psig whereas GOR predictions are between 36.5 and 51.2 scf/STB.

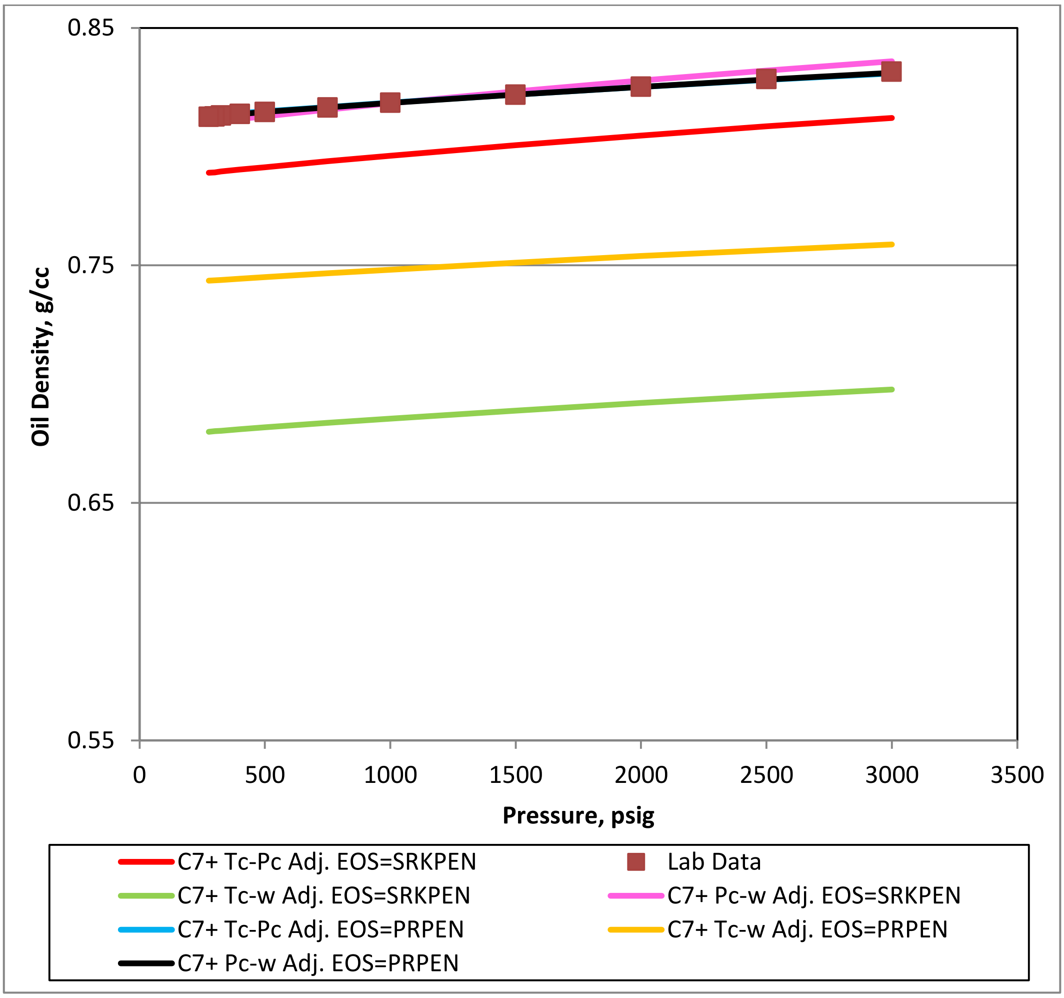

Figure 5.35 Pressure – Density Relationship for Well E2 Sample
(C7+ Adjustment – Correlated)

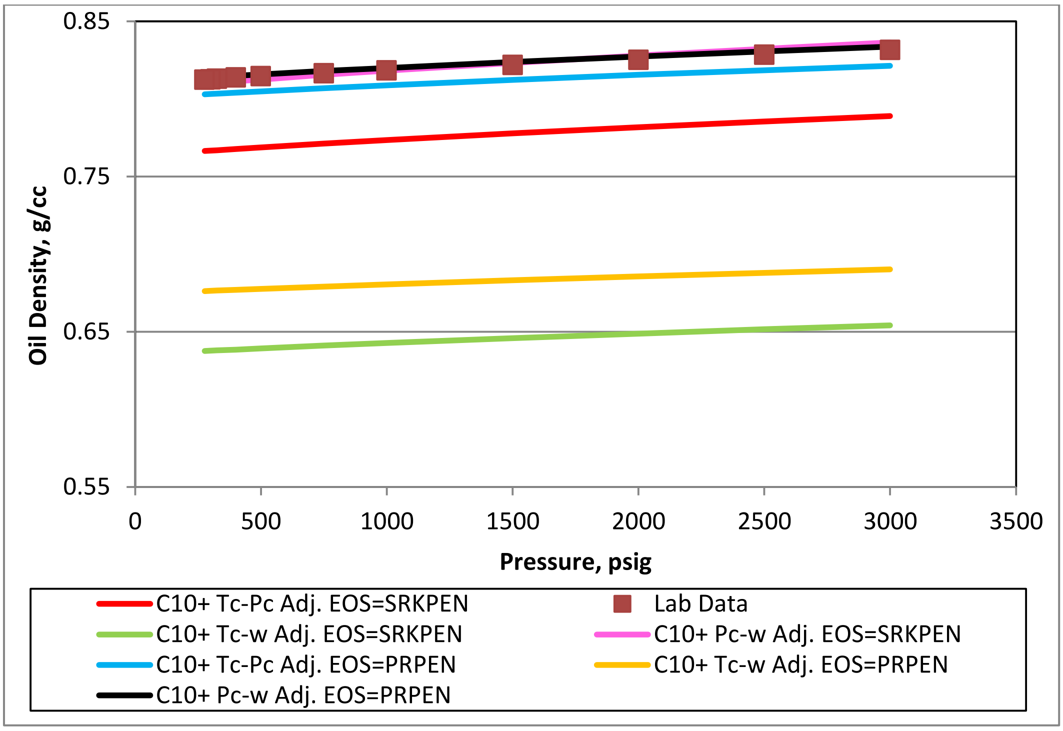

Figure 5.36 Pressure – Density Relationship for Well E2 Sample
(C10+ Adjustment – Correlated)

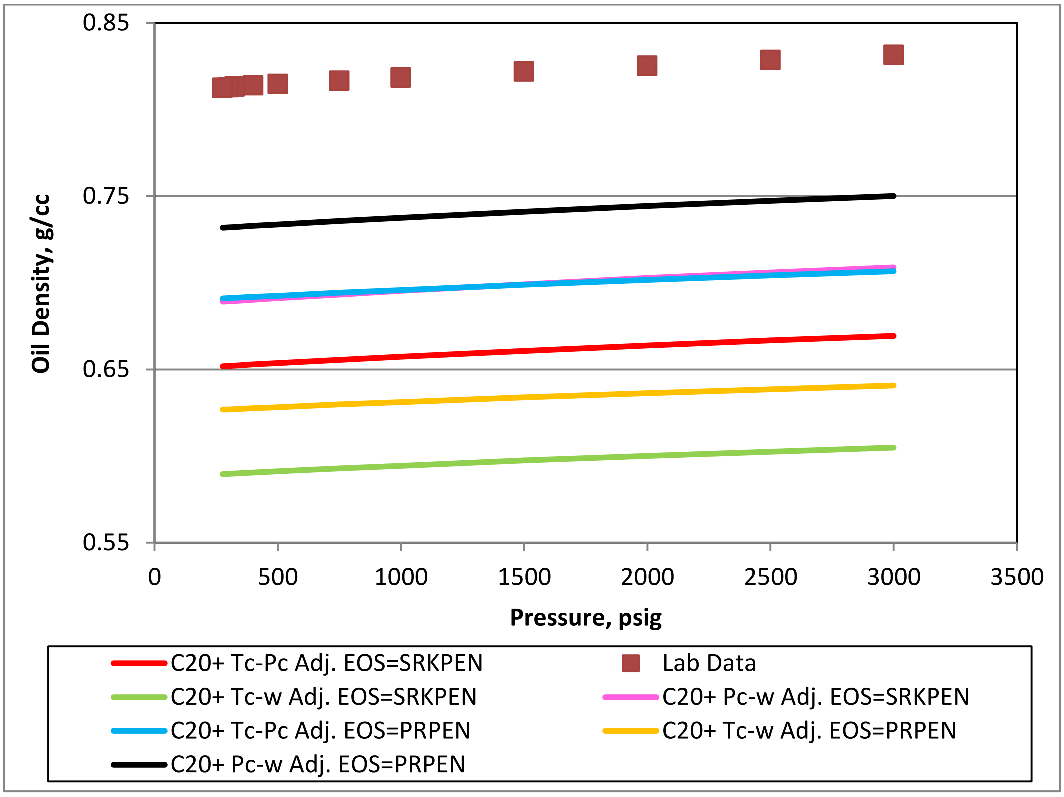

Figure 5.37 Pressure – Density Relationship for Well E2 Sample
(C20+ Adjustment – Correlated)

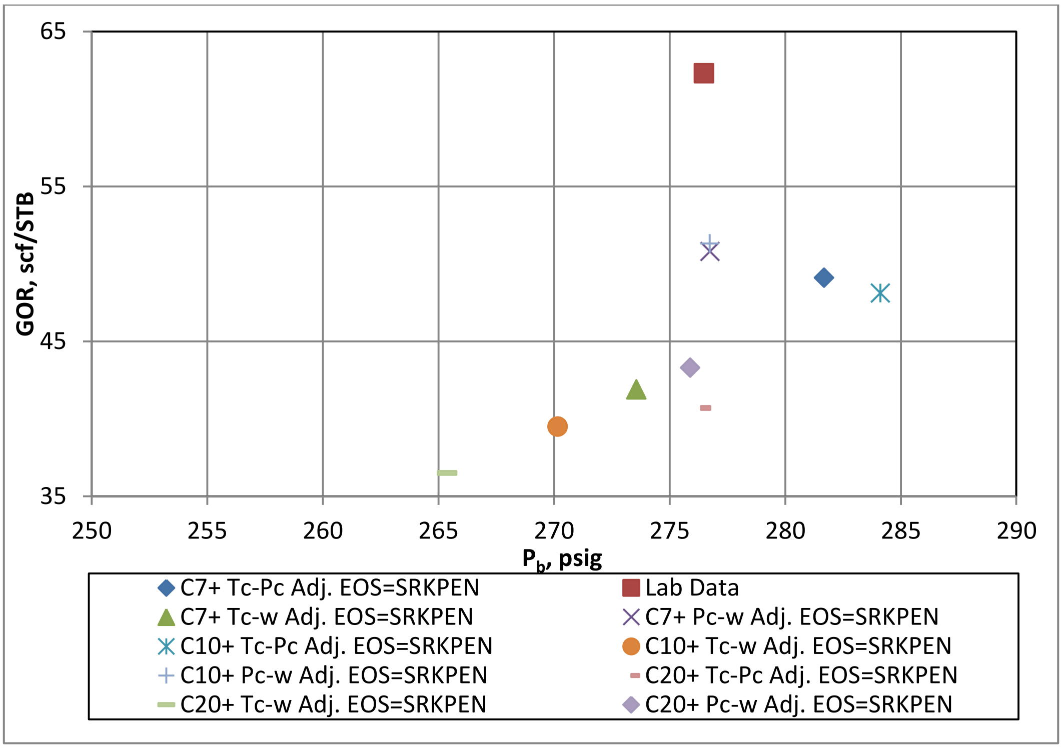

Figure 5.38 SRK - Pen EoS Predictions of GOR and P_b for Well E2 Sample (with S and E Values)

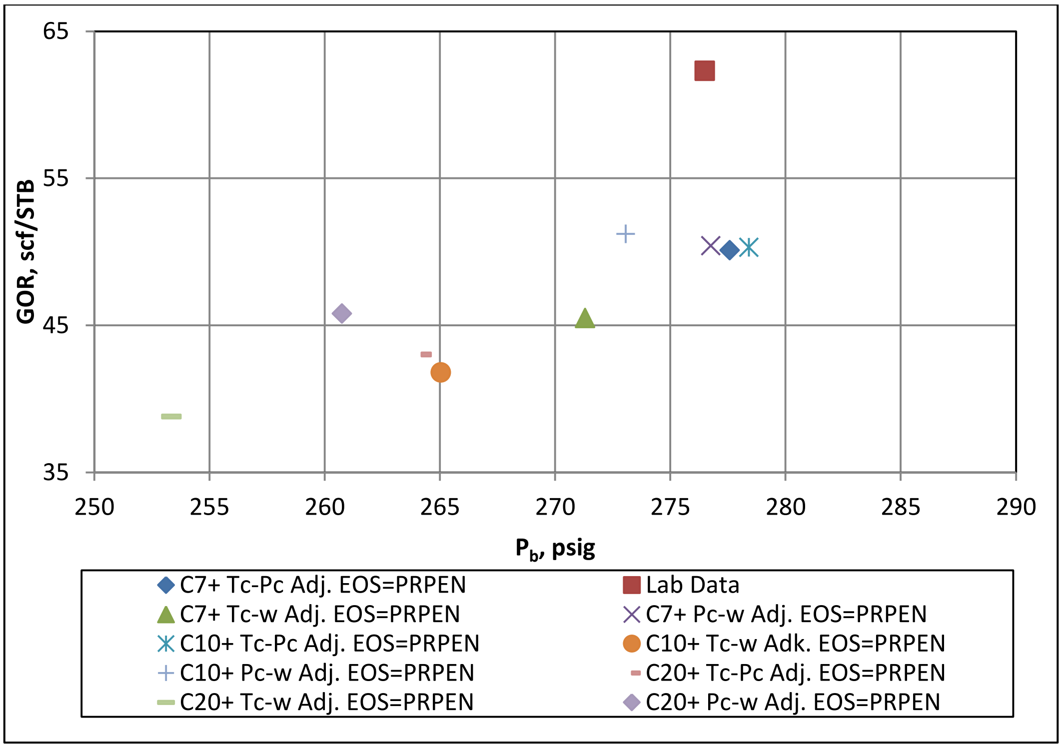

Figure 5.39 PR - Pen EoS Predictions of GOR and P_b for Well E2 Sample (with S and E Values)

Simulational B_{ob} values are very close to experimental B_{ob}. These B_{ob} values are obtained by using critical properties of Sancet and Edmister's correlations. Again, pseudoization effect is not observed and for both models, relative errors are within ± 1.5%. B_{ob} predictions are not affected by regressed parameter, equation of state models and pseudoization.

Table 5.43 B_{ob} Comparison for Well E2 Sample
(SRK-Pen EoS with S and E values)

Para.	SRK-Pen EoS								
	C7+			C10+			C20+		
	T_c-P_c	T_c-ω	P_c-ω	T_c-P_c	T_c-ω	P_c-ω	T_c-P_c	T_c-ω	P_c-ω
B_{ob}	1.069	1.060	1.076	1.068	1.058	1.077	1.060	1.056	1.065
Rel. Error, %	0.55	-0.30	1.20	0.45	-0.49	1.30	-0.30	-0.68	0.17

Table 5.44 B_{ob} Comparison for Well E2 Sample
(PR-Pen EoS with S and E values)

Para.	PR-Pen EoS								
	C7+			C10+			C20+		
	T_c-P_c	T_c-ω	P_c-ω	T_c-P_c	T_c-ω	P_c-ω	T_c-P_c	T_c-ω	P_c-ω
B_{ob}	1.061	1.057	1.065	1.062	1.054	1.067	1.057	1.053	1.063
Rel. Error, %	-0.21	-0.58	0.17	-0.11	-0.87	0.36	-0.58	-0.96	-0.02

Viscosity match under reservoir temperature and CSP viscosity coefficients for both models are presented below. Viscosities against pressure and CSP coefficients have no relationship between each other for Well E2. Moreover, relative difference between experimental and simulation data is high, especially for very high and low pressures. It is observed that equation of state models and pseudoization do not affect viscosity predictions.

Table 5.45 CSP Viscosity Coefficient for Well E2 Sample (SRK - Pen EoS)

CSP Visc. Corr. Factor	SRK-Pen EoS								
	C7+			C10+			C20+		
	T_c-P_c	T_c-ω	P_c-ω	T_c-P_c	T_c-ω	P_c-ω	T_c-P_c	T_c-ω	P_c-ω
1st	1.006	0.877	0.935	0.947	0.923	0.423	1.047	0.907	0.874
2nd	0.459	0.643	0.940	0.595	0.608	1.074	0.839	0.858	1.062
3rd	0.914	0.684	0.553	0.895	0.790	0.831	0.867	0.742	0.698
4th	4.310	1.624	1.655	3.385	2.179	3.807	2.957	1.936	1.155

Table 5.46 CSP Viscosity Coefficient for Well E2 Sample (PR - Pen EoS)

CSP Visc. Corr. Factor	PR - Pen EoS								
	C7+			C10+			C20+		
	T_c-P_c	T_c-ω	P_c-ω	T_c-P_c	T_c-ω	P_c-ω	T_c-P_c	T_c-ω	P_c-ω
1st	0.975	1.357	1.242	1.529	0.981	3.406	0.911	0.971	0.680
2nd	0.313	0.440	0.384	0.100	0.509	0.863	0.571	0.536	0.981
3rd	0.973	0.993	0.873	0.991	0.992	0.950	0.930	0.902	0.931
4th	1.155	5.499	4.148	5.862	4.971	6.120	3.519	2.923	4.121

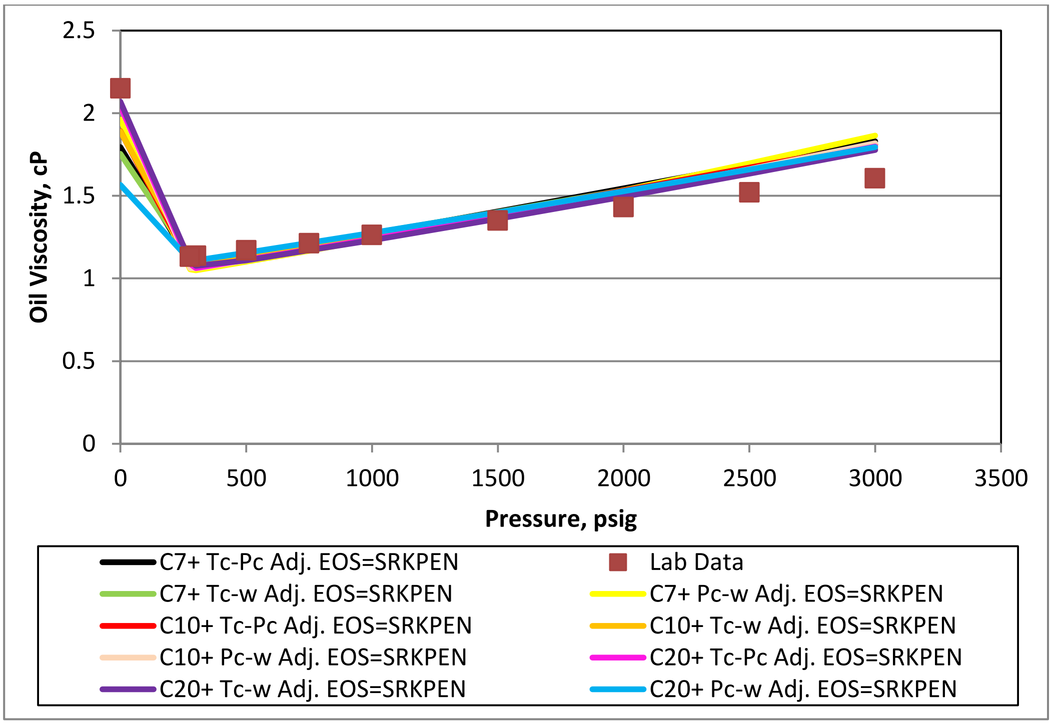

Figure 5.40 Pressure and Viscosity Relationship for Well E2 Sample (SRK - PEN EoS)

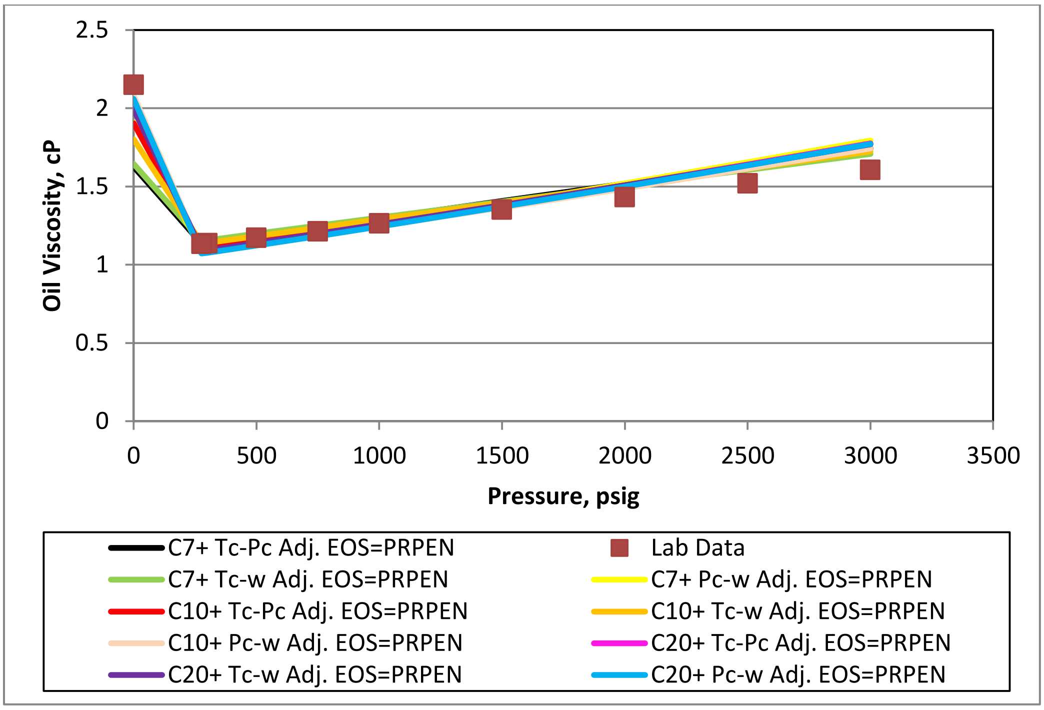

Figure 5.41 Pressure and Viscosity Relationship for Well E2 Sample (PR - PEN EoS)

5.3.4. Well BSS1 Sample

Gas and oil compositions are recombined with respect to GOR and ρ_{liquid} and then, they are lumped to investigate pseudoization effect as tabulated in Table 5.47. Then, properties of lumped compositions, after and before MW adjustment to predict P_b better, are given in Table 5.48 and 5.49.

After MW adjustment, according to density and viscosity data against pressure, regression is done. Density against pressure relationship is plotted in the following figures, Figure 5.42, 5.43 and 5.44. PR - Pen EoS predicts density better than SRK - Pen EoS. Moreover, predicted P_b and GOR are drawn in Figure 5.45 and 5.46 for each EoS model. GOR predictions of PR - Pen EoS are closer than those of SRK - Pen EoS. No pseudoization effect is observed in P_b and GOR predictions of SRK - Pen and PR - Pen equations of state.

Table 5.47 Lumped Reservoir Fluid Compositions for Well BSS1 Sample

Comp.	C7+	C10+	C20+	Comp.	C7+	C10+	C20+
N_2	0.096	0.096	0.096	C9		8.360	8.360
CO_2	0.545	0.545	0.545	C10 **(C10+)**		**(56.054)**	8.398
C1	3.232	3.232	3.232	C11			5.740
C2	0.596	0.596	0.596	C12			4.962
C3	1.174	1.174	1.174	C13			3.254
iC4	0.475	0.475	0.475	C14			2.870
nC4	2.109	2.109	2.109	C15			2.294
iC5	1.785	1.785	1.785	C16			1.987
nC5	2.985	2.985	2.985	C17			1.325
C6	6.979	6.979	6.979	C18			1.526
C7 **(C7+)**	**(80.025)**	7.624	7.624	C19			0.845
C8		7.987	7.987	**C20+**			**22.853**

Table 5.48 Parameters of Plus Fractions for Well BSS1 Sample

Para.	SRK-Pen EoS			PR-Pen EoS		
	C7+	C10+	C20+	C7+	C10+	C20+
MW	208.925	251.022	365.600	208.925	251.022	365.600
ρ_{liquid}	0.8440	0.8609	0.8915	0.8440	0.8609	0.8915
T_c	840.241	879.672	1000.044	888.393	950.742	1098.811
P_c	256.31	228.46	192.15	247.41	223.04	188.14
ω	0.8730	0.9480	1.1185	0.8142	0.8940	1.0913
C_{pen}	5.18E-5	4.95E-5	2.17E-5	3.93E-5	3.63E-5	9.68E-6

Table 5.49 Parameters of Plus Fractions After MW Adjustment
for Well BSS1 Sample

Para.	SRK-Pen EoS			PR-Pen EoS		
	C7+	C10+	C20+	C7+	C10+	C20+
MW	187.465	255.920	329.042	187.465	225.920	329.042
ρ_{liquid}	0.844	0.861	0.892	0.844	0.861	0.892
T_c	790.080	841.338	958.107	840.277	901.375	1043.835
P_c	280.66	247.22	204.18	246.30	236.67	196.97
ω	0.812	0.878	1.053	0.730	0.806	1.015
C_{pen}	4.31E-5	4.68E-5	2.88E-5	3.88E-5	3.86E-5	2.05E-5

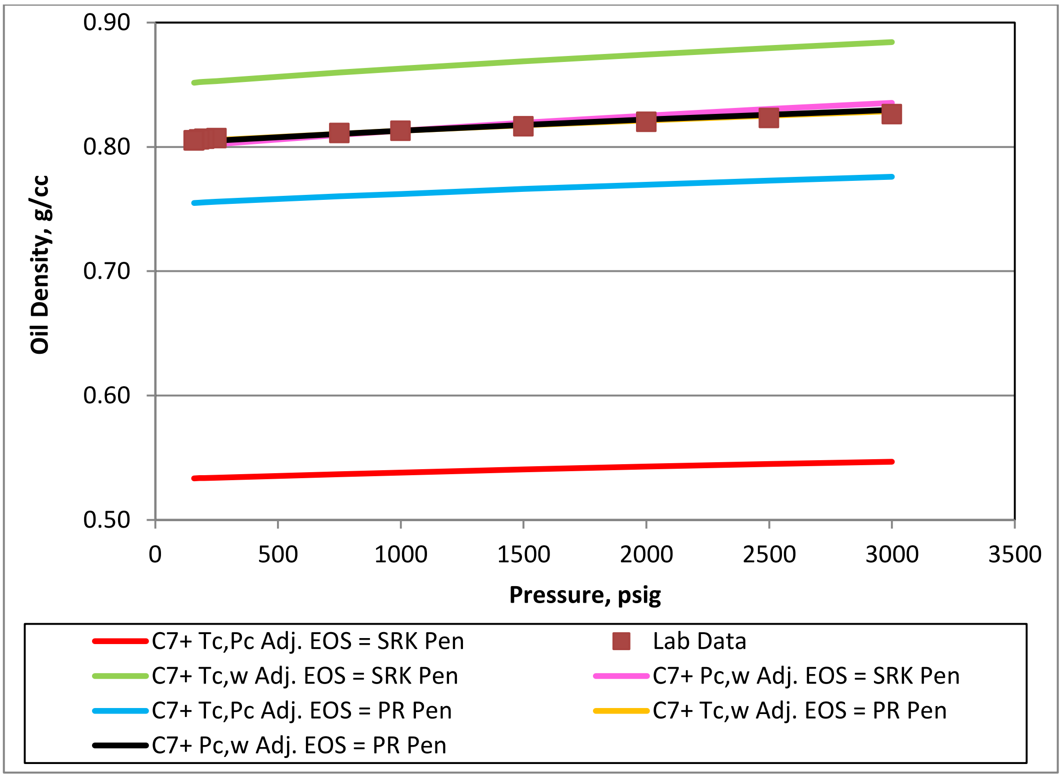

Figure 5.42 Pressure – Density Relationship for Well BSS1 Sample (C7+ Adjustment)

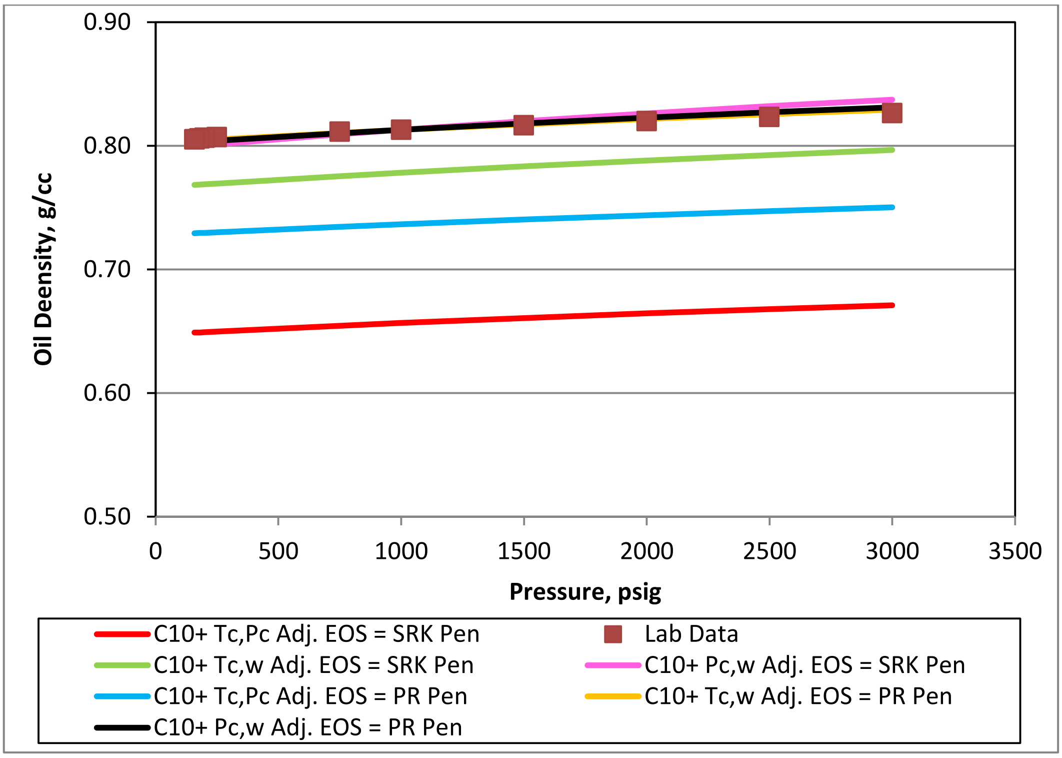

Figure 5.43 Pressure – Density Relationship for Well BSS1 Sample (C10+ Adjustment)

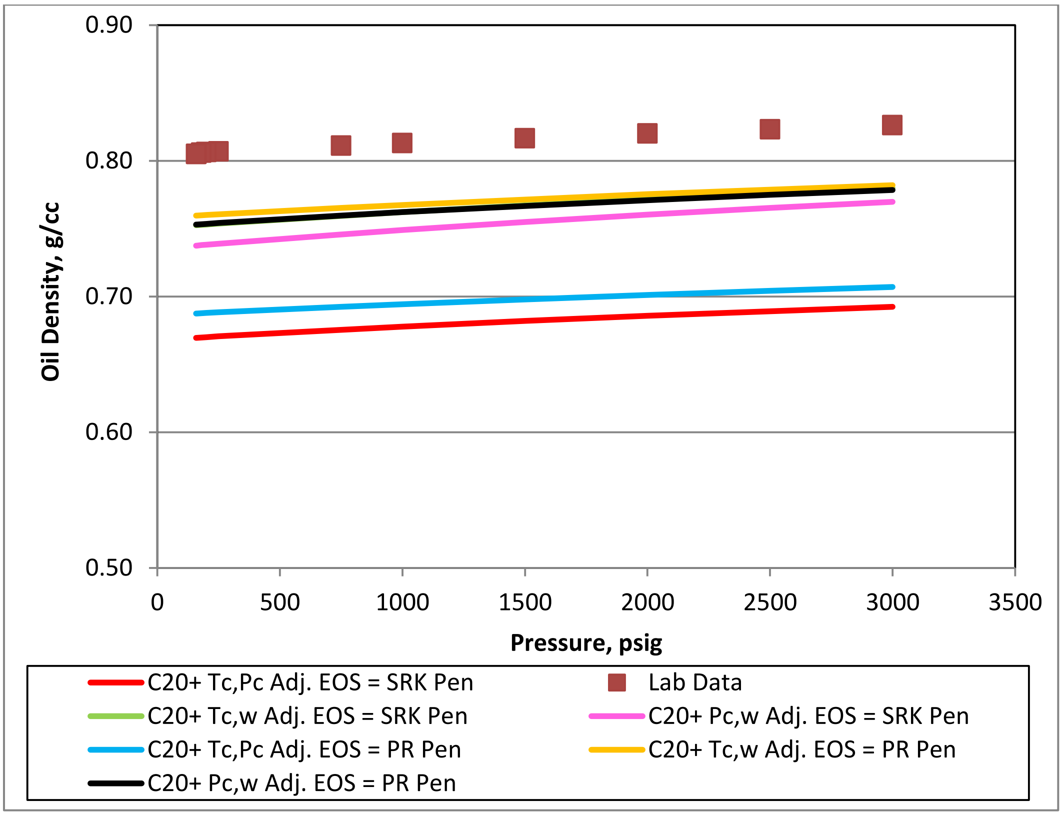

Figure 5.44 Pressure – Density Relationship for Well BSS1 Sample (C20+ Adjustment)

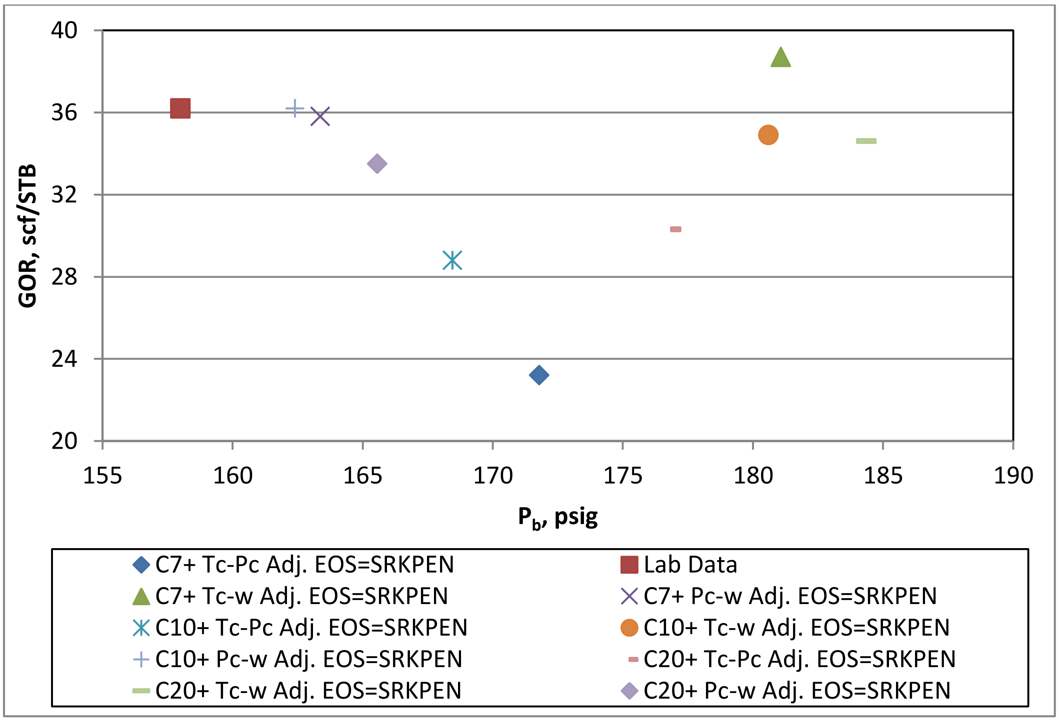

Figure 5.45 SRK - Pen EoS Predictions of GOR and P_b for Well BSS1 Sample

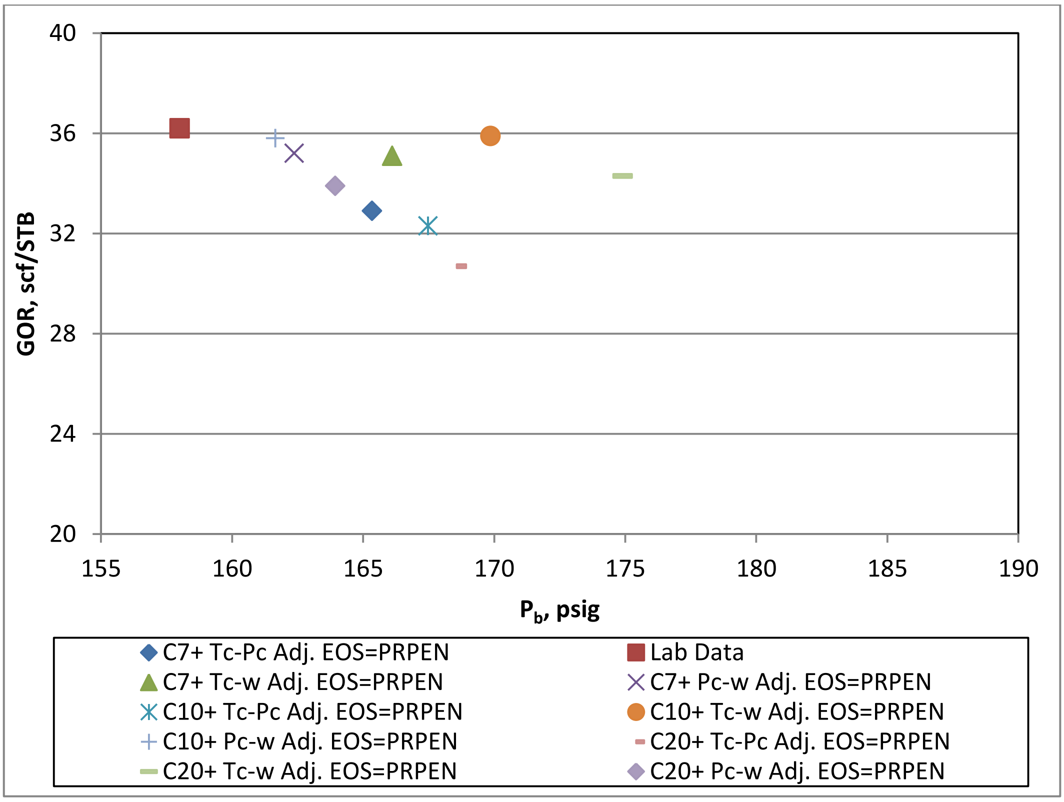

Figure 5.46 PR - Pen EoS Predictions of GOR and P_b for Well BSS1 Sample

In Table 5.50 and 5.51, B_{ob} values, obtained from simulations and experiment, are compared. Adjusted mole percentage does not affect the accuracy of predictions. Also, the most (1.058 bbl/STB) and the least (1.093 bbl/STB) deviated predictions are observed in SRK-Pen EoS.

Table 5.50 B_{ob} Comparison for Well BSS1 Sample (SRK - Pen EoS)

Para.	SRK - Pen EoS								
	C7+			C10+			C20+		
	T_c-Pc	T_c-ω	P_c-ω	T_c-P_c	T_c-ω	P_c-ω	T_c-P_c	T_c-ω	P_c-ω
B_{ob}	1.058	1.092	1.097	1.075	1.085	1.101	1.076	1.084	1.093
Rel. Error, %	-3.26	-0.16	0.30	-1.71	-0.80	0.67	-1.62	-0.89	-0.06

Table 5.51 B_{ob} Comparison for Well BSS1 Sample (PR - Pen EoS)

Para.	PR - Pen EoS								
	C7+			C10+			C20+		
	T_c-Pc	T_c-ω	P_c-ω	T_c-P_c	T_c-ω	P_c-ω	T_c-P_c	T_c-ω	P_c-ω
B_{ob}	1.072	1.077	1.080	1.072	1.079	1.084	1.069	1.074	1.080
Rel. Error, %	-1.98	-1.53	-1.25	-1.98	-1.34	-0.89	-2.26	-1.80	-1.25

Correlation - calculated critical properties are used for this well, too. In Table 5.52, critical properties, calculated by Sancet and Edmister's correlations are seen. Pedersen's correlations predict T_c, P_c and ω more than Sancet and Edmister's correlations.

Table 5.52 Correlation – Calculated Critical Properties of Plus Fraction for Well BSS1 Sample

Para.	SRK-Pen EoS			PR-Pen EoS		
	C7+	C10+	C20+	C7+	C10+	C20+
MW	187.465	255.920	329.042	187.465	255.920	329.042
ρ_{liquid}	0.844	0.861	0.892	0.844	0.861	0.892
T_c	760.154	881.800	979.558	760.154	881.800	979.558
P_c	230.392	165.718	124.820	230.392	165.718	124.820
ω	0.621	0.786	0.959	0.621	0.786	0.959
T_b	462.251	603.802	725.978	462.251	603.802	725.978

Density against pressure relationship under T_{res} for three lumping schemes is presented in Figure 5.47, 5.48 and 5.49. Pseudoization effect on density is clearly seen. Prediction ability with new properties is measured by drawing P_b versus GOR. P_b predictions of SRK - Pen EoS are usually more than experimental data. Also, both equations of state predict GOR less than experimental data.

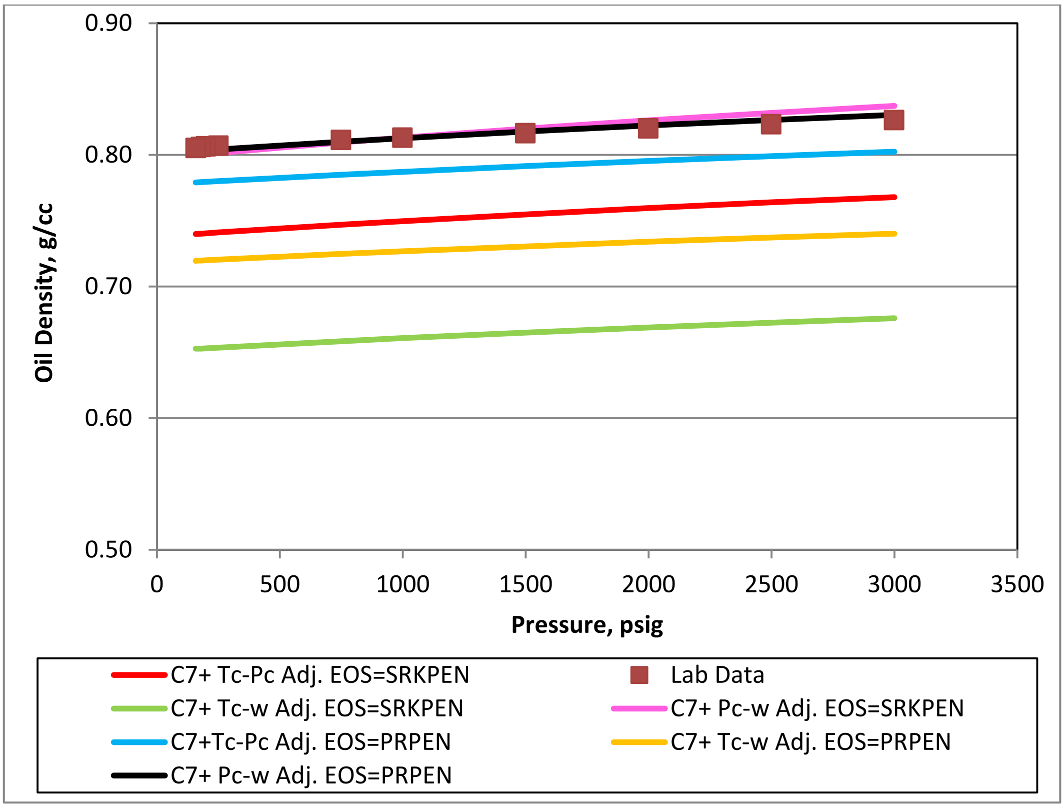

Figure 5.47 Pressure – Density Relationship for Well BSS1 Sample (C7+ Adjustment – Correlated)

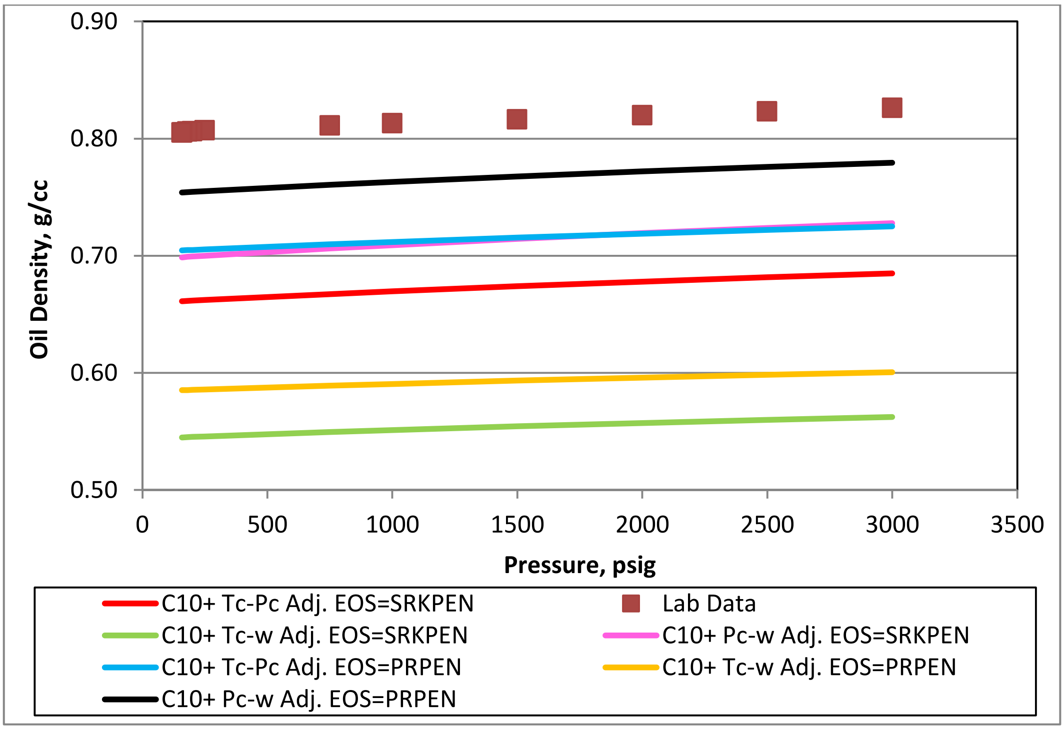

Figure 5.48 Pressure – Density Relationship for Well BSS1 Sample (C10+ Adjustment – Correlated)

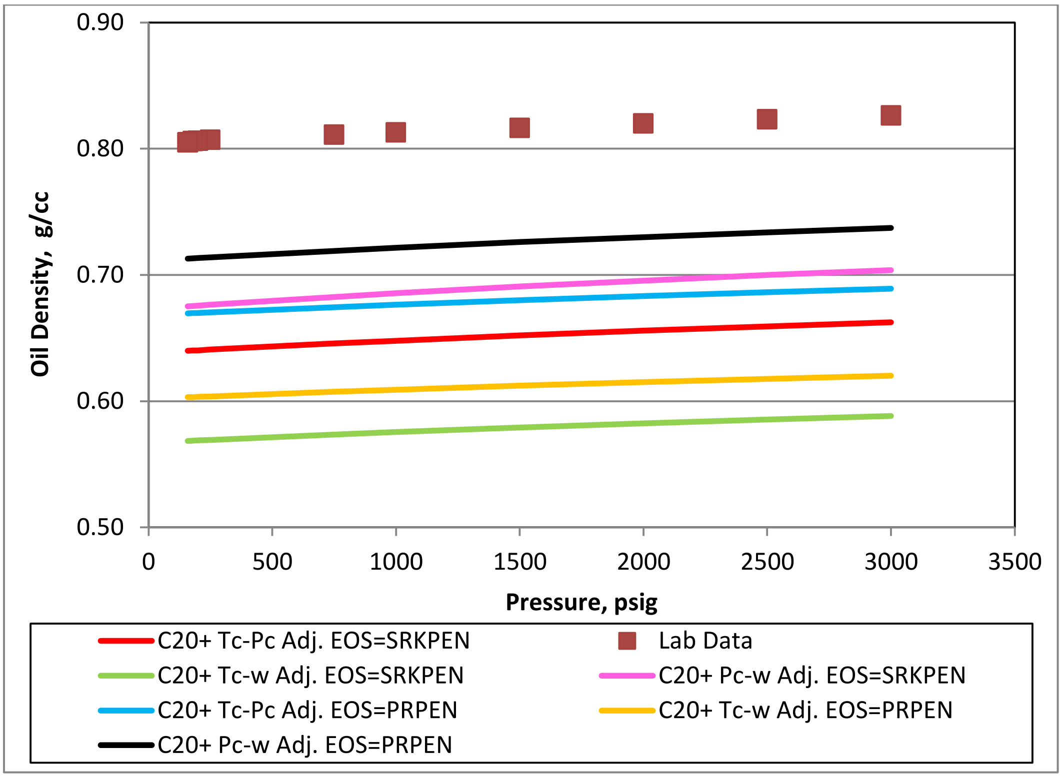

Figure 5.49 Pressure – Density Relationship for Well BSS1 Sample (C20+ Adjustment – Correlated)

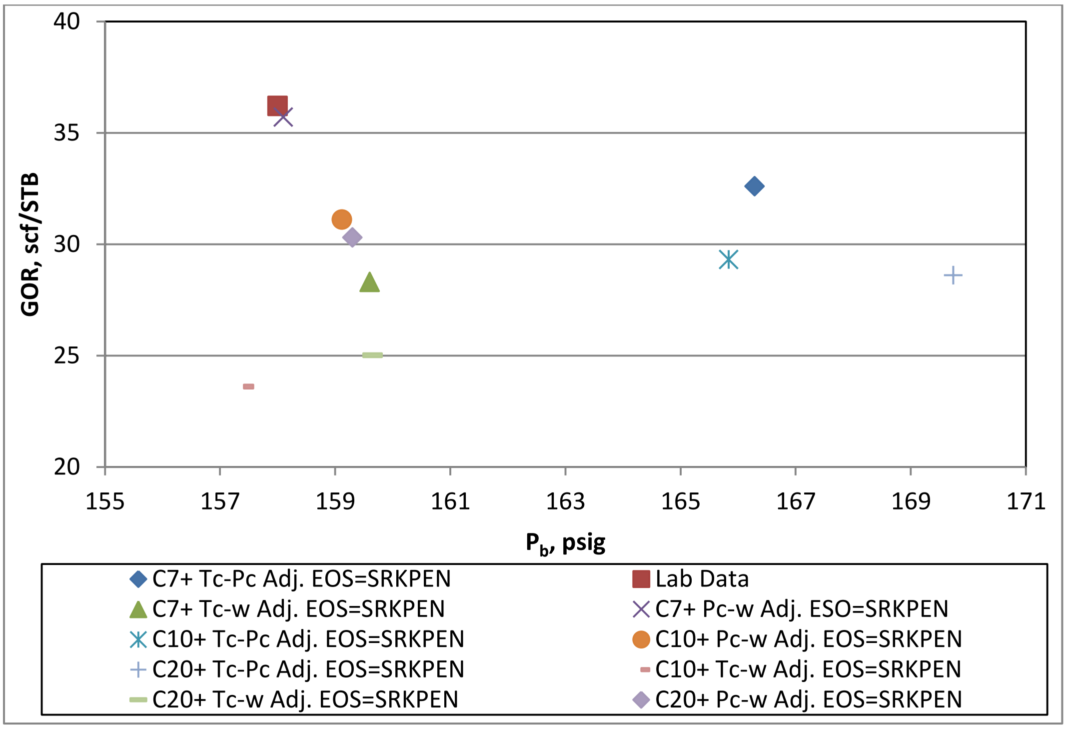

Figure 5.50 SRK - Pen EoS Predictions of GOR and P_b for Well E2 Sample (with S and E Values)

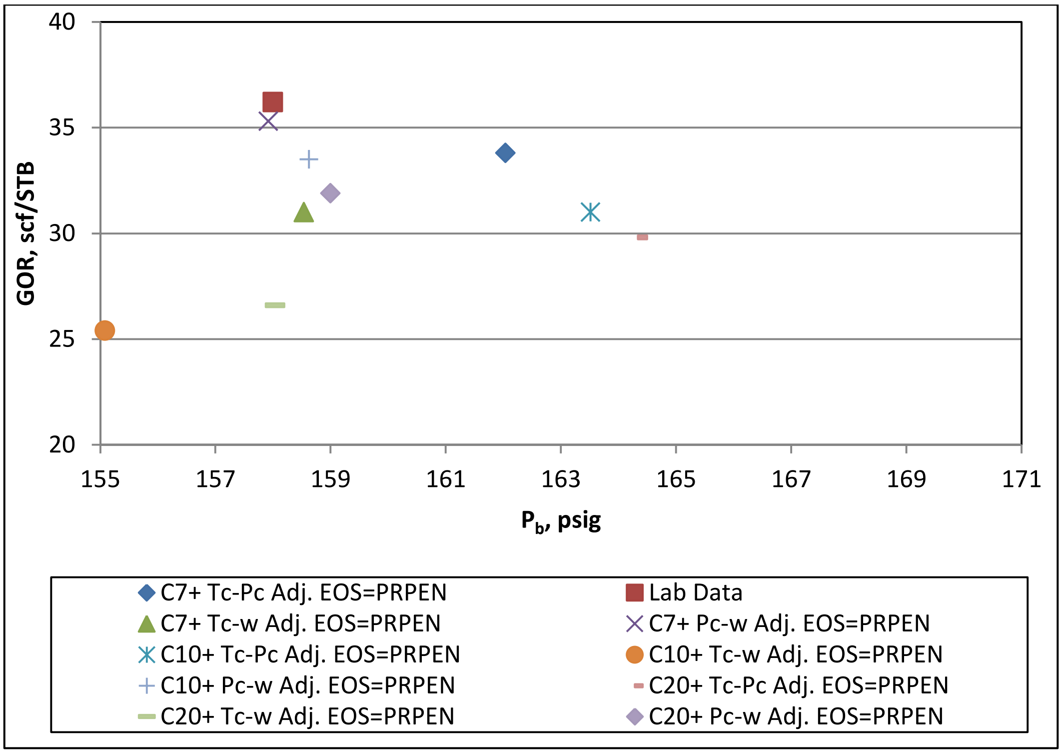

Figure 5.51 PR - Pen EoS Predictions of GOR and P_b for Well E2 Sample (with S and E Values)

Predictive ability of new critical properties is also shown in Table 5.53 and 5.54 by tabulating B_{ob} values and calculating relative errors with respect to experimental B_{ob}. Critical properties, calculated with Sancet and Edmister's correlations, are less successful when they are used in PR - Pen EoS.

Table 5.53 B_{ob} Comparison for Well BSS1 Sample (SRK - Pen EoS with S and E values)

Para.	SRK - Pen EoS								
	C7+			C10+			C20+		
	T_c-Pc	T_c-ω	P_c-ω	T_c-P_c	T_c-ω	P_c-ω	T_c-P_c	T_c-ω	P_c-ω
B_{ob}	1.083	1.075	1.101	1.077	1.066	1.088	1.075	1.070	1.087
Rel. Error, %	-0.98	-1.71	0.67	-1.53	-2.53	-0.52	-1.71	-2.17	-0.61

Table 5.54 B_{ob} Comparison for Well BSS1 Sample
(PR - Pen EoS with S and E values)

Para.	PR - Pen EoS								
	C7+			C10+			C20+		
	T_c-Pc	T_c-ω	P_c-ω	T_c-P_c	T_c-ω	P_c-ω	T_c-P_c	T_c-ω	P_c-ω
B_{ob}	1.076	1.071	1.085	1.071	1.061	1.082	1.069	1.064	1.079
Rel. Error, %	-1.62	-2.08	-0.80	-2.08	-2.99	-1.07	-2.26	-2.72	-1.34

Viscosity match under reservoir temperature and CSP viscosity coefficients for both models are presented below. Viscosities against pressure and CSP coefficients have no relationship between each other for Well BSS1 however, for PR - Pen EoS, 3rd and 4th viscosity correction factors are usually the most regressed coefficients. Relative difference between experimental and simulation data is high especially for very high and low pressures.

Table 5.55 CSP Viscosity Coefficient for Well BSS1 Sample (SRK - Pen EoS)

CSP Visc. Corr. Factor	SRK - Pen EoS								
	C7+			C10+			C20+		
	T_c-P_c	T_c-ω	P_c-ω	T_c-P_c	T_c-ω	P_c-ω	T_c-P_c	T_c-ω	P_c-ω
1st	0.717	1.124	0.742	1.19	0.932	0.923	1.184	0.707	1.028
2nd	1.002	0.989	1.117	1.007	1.050	1.101	1.030	0.689	1.099
3rd	0.609	0.421	0.655	0.847	0.579	0.543	0.592	0.689	0.975
4th	1.000	1.163	1.629	3.344	1.185	1.662	1.201	1.784	1.032

Table 5.56 CSP Viscosity Coefficient for Well BSS1 Sample (PR - Pen EoS)

CSP Visc. Corr. Factor	PR - Pen EoS								
	C7+			C10+			C20+		
	T_c-P_c	T_c-ω	P_c-ω	T_c-P_c	T_c-ω	P_c-ω	T_c-P_c	T_c-ω	P_c-ω
1st	0.820	0.944	0.700	0.968	0.641	0.981	0.372	0.799	0.788
2nd	0.875	0.900	1.086	1.000	1.024	1.073	1.095	1.039	1.094
3rd	0.589	0.782	0.566	0.738	0.685	0.609	0.851	0.816	0.774
4th	1.696	3.582	1.278	1.83	1.577	1.179	2.348	2.202	1.664

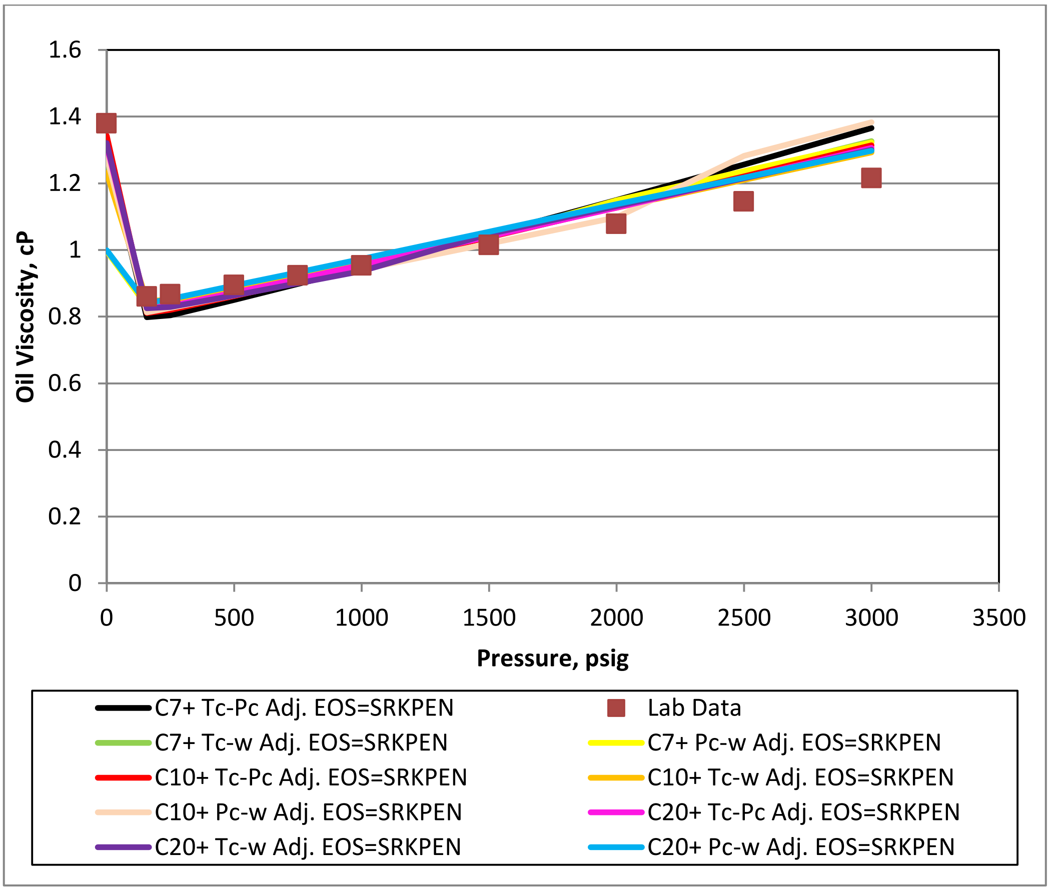

Figure 5.52 Pressure and Viscosity Relationship for Well BSS1 Sample (SRK - PEN EoS)

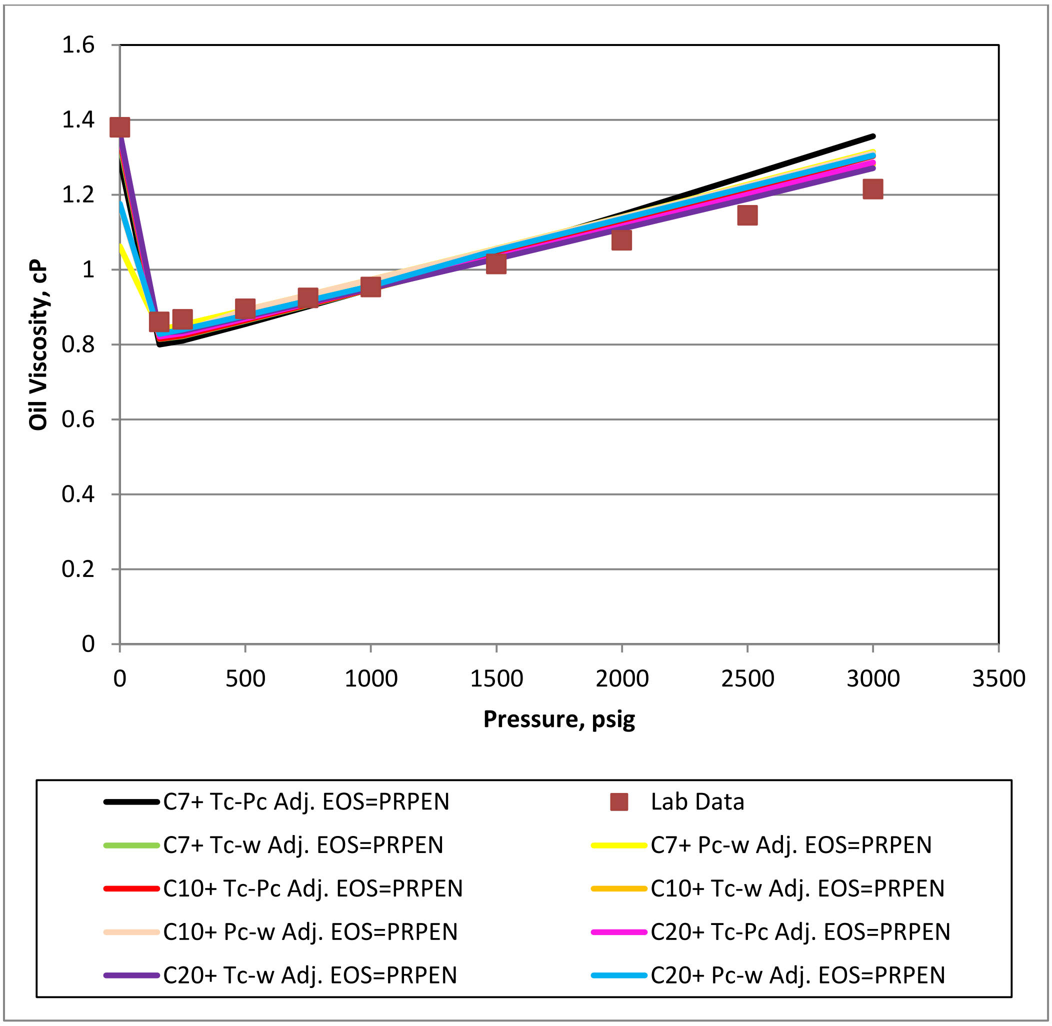

Figure 5.53 Pressure and Viscosity Relationship for Well BSS1 Sample (PR - PEN EoS)

To sum up, according to results of Constant Composition Experiment, oil compressibility near the Bubble Point Pressure is not constant as it is at high pressures. Pb and GOR data show that, they are not well correlated for the samples, studied. Simulation results show that adjusting the critical properties of more mole percentage results in better density predictions. However, for heavy hydrocarbons, adjustments on C20+ fractions give acceptable results. Consequently, viscosity predictions are independent on adjusted mole percentage. They are dependent on adjusted CSP viscosity correction factors but, for every well or field, CSP coefficients should be determined separately, instead of the usage of generalized CSP coefficients. Density predictions of critical pressure -

acentric factor (P_c - ω) pair are usually better than predictions of critical temperature - critical pressure (T_c - P_c) and critical temperature - acentric factor (T_c - ω) pairs. In addition, Peng - Robinson EoS with Peneloux correction is found to be more successful in density predictions. It is also, observed that Sancet and Edmister's correlations predict critical properties less than that of Pedersen. Density versus pressure plots show that critical properties, calculated by Pedersen et. al.'s correlations, give more promising results than critical properties, calculated by Sancet and Edmister's correlations. Relative error in B_{ob} predictions for all models and correlation sets are between -3.3 - 2.4%.

CHAPTER 6

CONCLUSIONS

Based on the samples studied in the thesis, following conclusions are obtained:

Bubble point pressure (P_b), Gas - Oil Ratio (GOR), oil formation volume factor at P_b (B_{ob}), API gravity and C7+ mole percentage of black oil samples, used in this study, are in between 90.5 - 276.5 psig, 20.7 - 62.3 scf/STB, 1.05 - 1.09 bbl/STB, 18.9 - 33.7 °API and 80 - 90 %, respectively.

Although the sample of Well E2 has the highest GOR (62.3 scf/STB) and the highest P_b (276.5 psig); experimental GOR and P_b are not correlated.

Samples with the highest and the lowest P_b do not have the highest and the lowest viscosity and density values with respect to pressure under reservoir temperature.

Adjusted mole percentage highly effects density predictions. Adjustments, done on C7+ fractions, give more accurate results than the ones, done on C10+ and C20+ fractions. In addition, Peng - Robinson EoS with Peneloux Correction predicts density better than Soave - Redlich - Kwong EoS with Peneloux Correction. Also, it is observed that, abundancy of heavy components makes a positive impact on density prediction. It is concluded that, highest accuracy in density predictions can be achieved by using C7+ fraction and PR - Pen EoS. The reason of inconsistency between density and B_{ob} predictions is that, density data is used for regression and B_{ob} values are predicted after critical properties are regressed according to density data. Critical pressure (P_c) - acentric factor (ω) pairs for all lumping schemes and equations of state are more successful than other pairs (T_c - P_c and T_c - ω) in density predictions.

Viscosity predictions do not depend on both equations of state and adjusted mole percentage. However, they depend on viscosity correction factors of Corresponding States Model (CSP) and instead of using generalized coefficients, those should be determined for each well.

Sancet and Edmister’s correlations predict critical properties of plus fractions, which are critical temperature, critical pressure and acentric factor, less than Pedersen’s correlations.

Equations of States and adjusted mole percentage do not effect P_b and GOR predictions.

Percentage of deviation from experimental data in all Oil Formation Volume Factor at Bubble Point Pressure (B_{ob}) predictions varies in between -3.3 and 2.4 %.

CHAPTER 7

RECOMMENDATIONS

1. By working on more black oil samples in Turkey, regional correlation sets, to predict bubble point pressure, gas - oil ratio, oil density and viscosity as a function of separator gas - oil ratio, API gravity, reservoir pressure and temperature, should be formed.

2. Map of compositions of black oils in Turkey is recommended to be constructed and its effects to phase behavior should be investigated.

3. This study should be expanded to cover more equations of state and correlations to predict the critical properties of plus fractions.

4. Since black oils in Turkey contain heavy fractions, studies about wax and asphaltene occurrences and depositions should be done both experimentally and on a compositional simulation package.

REFERENCES

1. Adepoju, O.O.: “Coefficient of Isothermal Oil Compressibility For Reservoir Fluids By Cubic Equations Of State”, M.Sc Thesis in Petroleum Engineering, Texas Tech University, 2006.

2. Ahmed, T.H.: “Comparative Study of Eight Equations of State for Predicting Hydrocarbon Volumetric Phase Behavior”, SPE 15673, presented at SPE Annual Technical Conference and Exhibition, New Orleans, Oct. 5-6, 1988.

3. Ahmed, T.H.: “Hydrocarbon Phase Behavior”, Gulf Publishing Company, Houston, Texas, 1989.

4. Ahmed, T.: “Reservoir Engineering Handbook”, 2nd Edition, Gulf Professional Publishing, Houston, Texas, 2001.

5. Alavian, S. A., Whitson, C. H., and Martinsen, S. O.: “Global Component Lumping for EOS Calculations”, Society of Petroleum Engineers. doi:10.2118/170912-MS, 2014.

6. Al-Marhoun, M.A. et. al.: “Adjustment of Differential Liberation Data to Separator Conditions”, Society of Petroleum Engineers. doi:10.2118/84684-PA, 2003

7. Archer, J.S. and Wall, C.G.: “Petroleum Engineering: Principles and Practice”, Graham and Trotman, London, UK, 1986.

8. Ashrafi, M. et. al.: “Experimental PVT Property Analyses for Athabasca Bitumen”, Society of Petroleum Engineers. doi:10.2118/147064-MS, 2011.

9. Bergman, D.F. et. al.: “Retrograde Condensation in Natural Gas Pipelines”, Monograph Series, American Gas Association, New York, 1975.

10. Bon, J. et. al.: “Reservoir Fluid Sampling Revisited - A Practical Perspective”, Society of Petroleum Engineers. doi:10.2118/101037-MS, 2006.

11. Burke, N.H. et. al.: “Extended Analysis of Live Reservoir Oils by Gas Chromatography”, Society of Petroleum Engineers. doi:10.2118/21003-MS, 1991.

12. Canas, J.A. et. al.: “Viscous Oil Dynamics Evaluation for Better Fluid Sampling”, Society of Petroleum Engineers. doi:10.2118/97767-MS, 2005.

13. Christensen, P.L.: “Regression to Experimental PVT Data”, Petroleum Society of Canada. doi: 10.2118/99-13-52, 1999.

14. Danesh, A.: “PVT and Phase Behavior of Petroleum Reservoir Fluids”, Elsevier Science B.V., 1998.

15. Edmister, W.C.: “Applied Hydrocarbon Thermodynamics Part 4: Compressibility Factors and Equations of State”, Pet. Refiner, Vol: 37, pp. 173 - 179, 1958.

16. Elias, R. and Gelin, F.: “Vertical Heterogeneity of Kerogen and Fluid Compositions in the Vaca Muerta Unconventional Shale Play and Assessment of Producible Fluid Composition and Quality”, International Petroleum Technology Conference. doi:10.2523/IPTC-18351-MS, 2015.

17. Evans, R.B. and Harris, D.: “Equilibrium Vaporization Ratios - Hydrocarbon Mixture Containing Two Concentrations of Heptanes and Heavy Fractions”, Ind. Eng. Chem., pp. 45 - 50, 1956.

18. Gharbi, R.B.C. and Elsharkawy, A.M.: “Neural Network Model for Estimating the PVT Properties of Middle East Crude Oils”, Society of Petroleum Engineers, 2001.

19. Heyen, G.: “A Cubic Equation of State with Extended Range of Application”, Proc., Second World Congress Chem. Eng., Montreal (Oct. 4-9), 1983.

20. Hoffmann, A.E. et. al.: “Equilibrium Constants for a Gas-Condensate System”, Society of Petroleum Engineers. 1953.

21. Imo-Jack, O. and Emelle, C.: “An Analytical Approach to Consistency Checks of Experimental PVT Data”, Society of Petroleum Engineers. doi:10.2118/167560-MS, 2013.

22. Joergensen, M., and Stenby, E. H.: “Optimization of Pseudo-component Selection for Compositional Studies of Reservoir Fluids”, Society of Petroleum Engineers. doi:10.2118/30789-MS, 1995.

23. Katz, D.L. and Firoozabadi, A.: “Predicting Phase Behavior of Condensate / Crude-Oil Systems Using Methane Interaction Coefficients”, SPE-6721-PA, J. Pet. Tech. Vol: 30, pp. 1649-1655, 1978.

24. Lawrence, J.J. et. al.: “Representative Reservoir Fluid Sampling: Challenges, Issues, and Solutions”, International Petroleum Technology Conference. doi:10.2523/IPTC-12401-MS, 2008.

25. Lindeloff, N. et. al.: “The Corresponding States Viscosity Model Applied to Heavy Oil Systems”, Journal of Canadian Petroleum Technology, Sept. 1964, Vol: 43, No: 9, 2004.

26. Ling, K. et. al.: “New Method To Estimate Surface-Separator Optimum Operating Pressures”, Society of Petroleum Engineers. doi:10.2118/163111-PA, 2013.

27. Lohrenz, J., Bray, B. G., and Clark, C. R.: “Calculating Viscosities of Reservoir Fluids from Their Compositions”, Society of Petroleum Engineers, SPE 915, presented at SPE Annual Technical Meeting, Houston, Texas, Oct. 11 -14, 1964.

28. McCain, W.D.: “The Properties of Petroleum Fluids”, PennWell Publishing Company, 2nd Edition, Tulsa, Oklahoma, 1990.

29. Michaels, J., Moody, M. and Shwe, T.: “Wireline Fluid Sampling”, Society of Petroleum Engineers. doi:10.2118/30610-MS, 1995.

30. Moses, P. L.: “Engineering Applications of Phase Behavior of Crude Oil and Condensate Systems”, Society of Petroleum Engineers. doi:10.2118/15835-PA, 1986.

31. Osman, E.A. et. al.: “Prediction of Oil PVT Properties Using Neural Networks”, Society of Petroleum Engineers, 2001.

32. Patel, N. and Teja, A.: “A New Equation of State for Fluids and Fluid Mixtures”, Chem. Eng. Sci. 37, No.3, pp. 463-73, 1982.

33. Pedersen, K.S. et. al.: “PVT Calculations on Petroleum Reservoir Fluids Using Measured and Estimated Compositional Data for The Plus Fraction”, Ind. Eng. Chem. Res., Vol: 31, pp. 1378 - 1384, 1992.

34. Pedersen, K.S. et. al.: “Phase Behavior of Petroleum Reservoir Fluids”, CRC Press Taylor & Francis Group, 2nd Edition, 2015.

35. Peneloux, A. et. al.: "A Consistent Correction for Redlich-Kwong-Soave Volumes", Fluid Phase Equilibria, Vol: 8, pp. 9 - 10, 1982.

36. Peng, D. and Robinson, D.: "A New Two Constant Equation of State", Ind. & Eng. Chem. Fund. 15, No.1, pp. 59 - 64, 1976.

37. PVTsim® Compositional Simulation Software, Version 16: Calsep.

38. Rackett, H.G.: "Equation of State for Saturated Liquids", J. Chem. Eng. Data, Vol: 15, pp. 514 - 517, 1970.

39. Rastegar, R. and Jessen, K.: "A Flow Based Lumping Approach for Compositional Reservoir Simulation", Society of Petroleum Engineers. doi:10.2118/119160-MS, 2009.

40. Reid, R.C. et. al.: "The Properties of Gases and Liquids", McGraw-Hill Companies, 4th Edition, 1987.

41. Riazi, M.R. and Daubert, T.E.: "Characterization Parameters for Petroleum Fractions", Ind. Eng. Chem. Res., Vol: 26, No: 24, pp. 755-759, 1987.

42. Sancet, G.F.: "Heavy Fraction C_{7+} Characterization for PR-EOS", SPE-113026-STU (Student 6), 2007.

43. Schmidt, G. and Wendel, H.: "A Modified van der Waals Type Equation of State", Chem. Eng. Sci., Vol: 135, pp. 1503-12, 1980.

44. Sınayuc, C. and Gumrah, F.: "Predicting the Critical Properties of Heptanes-Plus in Gas Condensates: Genetic Algorithms as an Optimization Tool", Petroleum Society of Canada, 2004.

45. Soave, G.: "Equilibrium Constants from a Modified Redlich-Kwong Equation of State", Chemical Engineering Science, Vol: 27, no. 6, pp. 1197-1203, 1972.

46. Twu, C.H. et. al.: "A New Generalized Alpha Function for a Cubic Equation of State Part 1. Peng-Robinson Equation", Fluid Phase Equilibria, Vol: 105, pp. 52 - 57, 1995.

47. van der Waals, J.D.: "Continuity of the Gaseous and Liquid State of Matter", 1873.

48. Van Orsdal, F.G.: "Natural Gas Measurement, Sampling, and Analysis", Society of Petroleum Engineers. doi:10.2118/17753-PA, 1990.

49. VINCI Technologies, Catalogue of Products, 2012. [ONLINE] Available at: http://www.vinci-technologies.com/images/contenu/documents/catalog%20 PVT.pdf. [Accessed 11 February 2016].

50. Whitson, C.H.: "Characterizing Hydrocarbon Plus Fraction", Soc. Pet. Eng. J., pp. 683-694, 1983.

51. Whitson, C.H.: "Effect of C_{7+} Properties on Equation-of-State Prediction", Soc. Pet. Eng. J., pp. 685 - 696, December, 1984.

52. Yang, T. et. al.: "LBC Viscosity Modeling of Gas Condensate to Heavy Oil", Society of Petroleum Engineers, doi: 10.2118/109892-MS, 2007.

APPENDIX A

INSTRUMENTS OF THE PVT TEST SYSTEM

This section consists of the information about the instruments, which are used during PVT experiments.

Fluid-Eval ® (Standard Version) of VINCI Technologies© is a mercury free and versatile PVT instrument. It is used to determine the PVT properties of oil and gas samples. The instrument has a stirrer mechanism based on a combined rocking mechanism and magnetic driven stirrer. Also, automatic phase detections are available (VINCI Technologies, 2012, p.6). Technical specifications are provided in Table A.1.

Table A.1. Technical Specifications of Fluid-Eval Standard®
(VINCI Technologies, 2012, p.6)

Volume Capacity (cc)	500
Operating Pressure (psi)	10000
Operating Temperature (°C)	ambient to 175
Volume Accuracy (ml)	0.01
Pressure Accuracy	0.1% Full Scale
Chamber Material	Stainless Steel

Electromagnetic Viscometer, EV1000® of VINCI Technologies© is designed based on a simple and reliable electromagnetic concept. A controlled heating jacket provides viscosity measurements under different temperatures. Travel time of backward and forward movement of piston between two coils determines the absolute viscosity (VINCI Technologies, 2012, p.23). Technical specifications of this instrument are provided in Table A.2.

Table A.2. Technical Specifications of EV1000®
(VINCI Technologies, 2012, p.23)

Viscosity Range (cP)	0.02 - 10000
Reproducibility	± 0.8% of reading
Pressure Range (psi)	up to 15000
Temperature Range (°C)	up to 190
Accuracy	± 1% Full Scale
Temperature Regulation (°C)	± 0.5
Wetted Material	Inconel 718

Automated Gasometer® of VINCI Technologies© is designed to measure and monitor the volumes of gas under atmospheric conditions. The instrument consists of a calibrated chamber and a motor driven piston. Pressure and temperature within the chamber are controlled automatically (VINCI Technologies, 2012, p.14). Technical specification of this instrument is presented in Table A.3.

Table A.3. Technical Specifications of Automated Gasometer®
(VINCI Technologies, 2012, p.14)

Volume Capacity (cc)	10000 cc
Operating Pressure (psi)	Vacuum to 20
Operating Temperature (°C)	Ambient
Pressure Accuracy	0.1%
Volume Accuracy (ml)	0.1
Temperature Resolution (°C)	0.1
Wetted Parts	Stainless Steel

Hydrocarbon Compositional Analyser® of VINCI Technologies© consists of two standard Gas Chromatographs, which analyze the compositions of gas and liquid fractions of the reservoir fluid. Compositional analyses of separator gas, separator liquid and recombined sample are generated from the values of these Gas Chromatographs. Liquid analyzer works for up to C36+, while natural gas analyzer works for up to C14. Natural gas analyzer works based on the standard GPA 2286. Weight, mole and volume percentages are provided (VINCI Technologies, 2012, p.28).

APPENDIX B

SAMPLE CHROMATOGRAM

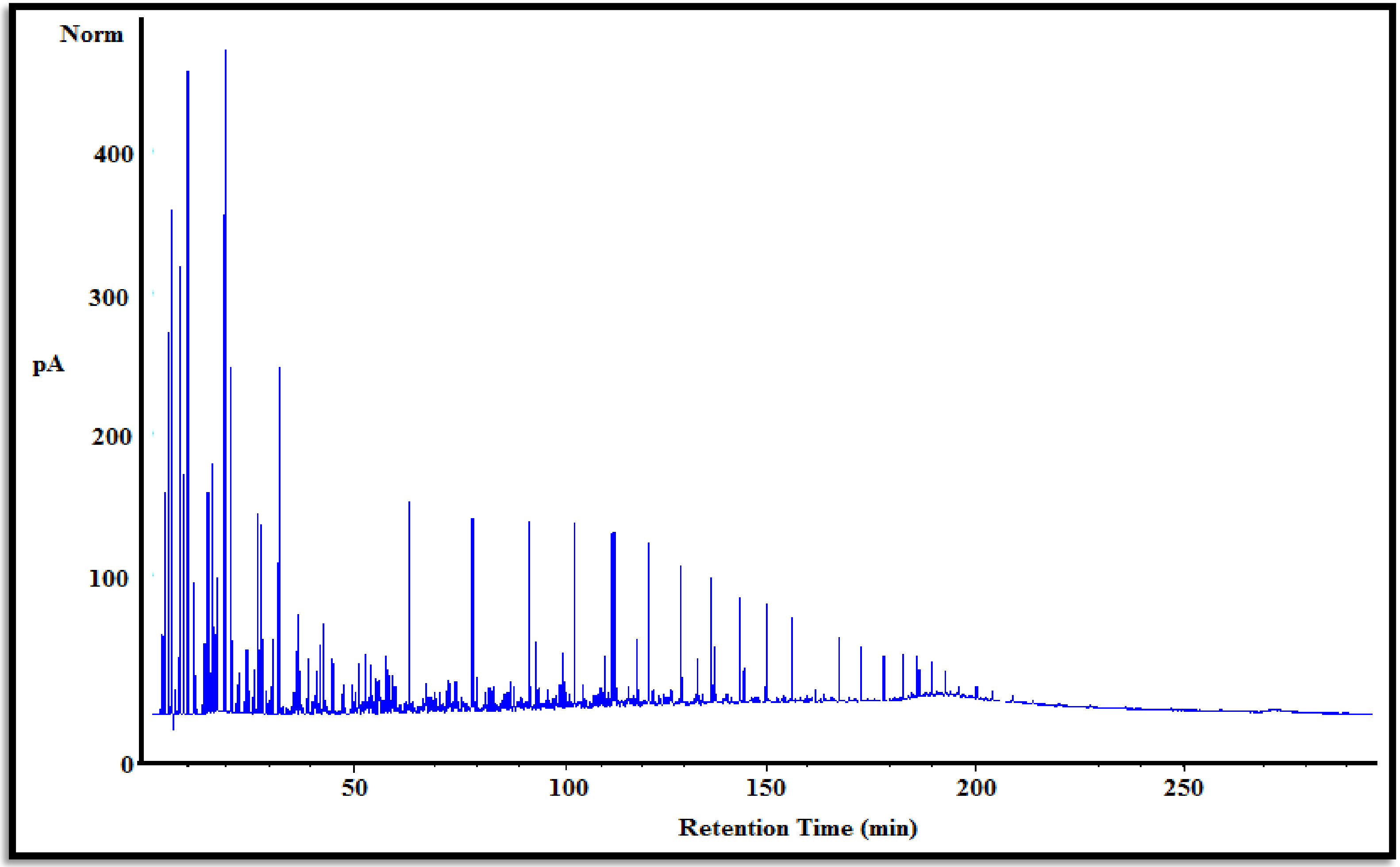

Figure B.1 Liquid Chromatogram Sample for Well B60